Direct Labeling Rolling Circle Amplification for Straightforward Signal Increase in Biodetection Formats Based on Fluorescence Spectroscopy Studies

Dissertation zur Erlangung des akademischen Grades des
Doktors der Naturwissenschaften (Dr. rer. nat.)

eingereicht im Fachbereich Biologie, Chemie, Pharmazie
der Freien Universität Berlin

vorgelegt von
Diplom Biochemikerin LENA LINCK
aus Berlin
2011

1. Gutachter: Prof. Dr. Volker A. Erdmann
2. Gutachter: Prof. Dr. Burghardt Wittig
Disputation am 29.05.2012

Die vorliegende Arbeit wurde unter der Anleitung von Dr. Ute Resch-Genger in der Zeit von März 2008 bis Oktober 2011 an der Bundesanstalt für Materialforschung und- prüfung Berlin angefertigt.

The submitted work was composed in the time from March 2008 to October 2011 under the supervision of Dr. Ute Resch-Genger at the Federal Institute of Materials Research and Testing Berlin.

Ich, Lena Linck, erkläre an Eides statt, dass ich die vorgelegte Dissertationsschrift mit dem Thema: *Direct Labeling Rolling Circle Amplification for Straightforward Signal Increase in Biodetection Formats Based on Fluorescence Spectroscopy Studies,* selbst verfasst und keine anderen als die angegebenen Quellen und Hilfsmittel benutzt, ohne die unzulässige Hilfe Dritter verfasst und auch in Teilen keine Kopien anderer Arbeiten dargestellt habe.

TABLE OF CONTENT

1 SUMMARY

The goal of this work was to develop a direct labeling rolling circle amplification (RCA)-based detection protocol as a straightforward and preferable general amplification strategy applicable to various detection platforms.

To this end an alternative fluorophore label to Cy3, the most commonly used green excitation dye in biodetection formats, were sought. The most suitable dye, DY-555, was employed in microarray assays yielding a protocol that reduces handling and reaction time efficiently with lesser costs while providing a great signal yield.

Seven fluorophores from different dye classes were investigated with steady-state and time-resolved spectroscopy to identify a candidate yielding maximum fluorescence with a minimum amount of dye molecules in a DNA template with defined labeling site spacing for the enzymatic integration of the dye-dUTPs. The most favorable properties were: High fluorescence quantum yield, absorption/emission features with a minimum sensitivity to the dye's microenvironment, and good photochemical stability.

For future for multiplexed real-time detection a fluorescence lifetime well above the signal for the scattered excitation light for potential detection with time-resolved fluorescence would be favorable. DY-555 offered all of these properties along with lesser cost than Cy3 and was subsequently chosen as the fluorophore label for assay studies.

An enzymatic direct labeling protocol for RCA-based signal amplification on a DNA microarray via dye-dUTPs was established. Next to the fluorophores, the labeling strategy, composition of reaction solution, and number of handling steps where optimized. With the resulting protocol, the assay's runtime and handling steps could be reduced while increasing the signal yield. The procedure was also carried out on an antibody microarray portraying the feasibility of applying this protocol to other RCA-based platforms.

These features are very attractive for many detection formats but especially for point-of-care diagnostic kits that need to be easy enough to be performed by scientifically untrained personnel.

2 ZUSAMMENFASSUNG

Das Ziel dieser Arbeit war die Entwicklung eines rolling circle amplification (RCA) basierten Nachweisprotokols als einfache und auf verschiedene Untersuchungsplattformen anwendbare Signalamplifikationsstrategie.

Für dieses Ziel wurden Alternativen zum Fluoreszenzlabel Cy3 gesucht, dem am häufigsten verwendeten Farbstoff im grünen Anregungsbereich. Der am Besten geeignete Farbstoff, DY-555, wurde in Mikroarray-Assays verwendet und führte zu einem Protokoll das die Handhabungs- und Reaktionszeit ökonomisch verringert während das Nachweissignal verstärkt wurde.

Sieben Fluorophore verschiedener Farbstoffklassen wurden mit statischer und zeitaufgelöster Spektroskopie untersucht um einen Kandidaten zu finden der die maximale Fluoreszenz mit der minimalen Menge an Farbstoffmolekülen, in einem DNA Templat mit definierten Einbaustellen für die enzymatische Integration von Farbstoff-dUTPs, ermöglicht. Die günstigsten Eigenschaften waren: hohe Quantenausbeute, Absorptions-/ und Emissions-Eigenschaften die in verschiedenen Mikroumgebungen stabil sind und gute photochemische Stabilität.

Für zukünftige Multiplex-Echtzeit-Detektion wäre eine möglichst lange Fluoreszenzlebenszeit, oberhalb des Signals des Anregungsstreulichts, für zeitaufgelöste Fluoreszenzmessungen von Vorteil. DY-555 zeigte alle diese Eigenschaften zusammen mit geringeren Kosten als Cy3 und war daher für Fluoreszenzlabel-Assaystudien ausgewählt.

Ein enzymatisches Direktmarkierungsprotokoll für RCA-basierte Signalamplifikation auf DNA-Mikroarrays mittels Farbstoff-dUTPs wurde erstellt. Neben den Fluorophoren wurde die Markierungsstrategie, Zusammensetzung der Reaktionslösung und die Anzahl der Handhabungsschritte optimiert. Mit dem resultierenden Protokoll konnten die Assay-Laufzeit und die Handhabungsschritte reduziert werden während das Signal verstärkt wurde. Die Prozedur wurde auch auf einem Antikörper-Mikroarray durchführt, um die Möglichkeit zu zeigen, dieses Protokoll auf anderen RCA-basierten Plattformen anzuwenden.

Diese Eigenschaften machen es sehr attraktiv für viele Detektionsformate aber besonders für Vor-Ort-Diagnostikverfahren die einfach genug sein müssen um von wissenschaftlich ungeschulten Personal durchgeführt zu werden.

3 INTRODUCTION

3.1 MICROARRAYS

Miniaturization is a dominant trend in the life sciences, especially in the field of diagnostics. Small scale detection formats like microarrays are excellent tools for analyzing many samples in small quantaties and thus reduced costs.[1][2] They are helpful tools for parallel and high throughput investigations [3][4] and have been employed for multiplexed and high-throughput analysis since the 1990s.[5] The growing number of microarray applications are used due to the versatility - DNA, protein, peptide, carbohydrate, small molecule microarrays. Antibody microarrays, e.g., are useful for the multiplexed analysis of low abundance proteins in serum samples such as health-related biomarkers and can provide more than 1000-fold sensitivity than the corresponding ELISAs when combined with *in situ* amplification methods.[6][7] DNA microarrays are valuable tools in gene expression profiling and single nucleotide polymorphism (SNP) detection, while antibody microarrays are used to detect various serum markers or illustrate protein-protein interactions.[4][8]

Yet, for some samples the detection limit is still insufficient. There are two strategies two improve the sensitivity of biodetection platforms – preamplification of the analyte molecules prior to detection or amplification of the signal.[9] For example, samples for DNA microarrays such as mRNA are transcribed into cDNA and consecutively labeled with fluorescent nucleotides during the DNAs amplification via polymerase chain reaction (PCR) (Figure 1).
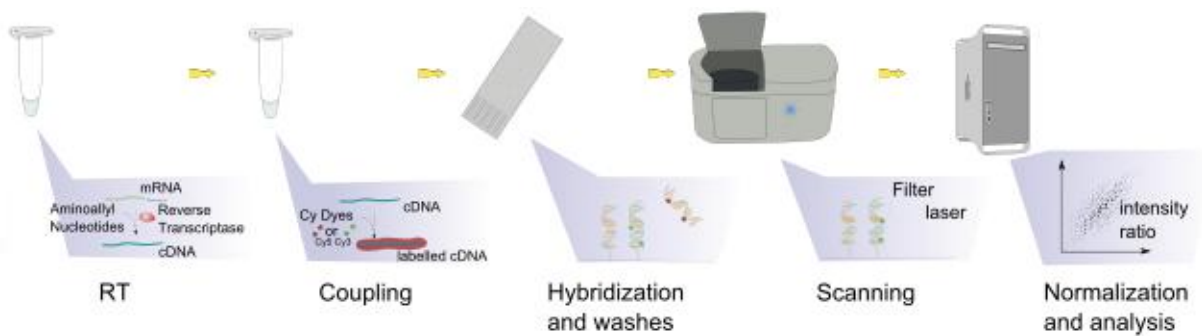
Figure 1: Steps in a microarray experiment. The nucleic acids of interest are purified and labeled by reverse transcription and/ or PCR amplification. The product is either labeled directly by typically adding fluorescent labels to the reverse transcription (RT) or PCR solution or indirectly via a post-synthetic coupling stage. The labeled DNA strands are added to the microarray where they hybridize to the complementary strands while all nonspecific sequences are washed off. The microarray is dried and scanned via laser excitation (see 3.3.11) (source: Anon).[10]

Microarrays are employed not only in research, but also in clinical analytic and are promising tools for personalized medicine and point-of-care (POC) diagnostics.[11][12][13] But proteins or health-related biomarkers, cannot be amplified prior to detection and can thus only be detected in greater amounts or need to be concentrated beforehand (see 3.3.11). These markers are so far poor candidates for POC diagnostic as this preconcentration would require several steps of laboratory work.

3.1.1 Point-of-care detection

Point-of-care (POC) diagnostic accepts a sample with little or no pre-preparation and provide the results in seconds to hours. It does not require laboratory staff and facilities and can thus be employed near-patient. Classical examples POC that are so simple that they allow diagnostic at home are strips that monitor the blood sugar levels for diabetics or pregnancy tests. Other platforms in clinics enable doctors to screen for cardiac and septic markers to ensure fast and cause specific treatment.[11]

As most health-related biomarkers cannot be amplified prior to detection an increase of their signal would allow to detect them in low concentration, as it is the case at the onset of a disease. For these, signal amplification is needed and rolling circle amplification (RCA) is a promising strategy that can enhance the detection limit in various bioanalytical formats.[14]

3.2 ROLLING CIRCLE AMPLIFICATION

3.2.1 Rolling circle replication

Small circular DNA strands, such as the human mitochondrial or bacterial genomes, employ the displacement replication to create two semiconservative copies of the genome. This involves continuous copying of one strand of the helix, the second strand being displaced and subsequently copied after synthesis of the first daughter genome has been completed.

In contrast, fast generation of multiple genome copies is achieved by rolling circle replication (RCR), a special type of displacement process.[15]

RCR is found in λ and various other bacteriophages and initiated at a nick which is made in one of the parent polynucleotides. The free 3′ end that results is extended, displacing the 5′ end of the polynucleotide. Continuous synthesis 'rolls off' a complete copy of the genome, and further synthesis eventually results in a series of linked genomes, called concatemers. These genomes are single-stranded and linear, but can easily be converted to double-stranded circular molecules by complementary strand synthesis followed by cleavage at the junction points between genomes and circularization of the resulting segments by ligation.[16]

3.2.2 Rolling circle amplification

While the Rolling Circle Replication mechanism was known since the 1970s, it was at the end of the 1990s that RCR found application in the life sciences under the name "rolling circle amplification" (RCA) when its potential was realized.[17][18] The thousands of concatemers produced can function as a platform for signal amplification in numerous detection formats if they can be equipped with a DNA primer (Figure 2).
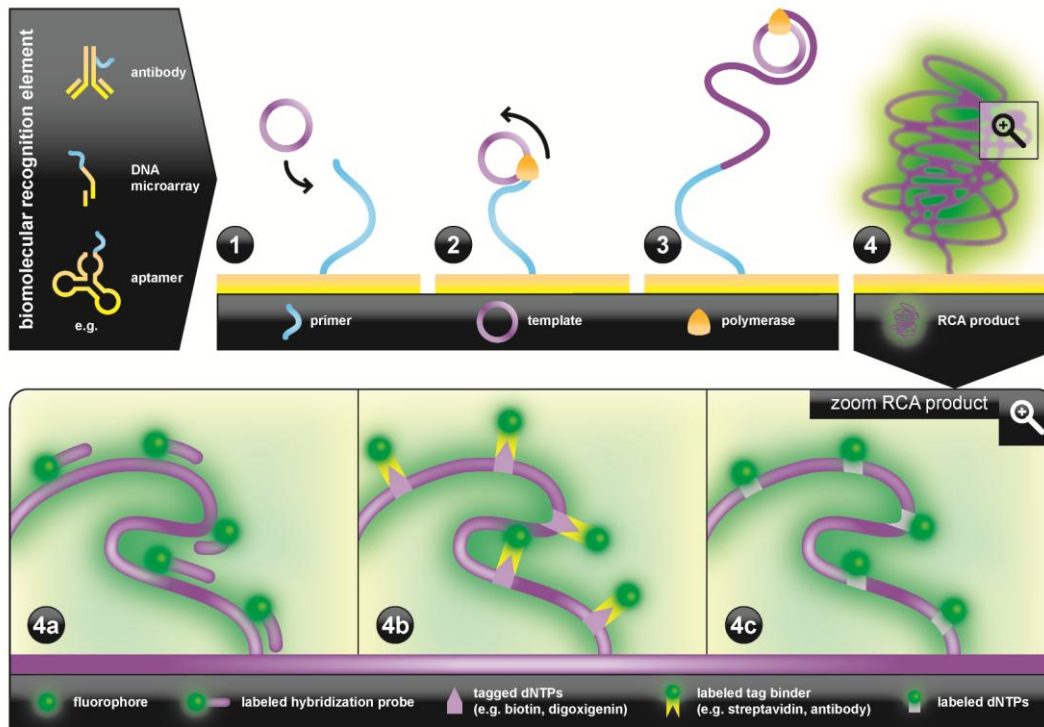
Figure 2: Signal amplification by rolling circle amplification in various biodetection formats. The circular template hybridizes to the DNA primer (1). ϕ29 polymerase binds to the double strand and initiates the RCA (2), generating a long single strand of concatemers (3). The RCA product is fluorophore labeled (4), either post-synthetically via hybridization probes to the concatemers (a), by the binding of affinity probes to tagged dNTPs (b) or directly during synthesis by the incorporation of fluorescent dNTPs into the nascent strand (source: Linck et.al).[19]

A primer binds to the circular template and replicates it, displacing the product strand, creating thousands of concatemers. It can be performed at room temperature as linear amplification with a single primer or as double primed exponential amplification, called geometric, branched, ramification, cascade or hyper-RCA. For linear amplification, the RCA product (RCP) is an extension of the DNA primer and thus tethered to whatever molecular recognition element the primer is bound. The multiple primers of the exponential RCA peel off most of the labeled strands and are performed in solution.[20][21]

While RCA can be performed with various polymerases the most commonly used is ϕ29 DNA polymerase, a mesophilic enzyme of the *Bacillus subtilis* bacteriophage ϕ29.

3.2.3 ϕ29 DNA polymerase

It has a great strand displacement ability that is crucial for the RCR of the bacteriophage and high processivity.[22][23] Its high fidelity is due to the $3' \to 5'$ proofreading exonuclease function which has been employed for whole genome replication.[24] ϕ29 DNA polymerase can produce more than 70 kb long strands per template. It has been used for cell-free amplification of DNA,[25][26] multiple displacement amplification (MDA),[27] cell-free cloning of lethal DNA,[28] and, of course, RCA.

Other polymerases have been employed for RCA as well, including thermophilic ones like Sequenase™, Klenow and Vent™ exo- enzymes, and the large fragment of Bst DNA polymerase.[29]

ϕ29 DNA polymerase and Sequenase, are considered to be most effective for performing linear RCA, while Vent exo- DNA polymerase is preferable in the exponential RCA.[29] The RCA efficiency is normally increased by the addition of proteins that bind ssDNA such as the *Escherichia coli* SSB protein.[30][31]

A number of ϕ29 DNA polymerase mutants have been produced.[22][23] As the high fidelity may hinder the incorporation of labeled dNTPs into the nascent strand, a mutant with lesser fidelity may serve the direct labeling RCA better.

3.2.4 RCA applications

RCA is a robust, simple to apply, isothermal enzymatic synthesis of a single-stranded DNA molecule from a small circular template[32] producing a strand of several hundred nanometers of length without requiring advanced laboratory equipment or experimental expertise.[18][33] Due to these properties, the rolling replication of circular DNA probes holds a distinct position in DNA diagnostics among other isothermal methods of target, probe, or signal amplification. The realization of this potential has led to a reliable strategy for probe/signal amplification in DNA diagnostics. RCA methodology provides highly sensitive and efficient contamination-resistant diagnostic assays that are capable of high multiplexity and can be used in a variety of testing formats.

RCA can be adapted to a number of detection platforms. Prerequisite is a DNA primer for the ligation and/ or polymerization that has to be conjugated to the surfaces/ molecular recognition elements desired. This has been successfully used to achieve a signal increase for DNA-microarrays[17][34], antibody-[35], aptamer-[36] and microbead-based[37] assays, and intracellular agents[38]. The detection limit was increased by a factor of 10^2 to 10^5 and the detection range usually consists of nM to fM concentrations[39]. In combination with other amplification methods, aM analyte concentrations can be measured.[40][41][42] Single molecule detection in and on cells has been reported, even multiplexed detection of several biomolecules simultaneously by employing different fluorescent reporters.[43][44]

That is why the RCA-based approaches are employed in SNP detection via padlock probes, prostate cancer tests or immuno-RCA-based proximity ligation assays.[29]

3.2.4.1 Padlock probes

RCA was first used to detect genomic sequences via padlock probes. These circularizable probes have a small gap, which is bridged by binding and ligation of a small phosphorylated oligonucleotide, or by DNA polymerase incorporation of dNTP's. The DNA target acts as the complementary primer for rolling circle amplification and the concatemers are generated (Figure 3). This allows the detection of single copies of single nucleotide polymorphisms (SNPs)[45][46][47] and *in situ* detection of DNA sequences within cell lines and tissues[17][43] with high specificity and selectivity.
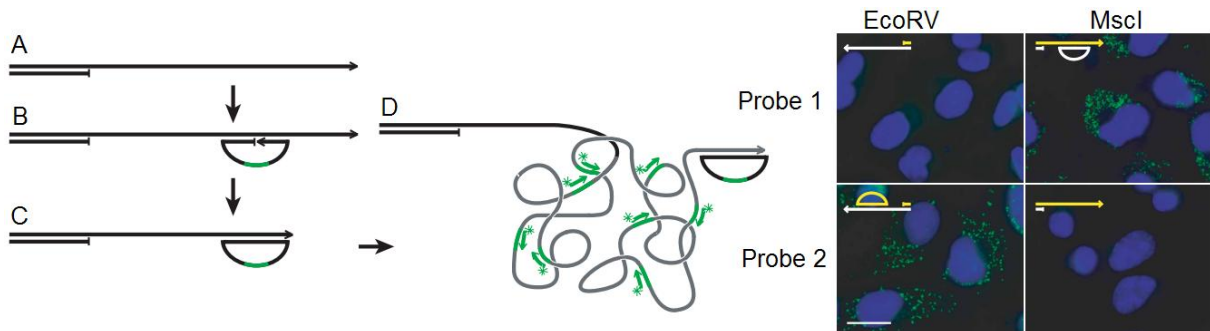
Figure 3: Padlock probe *in situ* detection. A) The single stranded DNA is the target of B) a hybridization probe and C) the probe's ends are joined through ligation. D) The RCA is initiated and the product (grey) is detected via hybridization of fluorescent labels (green). The probes (1 and 2) allow the strand-specific detection of EcoRV and MscI digestion, respectively (source: Larsson et.al).[43]

3.2.4.2 Immuno-RCA

Immuno-RCA employs antibodies (AB) that are equipped with DNA primers. To date they are the most common detection strategy that employs RCA. It is used *in situ* in tissue sections or in solid support sandwich assay to identify targets in solution or cell lysates.[7][34][48] This was employed to detect a total of 150 cytokines simultaneously[49], several prostate cancer markers[6] and in immonuhistochemistry to stain proteins in and on cells.[50]

The *in situ* immuno-RCA detection can label the target molecule directly.[50] But due to the specific need for a circular target it can also reveal protein-protein interactions via proximity ligation.[51] Here, two antibodies are applied that bind their target proteins. Secondary antibodies with DNA primers provide the scaffold for two ssDNA strands that form the circular template by ligating the strands ends. Therefore, the RCA is only initiated if these two targets are in close proximity to one another allowing the monitoring of protein interactions (Figure 4).
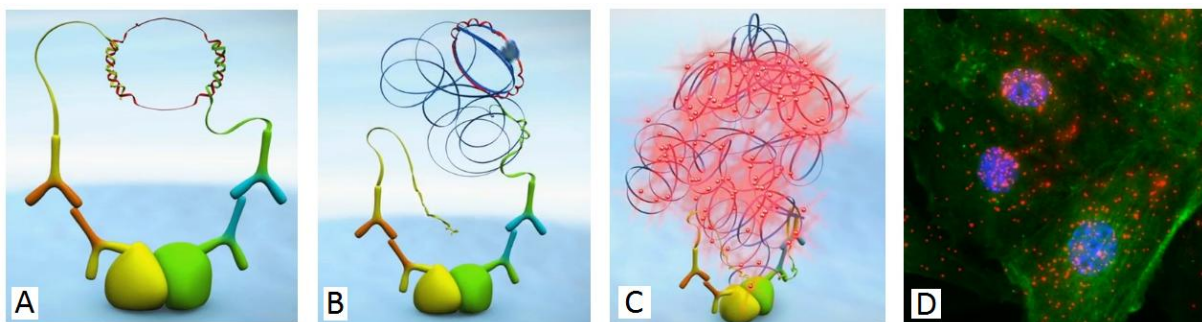
Figure 4: *In situ* proximity ligation assay. A) Two ABs of different animals (blue, orange) are incubated with their target proteins (green, yellow). The secondary ABs bind and their DNA primers function as a scaffold for two short ssDNA strands (red). They form a partial dsDNA strand with the AB's primer allowing a ligation reaction that produces the circular templatet. B) The polymerase binds to the double-stranded section of the circular template initiating the RCA. C) The RCP is post-synthetically labeled and D) can be microscopically detected (source: Olink).[51]

3.2.4.3 Aptamer-RCA

Like antibodies, aptamers bind to a target molecule with high specificity and selectivity. Unlike antibodies they are not produced *in vivo* but can be generated *in vitro.* Thus, they are offering a greater range of possible targets including potent poisons.

Aptamer-RCA can employ sandwich assays[52][53] analogue to those of antibody platforms. But due to their oligonucleotide nature the options to initiate RCA are more versatile. For proximity-dependent detection two aptamers are needed to initiate the reaction: a linear one as the RCA primer and a circular as the RCA template.[54] A structure switching aptamer can bind to the target that initiates a conformational change and promotes the formation of a ligation junction and circularizing the aptamer itself to serve as the template for RCA.[55] The aptazyme also switches conformation upon target binding but it catalyzes the DNA ligation of an added padlock probe and acts as a primer (Figure 5).[36]
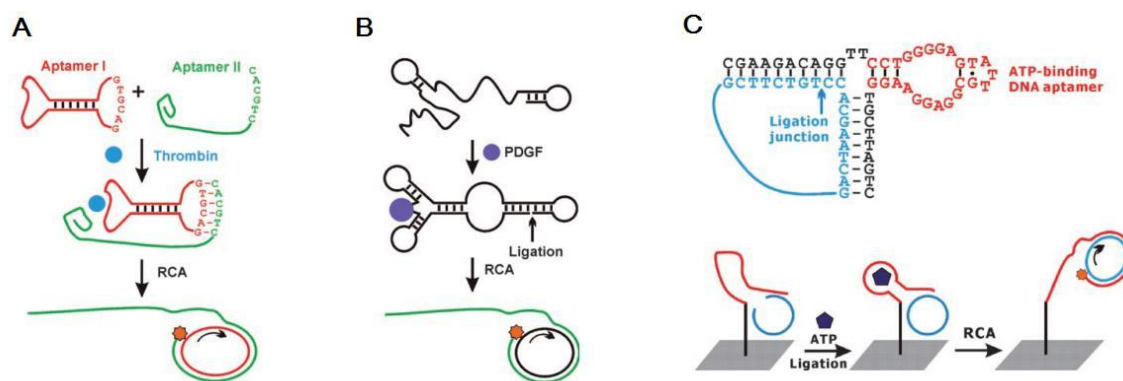
Fi

Figure 5: Aptamer RCA. A) Proximity-dependent thrombin-detection - the simultaneous binding of a thrombin molecule by a linear aptamer (which also serves as the RCA primer) and a circular aptamer (which serves as the RCA template) facilitates an RCA reaction. B) Structure switching aptamer - an assay for PDGF detection using a structure-switching aptamer. The binding of PDGF to the aptamer causes a conformational change in the aptamer and thus promotes the formation of a ligation junction. Following ligation by a DNA ligase, the circularized aptamer serves as the template for RCA. C) Aptazyme - an aptamer that catalyzes a DNA ligation reaction upon ATP binding. Black: DNA ligase, red: ATP-binding aptamer domain, blue: RCA padlock probe. The aptazyme is attached to a glass slide and activated by ATP. It ligates the padlock probe for the subsequent RCA reaction (source: Zhao et. al.).[33]

3.2.4.4 Nanostructures

RCA has also been employed for the construction of well-defined nanostructures.[56] The long single-stranded DNA molecule with periodic sequence is an attractive building block for DNA nanotechnology.[56] These can be one dimensionally or, in combination with other particles (gold, thrombine), yield three dimensional structures[33] that may be utilized as a scaffold and functionalized with nanoparticles or conductive metals.[57]

It can also be used for biosensing by generating DNAzymes, utilizing aptazyme mediated enzymatic-like reactions. RCA has been used to produce thousands of DNAzymes, which, upon the binding of hemin, mimic the functions of peroxidize allowing a photometric signal detection as employed for most ELISA assays (Figure 6).[58]
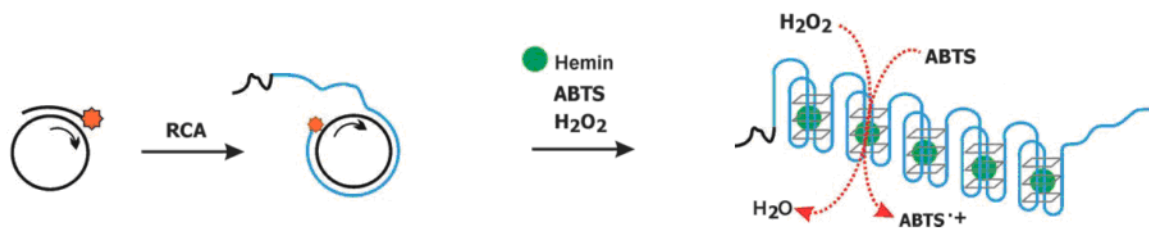
Figure 6: RCA production of DNAzymes that mimic peroxidase function and catalyse the oxidization of ABTS (source: Zhao et. al.).[33]

3.2.5 Detection and labeling strategies

The RCP can be detected electrochemically[52] by surface plasmon resonance[59], diffractometric[53] and colorimetric[48] means, but the most common detection of the RCP is via fluorescence spectroscopy.

Three techniques used to obtain a fluorescence signal are, in descending popularity: Fluorophore-labeled hybridization probes, affinity probes or dNTPs (Figure 2: 4a, b, c). Hybridization and affinity probes label the RCP post-synthetically, while dye-dNTPs allow for direct labeling during the polymerization, saving time, and handling steps.

When employing direct labeling, greater consideration has to be given to the choice of the dye-dNTPs and template design than for post-synthetic labeling.[60][61][62] Also, the most common post-synthetic labels are 5'-labeled oligonucleotides that form short dsDNA sections upon hybridization while the direct labeling strategy produces internally labeled long single strands. This can lead to changes in the spectroscopic properties for the same dye, which will be discussed in section 3.3.12.

To realize an optimal fluorescence signal, as many labels as possible should be integrated into the strand – yet, without quenching each other's fluorescence or hindering the processivity of the polymerase.[63]

3.3 SIGNAL-RELEVANT OPTICAL PROPERTIES

3.3.1 Fluorescence spectroscopy

Fluorescence has been known since the middle of the 19th century but it needed more than a century that the first spectrofluorometers were developed in the 1950's.[64] The visible spectrum usually employed for fluorescence measurements ranges from approximately 380 nm (violet) to 740 nm (red). Also the adjacent wavelengths are for used for detection, such as ultra-violet for DNA and proteins, or infra-red for molecule oscillation. Aromatic, organic dyes absorbing within this range are the most commonly employed fluorescent labels for detection.

Today fluorometric measurements are the dominant methodology used in genetic analysis, medical diagnostics, intracellular imaging, and many other fields of biochemistry.

3.3.2 Absorption and emission spectra

Any emission of light from an electronically excited state is called photoluminescence.[64] The return of an electron to the ground state from an excited singlet state is called fluorescence. Phosphorescence sees a return via a triplet state, resulting in slow emission rates due to a spin-forbidden transition. The process that occurs between the absorption and emission of energy is portrait in the Jablonski diagram (Figure 7).
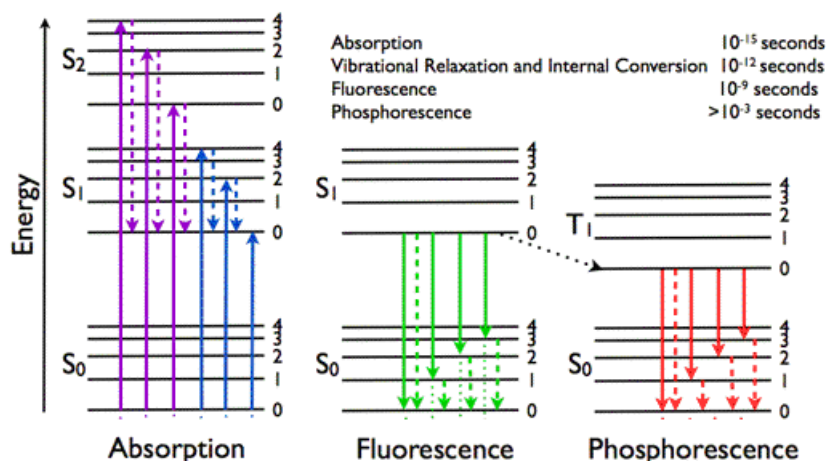
Figure 7: Jablonski diagram representing the ground state (S_0), excitation (S_1, S_2) and triplet (T_1) energy levels. Solid arrows indicate radiative transitions occurring by absorption (violet, blue) or emission (green for fluorescence; red for phosphorescence) of a photon. Dashed arrows represent non-radiative transitions (source: Rolinski A, Visser OJWG).[65]

The absorption and emission of photons is characterized by the electronic and vibrational levels individual to each fluorescent dye. These levels vary with the wavelength and result in the fluorophores individual spectra.

To obtain a corrected spectra and to quantify the spectroscopic data of these spectra a baseline, typically with the solution that the sample is dissolved in, is recorded first under the exact conditions the sample will be measured. This baseline will include all spectrometer inherent deviance at this setting and is thus subtracted from all sample spectra to eliminate these effects for future calculations.

Absorption, Transmission 0°/180°   **Fluorescence, Phosphorescence - 0°/90°**
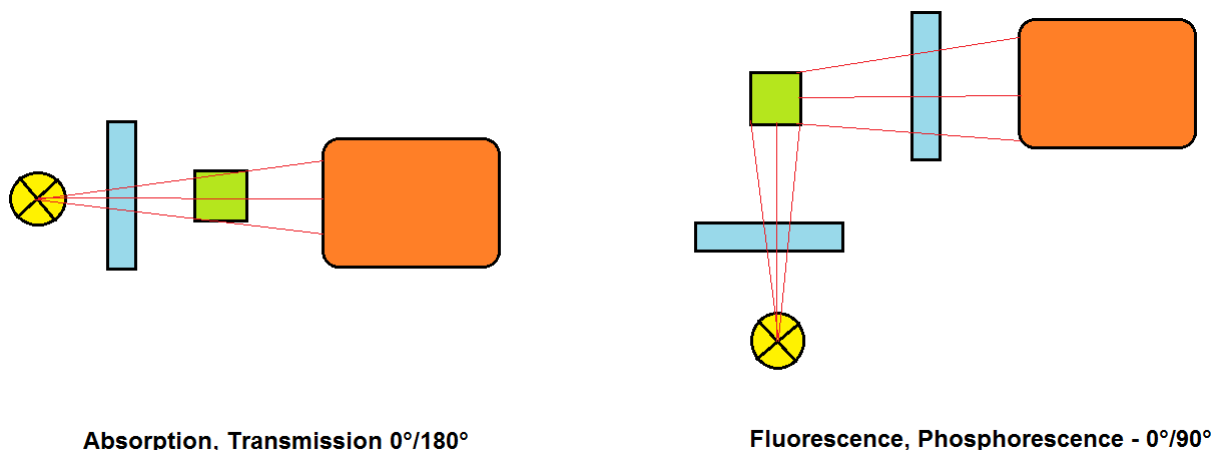
Figure 8: Measurement geometries in optical spectroscopy. Left: Absorption and transmission spectra are recorded in a 0°/180° setting, while right: Fluorescence and phosphorescence spectra are measured with a 0°/90° setting. Yellow: excitation source, blue: monochromator, green: sample, orange: photodetector, red: light pathway.(source: W.Schmidt) [66]

The spectrometers all have an excitation source like a lamp or a laser. The light passes through a prism or diffraction grating monochromator that selects a narrow band of wavelengths for the sample. The light that passed through the sample is either recorded in a straight line behind the sample for absorption and transmission spectra or in a right angle, after passing through another monochromator, for fluorescence or phosphorescence spectra. It is recorded by a photodetector that that amplifies the incoming light via photomultiplier tubes (PMT).

Absorption spectra record how much light is eliminated when the light passes through the sample in dependence of the light's wavelength (Figure 8). Emission spectra, on the other hand, excite the sample with a single wavelength and record the emission of the fluorophore in dependence of the wavelength. While in absorbance spectroscopy the the slight difference in the number of photons which pass through the sample and reference cell is detected, the emission spectra records only the photons of the fluorophore's emission.

Fluorescence spectroscopy offers more possibilities when employed for detection as more target properties can be investigated, for example via fluorescence quantum yield or anisotropy. Additionally it has a greater sensitivity allowing single molecule detection that has been on the rise over the last years.[67]

Next to the spectral position, width and shape of the fluorophore's absorption and emission bands, the Stokes shift, and the molar absorption coefficient ε are important spectroscopic features of a fluorescent label.[68] These spectroscopic properties along with the fluorescence quantum yield Φ_f, fluorescent lifetime τ and emission anisotropy r are used for the sensitive and selective detection of a broad variety of bioanalytes and provide information on dye-biomolecule interactions.[69][70][71]

3.3.3 Stokes shift
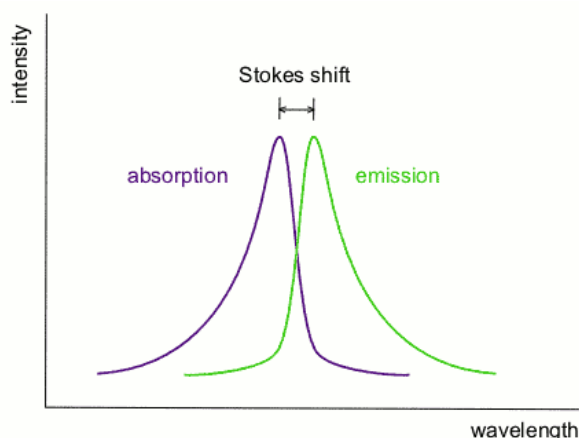
Figure 9: Stokes shift. The absorption (purple) and the emission (green) spectra are often mirroring one another, with the emission spectrum moved into the red. The distance between the respective peaks is called Stokes shift (source: Anon).[72]

The emission spectra are red-shifted as it has less energy than the absorption's spectra. This energy loss is observed universally for fluorophores in solution and is called the Stokes shift (Figure 9). A small Stokes shift results in a great spectral overlap and vice versa. For an effective collection of the emission signal a considerable separation of excitation and emission spectra is wanted.

One common cause of the Stokes shift is the rapid decay to the energy level of S_1 and S_0. In addition the fluorophore can display further shifts due to solvent effects, excited state reactions, complex formations and/ or energy transfers. This may occur when a fluorophore is bound to a biomolecule, indicating an interaction between the two.[68]

3.3.4 Molar absorption coefficient ε

The molar absorption coefficient ε is the measure of how strongly a chemical species absorbs at a certain wavelength.[64] It is an intrinsic property of the species and this wavelength specific absorption gives the spectrum of the species its characteristic form. Beer Lambert's law employs this fundamental property of ε to calculate the concentration of a solution. Most aromatic structures in biochemistry absorb light in the UV range like the DNA bases (260 nm) and the proteins amino acids tryptophan, tyrosine and phenylalanine (280 nm). The light pass is recorded before (I) and afterwards (I_0) and its log of the quotient yields the absorbance *A*, formerly also known as optical density (OD).

With the pathway length *d* and the molar absorption coefficient ε at a defined wavelength the concentration *c* can be calculated from the absorption at this wavelength (Figure 10).

$$\log \frac{I}{I_0} = \varepsilon \times c \times d = A$$
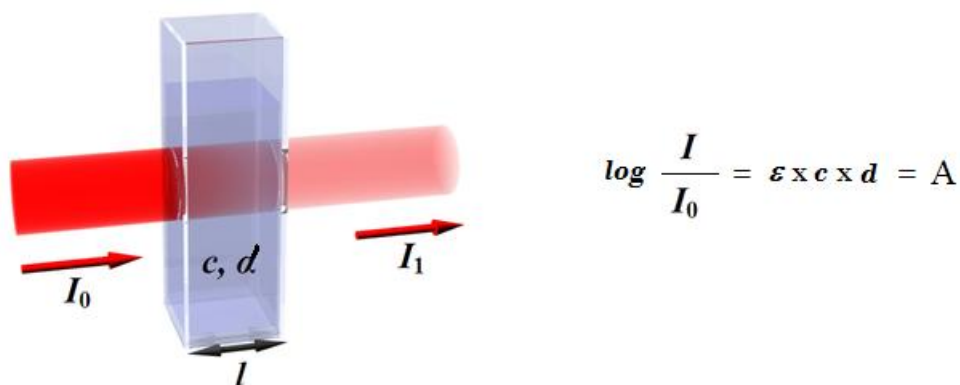
Figure 10: Beer Lambert Law. *I* is the light's intensity before and after (*I_0*) it passed through the sample. This equals the molar absorption coefficient ε, concentration *c* and pathway length *d* (source: Anon).[73]

Oligonucleotides are usually measured at their absorption maximum of 260 nm for this. For a standard cuvette of 1 cm the absorption is multiplied by a conversion factor. The conversion factors that yield the concentration in ng/ μL are 50 (*dsDNA*), *33 (ssDNA),* and 40 (*RNA).* The proteins' absorption maximum at 280 nm is used to determine the purity of oligonucleotide solutions. The ratio A_{260}/ A_{280} is calculated with 1.7 – 2.0 indicating a good purity.

3.3.5 Fluorescence quantum yield Φ_f

Fluorescence quantum yield Φ_f is the ratio of the number of emitted photons per number of absorbed photons and is independent of excitation wavelength.

$$\Phi f = \frac{\text{photons emitted}}{\text{photons absorbed}}$$

Φ_f is an important factor for the maximum signal yield one can obtain, as the brightness of a fluorophore is the product of the molar absorption coefficient ε and Φ_f at a given excitation wavelength. It presents a direct measure for the efficiency of the conversion of absorbed light to emitted light that equals 1.0 in an ideal system. But when a fluorophore absorbs a photon of light the excited state is formed it can be deactivated and return to the ground state without remitting a photon which is called fluorescence quenching.[64]

3.3.5.1 Fluorescence quenching
There are different mechanisms of quenching: internal conversion, intersystem crossing and photoinduced electron transfer (PET).[64]
Quenching is any process which reduces the lifetime τ (section 3.3.4.2), and thus decrease in the quantum yield, of the excited state of a fluorophore. It can occur by intra- or intermolecular processes.

The energy can be lost non-radiatively as heat by internal conversion, such as cis-trans isomerization, and vibrational relaxation. Due to this Φ_f of non-bridged molecules can be amplified with by an increased solvent viscosity and lowered by raising temperatures, which hampers the molecules movements.

Intersystem crossing is thought to be due to heavy atom halogens or triplet oxygen. They cause the excited single state (S_1, Figure 7) to become an excited triplet (T_1) which is then quenched, although the exact mechanism is still unknown.

PET is similar, as also an electron exchange between donor and acceptor takes place. But here a complex is formed and the fluorophore can fulfill either role. The direction of the electron transfer is determined by the oxidation and reduction potential of the ground and excited states. This charge transfer complex can return to the ground state without emission of a photon.

While one wants to avoid quenching when high signal yield is desired, this phenomenon can be also exploited as an important tool in DNA diagnostics (see 3.3.11).

3.3.6 Fluorescence lifetime τ

The fluorescence lifetime τ represents the average time a photon stays in the excited state.[64] It is an intrinsic dye property that is independent of the concentration of the fluorophore and is employed, for example, to measure component specific quantities to identify different species. The fluorescence lifetime of a molecule is very sensitive to its molecular environment and reveals much about the changes in the state of the fluorophore and can thus be used to investigate dynamic processes and gain insight into the chemical surroundings of the fluorophore. Fluorescent lifetime studies have seen a rise in application in recent years as the instrumentation has become more commercially available.[67]

The lifetime of a fluorophore in the absence of non-radiative decay is called radiative lifetime τ_0.[74] Both Φ_f and τ are diminished by this non-radiative decay or fluorescence quenching as:

$$\tau_0 = \frac{\Phi_f}{\tau}$$

This decay reaction is a photophysical reaction and due to this, the kinetics can be described as for chemical reaction.

$$k = k_F + k_N$$

The radiative rate constant k_F is a constant for the fluorophore and independent of the dye environment. k_N describes the non-radiative components, such as fluorescence quenching, that are dependend on the environment.

Lifetimes are measured with a pulsed laser that excites the fluorophore and records the time/s to return to the ground state in several cycles. Dyes with τ exceeding 1 ns enable time gated detection and can greatly reduce background radiation, such as scattered excitation light and short-lived fluorescence, such as biological components whose lifetimes are in the µs range (Figure 11).[75] Distinguishing different τ and eliminating unwanted background is also employed in biodetection formats (see 3.3.11).
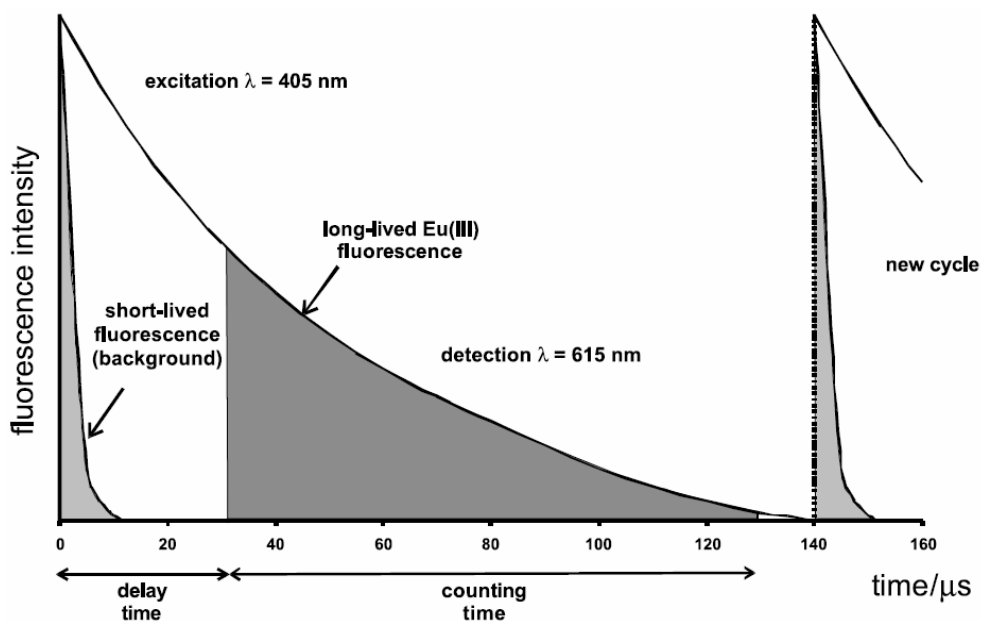
Figure 11: Schematic presentation of the gated (time-resolved) detection of EuTc-HP. The laser impulse excites the fluorophore generating a short-lived lifetime that is mostly background radiation, for example from buffer components or cell organelles. Therefore, a delay time is set in which the signal is not recorded and the background thus omitted. The counting time then allows to solely detect the fluorophores signal (source: Lei W et.al.).[76]

3.3.7 Emission anisotropy r

The emission anisotropy r is the measure for the polarization dependence of the emission of a fluorophore and presents a common tool to evaluate its rotational freedom.[64] Measurements of r are also often used to study energy transfer processes that are known to result in a change in emission anisotropy.[77] To measure r the sample is excited in two perpendicular measurements - the excitation polarizer is set to 0° while the emission polarizer records 0° and 90°.

$$r = \frac{F_{0°/0°} - F_{0°/90°}}{F_{0°/0°} + 2F_{0°/90°}}$$

When a fluorophore is attached to a larger molecule, such as DNA strand or proteins, r increases due to the restricted rotational freedom resulting in different values for the perpendicular measurements.[78] Conformational changes, such as protein folding or in DNA hybridizations, also alter r.

Although, principally, *r* can provide information on dye mobility care must be taken as *r* also depends strongly on fluorescence lifetime τ.[79][80] If τ increases, often accompanied by an increase in Φ_f, the fluorophore emits its fluorescence over a longer time span. A time, in which the molecule the fluorophore is attached to can travel or rotate more, thus giving the impression that *r* is smaller. Homo-FRET will also cause a decrease in *r* (see 3.3.8).

3.3.8 Fluorescence Resonance Energy Transfer

Fluorescence Resonance Energy Transfer (FRET) occurs between a donor in the excited state and an acceptor in the ground state when the donor emits a shorter wavelength that overlaps with the longer absorption spectrum of the acceptor (Figure 12).[64][81] This energy transfer takes place without radiation loss and is proportional to the 6th power of the distance between the molecules, called Foerster radius. Therefore, the two molecules need to be very close to each other (2–7 nm) and already minor conformational changes can induce or eliminate FRET giving information on their interactions. Universal FRET tags allow multiplexing, for example in nucleic acid sequencing the read out of four different acceptors, one for each DNA base, with only one excitation wavelength was accomplished by utilizing a donor common to all four of then.[82]
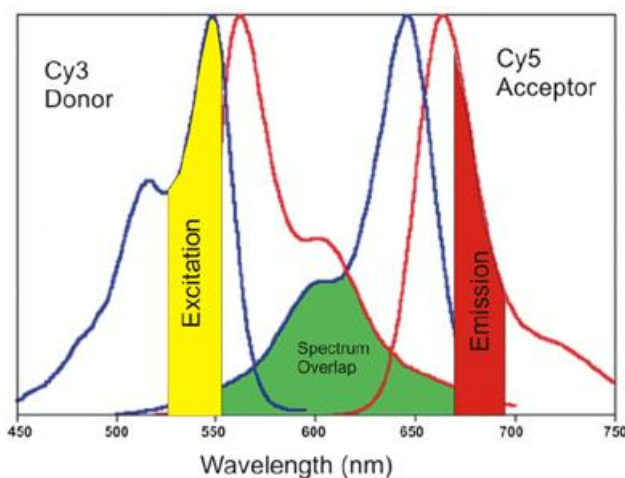
Figure 12: Fluorescence resonance energy transfer (FRET). Spectrum overlap (green) of Cy3 as the donor and Cy5 as the acceptor dye. The typical excitation (yellow) and emission (red) windows are given for the absorption (blue line) and emission (red line) spectra (source: Biotek Instruments).[81]

The two molecules engaging in FRET do not need to be two fluorophores or different molecules. In the first instance the acceptor may be a quencher that suppresses the fluorescent signal until it is separated from the donor as in real-time PCR probes (see 3.3.11). Homo-FRET takes place between chemically identical molecules which typically occurs for fluorophores with small Stokes shifts.[64] Energy is lost as well in this transfer and is the reason that biomolecules labeled with fluorophores do not become more fluorescent with higher degrees of labeling. The homotransfer can be detected by a decrease in *r* as the energy transfer and depolarization rate is fast compared to the rotational time of the biomolecules.

3.3.9 Photostability

An excellent photostability is required for fluorescence techniques using intense excitation light sources, such as lasers or laser diodes as are used for microarray experiments or microscopic readouts. This allows frequent remeasuring of the sample without signal loss and permits longer exposition times to collect more photons and thus yield a higher signal. But virtually all fluorophores are photobleached upon continuous illumination due to excited state reactions that yield non-fluorescent products.[64] The photostability of a dye can be affected by its local environment. In some cases it is increased by removal of oxygen, in others it has no effect. There seems to be no general principle to predict photostability. The photostability of Cy5 on DNA microarrays is strongly improved by the removal of ozone in the atmosphere while the structurally very closely related Cy3 is not affected by it.

3.3.10 Fluorophores

Fluorophores absorb energy of a specific wavelength and re-emit it at a different wavelength. The relevant spectroscopic features of a fluorescent label are the absorption and emission spectra, the Stokes shift, molecular absorption coefficient, fluorescence quantum yield, lifetime and anisotropy.

Classical fluorophores are aromatic molecules that have been known and studied since the 19th century.[64] Next to the classical aromatic dyes like cyanines, rhodamines or oxaxines, two new sets of fluorophores have been developed in the last twenty years: quantum dots and fluorescent proteins (Figure 12).[68][83]

Quantum dots (QDs) are luminescent semiconductor nanocrystals with 2 – 10 nm, composed of elements such as Cd, Zn, Se, Te, In, P and/ or As. They are fluorescent and the emission wavelength is size tuneable, decreasing with decreasing particle size due to an increase in the semiconductor band gap with decreasing size.[84] They have an excellent photostability, higher fluorescence quantum yield, larger Stokes shifts, longer fluorescent lifetimes, and narrow, symmetric emission bands than traditional organic fluorophores.[85]

The fluorescent proteins like green fluorescent protein (GFP) from the bioluminescent jellyfish can be incorporated into proteins by genetic fusion. Chimeric GFPs can be expressed *in situ* by gene transfer into cells and localized to particular sites with appropriate targeting signals, thereby allowing imaging of a range of biological events.[86] Various GFP-like proteins (e.g. Verde fluorescent protein, VFP) have been designed and are covering other ranges of the spectrum as well.
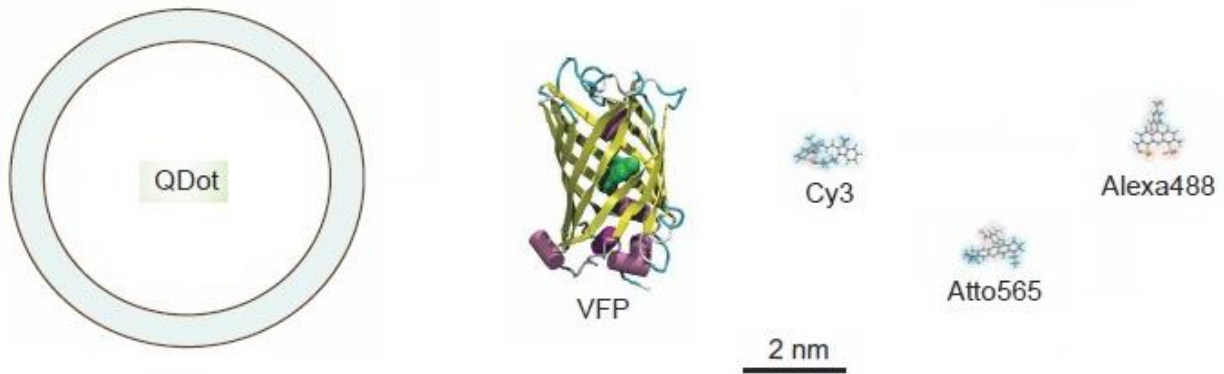
Figure 13: Comparative sizes of common fluorophores. From left to right: Quantum dot (QDot), Verde fluorescent protein (VFP), organic dyes (Cy3, Atto565, Alexa488) (source: Jares-Erijman EA, Jovin TM).[87]

The comparison of fluorophore sizes shows, that quantum dots and fluorescent proteins must be ruled out for direct enzymatic labeling as their size exceeds that of DNA polymerases. Additionally, labeled nucleotides are only available with small aromatic dyes (co-synthetic labeling) or biotin (post-synthetic labeling).

3.3.11 Fluorescence spectroscopy in biodetection

The sensitivity of fluorescence and its spectroscopic properties described above make it valuable for many applications in biochemistry of which a few will be presented here.

3.3.11.1 DNA microarrays

DNA microarrays identify the activity of genes under regular and altered condition, such as disease or stress, fast and efficiently (Figure 14).

For a gene expression profile microarray, the wild-type/ healthy and the altered/ ill mRNA is extracted and fluorescently labeled. The cDNA is incubated competitively and read out at two different wavelengths according to the applied dyes, usually red and green. The pixels of the spots of each scan images and the ratio of the two hybridized samples on the spot are quantified.
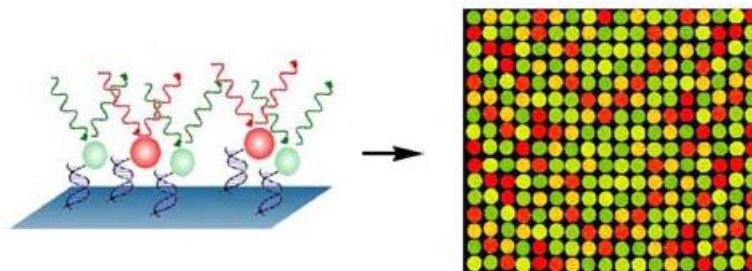
Figure 14: Differential gene expression microarray. DNA samples labeled with a green and a red fluorophores, representing the wild-type and altered respectively, are incubated competitively (source: Schäferling et. al.).[88]

3.3.11.2 Reporter-quencher probes

TaqMan probes and molecular beacons are both short oligonucleotides used for the real time detection of their target sequence to which they hybridize by using the interaction of fluorophores and quenchers.

TaqMan probes is used to quantify the exponential increase during the PCR amplification reporter.[89] The probe has fluorescent reporter dye on the 5' and a quencher at the 3' ends that are in close proximity. When intact, the reporter's fluorescence is quenched but during the PCR cycle the probe hybridizes to the target sequence and is digested by enzyme's 5'-3' exonuclease activity. This releases the reporter dye from the quencher quenching effect, and the fluorescent light from reporter dye can be detected (Figure 15, left).

Molecular beacons employ the same mechanism as TaqMan probes but the DNA strand is not digested in order to separate reporter and quencher to yield a signal. The length of 18-30 base pairs (ca. 6 – 10 nm) spaces the two so far apart that the quencher would not prevent fluorescent dye from emitting light. But the last base pairs of either end are complementary forming a loop and positioning the reporter and quencher next to each other. Only when the beacon binds to its target sequence the probe is unfolded to a linear form and a signal can be detected (Figure 15, right).
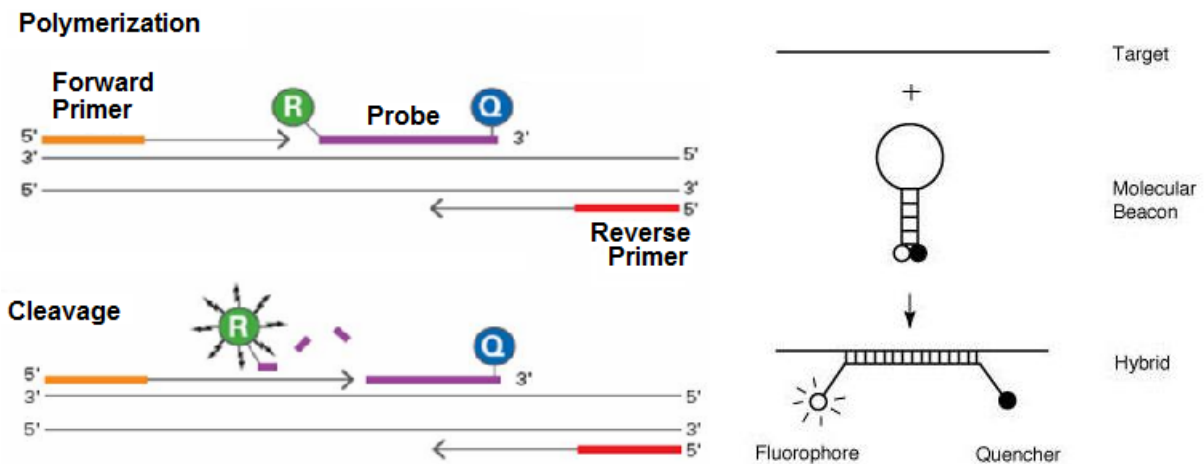
Figure 15: Reporter-quencher probes: The TaqMan probe (left), molecular beacon (right) (Source: Applied Gene)[90]

3.3.11.3 Intercalation dyes

To detect unspecific double stranded oligonucleotides intercalation dyes are often used. But unlike the reporter-quencher probes these dyes are initially almost fluorescent because the energy is lost non-radiatively (see 3.3.5). Binding to the DNA double strand restricts the torsional movements of a flexible non-bridged bonds in the fluorophore and blocks these channels. Ethidium bromide displays a 20-fold and TOTO-1 even a 1,100-fold fluorescence enhancement upon binding to DNA (Figure 16).[91]
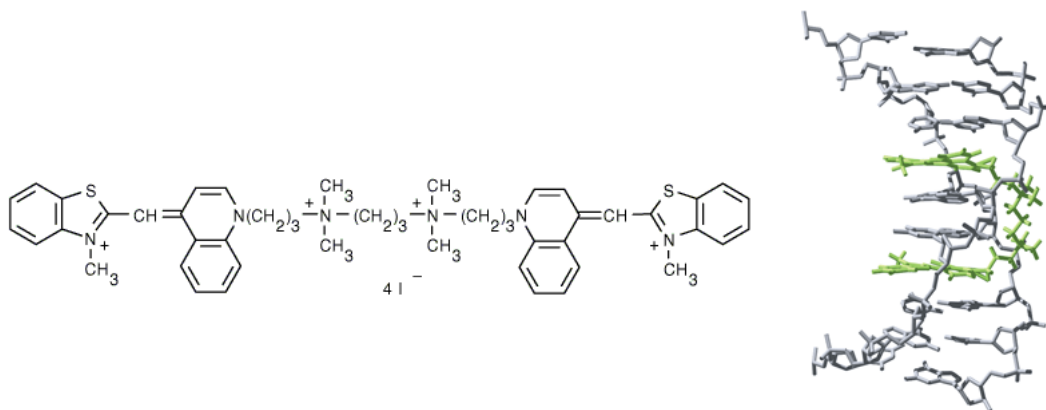
Figure 16: Left: Chemical structure of TOTO-1. Right: TOTO-1 (green) intercalated within the DNA double helix (gray)(source: Invitrogen).[92]

3.3.11.4 Signal enhancement strategies

Analyte concentrations are generally low and need to be amplified prior to detection. This can be accomplished by label- or enzyme-based amplification strategies.

Label-based strategies attach multiple fluorophores to the target molecule which limited by the available reaction sites, for example lysine residues, and the dye's self-quenching if they are too close together. Polymer particles require one reaction site but can carry multiple dyes, inside or on the surface, in a concentration that prevents or minimizes self-quenching.[93][94][95]

Enzyme-based strategies include PCR or ELISA assays. PCR amplifies the signal by increasing the analyte concentration of DNA available for labeling. ELISA assays increase the signal by generating fluorescent molecules form non-fluorescent precursors within the solution, usually via alkaline phosphatase or horseradish peroxidase.

RCA combines both strategies although the target molecule is neither amplified nor labeled itself. Instead it is "labeled" with a DNA primer that will be amplified and the generated strand acts as a scaffold for either direct or post-synthetic labeling.

3.3.12 5'-labeling and internal DNA labeling

DNA can be chemically or enzymatically synthesized. Commercially available oligonucleotides are chemically synthesized and can be ordered with various modifications. 5'-modifications are the most common (and inexpensive) and thus mostly 5'-labeled oligonucleotides are used in detection.

Building the DNA strand enzymatically with a polymerase sets limits to possible modifications, as they have to be attached to the dNTPs to be integrated into the nascent strand. Small molecules, like biotin or fluorescent dyes, are usually bound to the bases via an amino linker. 5'- and 3'-linker are used to couple the strand to proteins or to the surface of DNA microarrays (Figure 17).
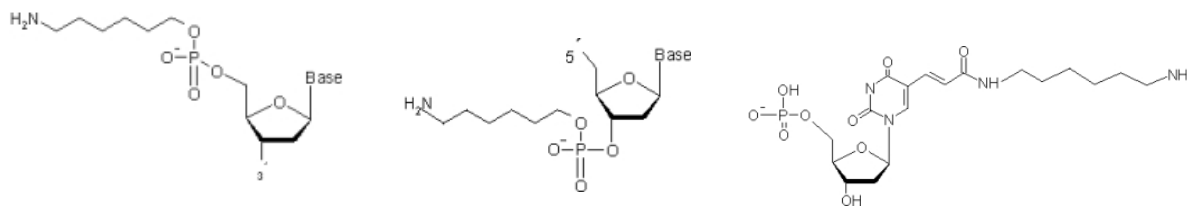
Figure 17: Modified nucleotides with an amino linker. From left to right: 5'-, 3'- amino link and amino-dT. The amino linker allows coupling other molecules to the dNTPs (source: Biomers). [96]

Systematic studies focusing on a methodical dye comparison are few and are usually on chemically synthesized 5' bound fluorophores.[97][98][99] But enzymatic labeling, as in polymerase chain reaction (PCR) or direct labeling RCA, result in internal fluorophores.[100][101][102] The position of the dyes in the DNA strand can alter their spectroscopic properties.

Cy3, for example, has an increased fluorescence quantum yield Φ_f when attached to DNA because the *cis-trans* photoisomerization of the double-bond bridge is restricted via nucleotide stacking. The aromatic bases of the DNA interact with one another via π-stacking and can also stabilize other molecules, like fluorophores, in their neighborhood via this mechanism. The Φ_f, however, can increase by a factor of two from internal to 5'-labeling.[97] This has been known to lead to a flawed interpretation of the results, i.e. for FRET calculations.[103]

4 AIM OF THE PROJECT

The goal of this work is to develop a rolling circle amplification (RCA)-based detection protocol applicable to various detection platforms that reduces handling and reaction time efficiently with reduced costs while providing a great signal yield. This technique can be valuable for formats that require simple and/or automated, as well as a sensible, target detection, for example, in point-of-care diagnostics.

The signal shall be produced *in situ,* rendering previous amplifications steps, such as PCR, unnecessary and enabling the analysis of low amounts of sample that could not be amplified prior to detection (proteins, antibody targets).

Seven fluorophores of different dye classes are investigated to optimize the signal yield in RCA-based assays and to gain maximum fluorescence with a minimum amount of dye molecules. They are chosen to spectrally resemble Cy3, the most commonly used green excitation dye in biodetection formats.

Before designing the RCA assay, various fluorophores were investigated to determine which has the most favorable properties for the cause: High fluorescence quantum yield, absorption/emission features with a minimum sensitivity to the dye's microenvironment, and good photochemical stability. Furthermore, a fluorescence lifetime well above the signal for the scattered excitation light for potential detection with time-resolved fluorescence for multiplexed real-time detection and low costs of material are desired. In order to choose the dye, the fluorophores were measured in six microenvironments: Free dye, dye-dUTP, ssDNA and dsDNA strands - single- and triple-labeled, with a previously optimized fluorophore distance, using steady-state and time-resolved fluorometry.

The most suitable dye is then used for a signal amplifying RCA on a DNA microarray via dye-dUTPs in a direct labeling protocol. Different parameters of standard post-synthetic labeling RCA protocols are optimized toward a simpler and more effective signal generation.

If the procedure is successful it will also applied out on an antibody microarray to portray the feasibility of applying this protocol to other RCA-based platforms.

5 MATERIAL AND METHODS

5.1 DNA SAMPLE PREPARATION

5.1.1 Linear sample preparation

The oligonucleotide sequences for the experiments with linear samples were obtained from Integrated DNA Technology. To investigate the enzymatically integrated dye-dUTP two 91 mer templates were designed, one single and one triple labeled. Based on previous studies with Cy3 the three integration sites for the fluorophores were spaced 10 bases apart to avoid dye-dye-quenching.[9] 5'-Phosphate allowed digesting the dsDNA to ssDNA after it had been spectroscopically measured.

The bold **A**'s indicate the labeling site for the dye-dUTPs in the complimentary strand synthesized by φ29 DNA polymerase from New England Biolabs.

Template 1A 5'-Phosphate	5' - TG CCT TTC CGT GCC TTT CCG TGC CTT TCC GTG CCT **A**TC CGT GCC TTT CCG TGC CTT TCC GTG CCT TTC CGT TC CAT CCG CGT CTG CAG TCT – 3'
Template 3A 5'-Phosphate	5' - TG CCT TTC CGT GCC TTT CCG TGC CT**A** TCC GTG CCT **A**TC CGT GCC T**A**T CCG TGC CTT TCC GTG CCT TTC CGT TC CAT CCG CGT CTG CAG TCT – 3'
Linear primer	5' – AGA CTG CAG ACG CGG ATG GA - 3'
Cy5 primer 5'-Cy5	5' – AGA CTG CAG ACG CGG ATG GA - 3'

The unlabeled dNTPs were purchased from Fermentas. 100 pmol of the 5'-phosphorylated templates was incubated in 100 µL with 100 pmol primer, dATP, dCTP, dGTP (1 mM each), dye-labeled dUTP (1 µM), and 10 U φ29 DNA polymerase in φ29 DNA polymerase buffer (50 mM Tris-HCl, 10 mM MgCl$_2$, 10 mM (NH$_4$)$_2$SO$_4$, 4 mM dithiothreitol; pH 7.5 at 25±1°C) for 16 h at 37 °C.

The dye-labeled dUTPs were obtained from Dyomics (DY-547, DY-548, DY-549, DY-555), Invitrogen (BODIPY-FL), and GE Healthcare (Cy3). All dye-labeled dUTPs were chosen to have a C6 spacer. For the Cy3B systems, Cy3B-NHS was purchased from GE Healthcare. The Cy3B-NHS was hydrolyzed to obtain the carboxylic acid for the measurements with the free dye. Coupling of Cy3B-NHS to dUTP and subsequent HPLC clean up was performed by IBA. To obtain labeled ssDNA, the dsDNA was incubated with λ-exonuclease from Fermentas according to the manufacturer´s protocol.

5.1.2 DNA clean up

The DNA clean up was performed with NucleoSpin Extract II from Macherey-Nagel. For the dsDNA samples NT buffer and for the ssDNA NTC buffer was used.

200 µL NT or NTC buffer were added to the reaction solution of 100 µL and transferred to the spin columns. The loaded samples were centrifuged for 30 s at 11,000 x g and the flow-through discarded. The column was washed with 600 µL NT3 buffer by centrifuging it for 30 s at 11,000 x g. The flow-through was again discarded and the column dried for 30 s at 11,000 x g. For elution the column was placed in a fresh 1.5 mL reaction tube and incubated with 15-50 µL buffer NE for 1-2 min and centrifuged for 1 minat 11,000 x *g*.

5.1.3. Gel electrophoresis

Gel electrophoresis is a widely used method to check quality, analyze samples and/ or purify oligonucleotides or proteins. The gel matrix functions as a sieve separating the samples by size, shape and charge by an electrical field. The smaller, more (positively) charged and linear a molecule is the faster it migrates towards the anode.

To neutralize the effects of secondary structures in nucleic acids denaturing gels with urea are used that do not allow for the formation of dsDNA and gives the strands a homogenous charge. Thus, they are separated by their length only resulting in various bands of the separates species that then need to be stained in order to make them visible, e.g. by ethidium bromide or SYBR dyes.

Successful circularization of the ligated template for RCA and the digestion of the unligated ssDNA strand was controlled by running the samples on a 15% PAA gel with 7M Urea, acrylamide/ bis-acrylamide (19:1) (Sigma-Aldrich). The gel was run in TBE-buffer (89 mM Tris, 89 mM Borate, 2 mM EDTA, pH 8.3; Merck) for 30 min at 200V before loading the samples in urea loading buffer (8M urea, 20 mM EDTA, 5 mM Tris-HCl, 0.5% (w/v) xylene cyanol, bromphenole blue, pH 7.5) and the Gene Ruler Ultra Low Range DNA Ladder (Fermentas) in 6x Loading buffer (0.03% Bromphenolblue, 0.03% Xylencyanol, 60% Glycerol, 10 mM Tris-HCl (pH 7.5), 60 mM EDTA (pH 8.0) (Fermentas).
 It was then run for further 2h. SYBR Green II (Invitrogen) staining in TBE buffer was carried out for 20 min while shaking gently. The read out was carried out with the GeneDoc X gel documentation system (Biorad).

5.2 SPECTROSCOPIC AND PHOTOPHYSICAL STUDIES

5.2.1 Absorption and Emission Measurements

All samples were measured at 25±1 °C in 1cm-quartz microcuvettes from Hellma using the DNA buffer (10 mM NaPi, 250 mM NaCl, pH 7.2) as solvent. All spectroscopic measurements were performed at least in triplicate. The absorption spectra were recorded on a CARY 5000 spectrometer (Varian Inc.). Fluorescence measurements were performed with a Spectronics Instruments 8100 (Spectronics Instruments Westbury) spectrofluorometer (Figure 18) equipped with Glan Thompson polarizers in the excitation and emission channel (set to 0° and 54.7°, respectively), that was previously calibrated with physical transfer standards.[104] The emission was excited at the blue vibronic shoulder of the dye's longest wavelength absorption band using absorbances of 0.05 to 0.10 at the excitation wavelength. All fluorescence emission spectra were corrected for scattering and autofluorescence from the solvent and dark counts from the detector (blank correction) as well as for the wavelength- and polarization-dependent spectral responsivity of the fluorometer´s detection system.[105]
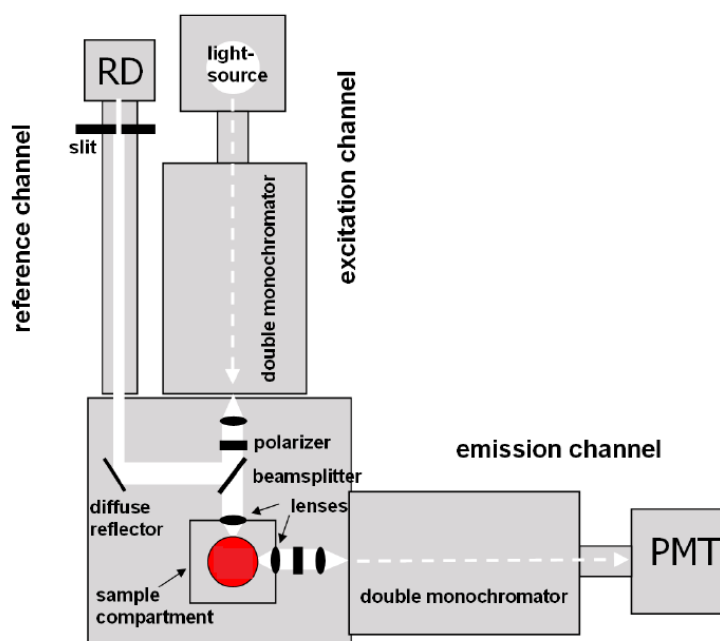
Figure 18: Spectronics Instruments 8100 fluorescence spectrometer. The light of the excitation channel is divided by the beamsplitter and directed towards the sample (red) and the reference detector (RD). The fluorescent light is collected in right angle to the excitation and direct to the photomultiplier tube (PMT) via the emission channel (source: Wuerth C et.al.).[106]

5.2.1.1 UV quantification (linear samples)

The absorption spectra were recorded in 130 μL DNA buffer with a CARY 5000 spectrometer (Varian Inc.). The DNA concentrations were calculated according to Beer Lamberts Law by multiplying A_{260} with the dilution factor and 50 ng/ μL (dsDNA) and 33 ng/ μL (ssDNA), respectively (Figure 10)
Purity of the oligonucleotide clean-up was determined by the ratio A_{260}/ A_{280} which should be 1.7 – 2.0.

5.2.1.2 UV quantification (circular samples)

For the circular samples, 1 μL volume was used for measuring the absorbance at 260 nm with a Nanodrop spectrophotometer ND-1000 (Peqlab). After calibrating the spectrometer with water, NE buffer was applied as blank that would be subtracted from all following measurements. The template concentration was determined in NE buffer directly after elution. 1 μL of the NucleoSpin Extract II the sample was applied and measured triplicate. The calculations of oligonucleotide concentration and purity were analogue to those for the linear samples.

5.2.2 Fluorescence quantum yield Φ_f

The fluorescence quantum yields Φ_f of the fluorophore systems were determined according to equation 1,[64] following a previously described procedure.[106]

$$\Phi_{f,x} = \Phi_{f,st} \times \frac{F_x}{F_{st}} \times \frac{f_{st}(\lambda_{ex})}{f_x(\lambda_{ex})} \times \frac{n_x^2}{n_{st}^2} \qquad \text{(eq. 1)}$$

In equation 2, $f(\lambda_{ex})$ is the absorption factor at the excitation wavelength λ_{ex}, F is the spectrally integrated photon flux $q_p(\lambda_{em})$ at the detector, i.e., the area under the emission spectrum $I_c(\lambda_{ex},\lambda_{em})$ corrected for blank emission and the wavelength dependence of the instrument´s spectral responsivity that has to be multiplied with λ_{em} prior to integration (see equation 2) to account for the energy of the emitted photons. *n* is the refractive index of the solvent(s) used.
The subscripts *x* and *st* denote sample and standard, respectively: rhodamine 101 (Φ_f = 0.90 in ethanol) for the cyanine and rhodamine dyes (λ_{ex} = 525 nm) and relative to fluorescein (Φ_f = 0.79 in 0.1 M NaOH) for BODIPY FL (λ_{ex} = 480 nm).[106] A a refractive index of 1.333 for the DNA buffer was used.

$$F = \int_{\lambda_1}^{\lambda_2} q_p(\lambda_{ex},\lambda_{em})d\lambda_{em} = (hc_0)^{-1}\int_{\lambda_1}^{\lambda_2} I_c(\lambda_{ex},\lambda_{em})\lambda_{em}d\lambda_{em} \qquad \text{(eq. 2)}$$

5.2.3 Photostability studies

The photostability studies were performed with dye-dUTP solutions: 300 µL sample volume, concentration of the dye-labeled dUTPs of 0.1 pmol/µL, DNA buffer in cuvettes with an optical path length of 1 mm. A 150 W Xenon lamp-monochromator assembly equipped with two detectors was used, one for measuring the light-induced changes in absorbance of the sample and one for controlling the stability of the lamp's output. An illumination wavelength (λ_{ill}) of 525 nm and a spectral irradiance of 1.52 ± 0.02 mW/cm² was used for Cy3, DY-547, DY-548, DY-549, Cy3B, and DY-555 and an illumination wavelength of 480 nm and a spectral irradiance of 1.35 ± 0.01 mW/cm² for BODIPY FL, respectively. The spectral bandwidth of the monochromator was set to 15 nm. The illumination light was cumulated inside the cuvette yielding an area of 1.5 cm² of the illuminated spot. All the samples were illuminated for 1000 min at a constant temperature. The absorption spectra of the samples were measured before and after illumination to calculate the percentage of photobleaching.

5.2.4 Emission Anisotropy r

For measurements of the emission anisotropy *r*, the samples were excited with the excitation polarizer set to 0° and the resulting fluorescence intensities were measured for emission polarizer settings of 0° and 90°, respectively. The emission anisotropy was calculated from blank and spectrally corrected integrated emission spectra according to equation 3.

$$r = \frac{F_{0°/0°} - F_{0°/90°}}{F_{0°/0°} + 2F_{0°/90°}}$$
(eq. 3)

5.2.5 Time-resolved Fluorescence Measurements

Fluorescence decay curves were measured with the FluoTime200 time-resolved spectrometer from Picoquant equipped with a PMA182 detector, a PicoHarp300 TCSPC module and a PDL800-B laser driver. The cyanine and rhodamine dyes were excited with a LDH-P-FA-530 green diode laser based on a master-oscillator fiber-amplifier (MOFA) concept with frequency conversion (531 nm, >50 ps FWHM (full width at half maximum) optical duration); BODIPY FL was excited with a LDH-P-C-470 gain switched picosecond laser diode (466 nm, 70 ps FWHM optical duration). 10,000 photon counts in the peak of the histogram were collected per measurement. The instrument response function (IRF, FWHM < 200 ps) was determined and accordingly considered for the analysis of the measured fluorescence decays.

The decay curves were analyzed by means of the FluoFit Pro software from Picoquant that implements global analysis using nonlinear reconvolution fitting.

The quality of the fits was judged by the value of χ^2 and by the randomness of the weighted residuals and further evaluated by support plane analysis as implemented in FluoFit Pro.[64] If a monoexponential model was not adequate to describe the measured decay, a multiexponential model was used to fit the decay.

All mean or average fluorescence lifetimes τ_{av} were calculated according to equation 4.

$$\tau_{av} = \frac{\sum_i a_i \times \tau^2_i}{\sum_i a_i \times \tau_i} \qquad\qquad \text{(eq. 4)}$$

τ_i and a_i represents the single lifetimes and amplitudes, respectively, contributing to the intensity-weighted average fluorescence lifetimes τ_{int}.

The relative amplitudes in % for each decay component or fluorescence lifetime given in Tables 2 and 3 were calculated according to equation 5 dividing the single amplitudes a_i by the sum of all amplitudes Σa_i of the sample

$$A_i = a_i / \Sigma a_i \times 100\% \qquad\qquad \text{(eq. 5)}$$

5.3 MICROARRAY STUDIES

5.3.1 DNA sequences for microarray studies

All DNA sequences for the RCA studies on microarrays were purchased from Biomers.

Primer *cF5* 5'-Aminolink C12	5'-<u>CTT ATC GCT TTA TGA CCG GAC C</u>-3'
Primer *cRCA15* 5'-Aminolink C12	5'- <u>TCA AGC CAG ACG AAC TCA AGC C</u>-3'
Control *F-prim* 5'-Cy3	5'-AAA AAA AAA – 3'
Template *RCA15* 5'-Phosphate	5'-GTT CGT CT <u>GGC TTG AGT TCG TCT GGC TTG A</u> GTT CGT CTG GCT TGA GTT CGT CTG GCT TGA **GCC TGC GTC GTT TA**-3'
Template *F1F9F10F5* 5'-Phosphate	5'-**CCT GCG TCG TTT A** AG GAA GTA CGT GGA AAG TGG CAA TCG TGA AGG GAC GAA TAC AAA GGC TAC ACG <u>GGT CCG TCA TAA AGC GA</u>TAA **G**-3'
Hybridization probe *Hyb-Cy3* 5'-Cy3	5'-**GCC TGC GTC GTT TA**-3'
Primer *Antibody-primer* 5'-Link to AB	5'-AAA AAA AAA AAA AAA GAC GAA TCG ATA CCA C-3'
Hybridization probe *AB-Cy3* 5'-Cy3	5'-GTG GTA TCG ATT CGT CTT TTT TTT TTT TTT T-3'

5.3.2 Ligation and RCA reaction

The ligation and RCA reactions were carried out according to the instructions of the supplier of the enzymes and the literature. [56][107]

5.3.2.1 Ligation

Per 20 µL reaction volume: 20 pmol DNA template, CircLigase II buffer (0.033 M tris-acetate, 0.066 M potassium acetate and 0.5 mM DTT, pH 7.5), 2.5 mM MnCl$_2$, 1 M Betaine, 100 U CircLigase II (Epicentre); 2 h incubation at 60°C and inactivation for 10 min at 85°C. Addition of 60 U exonuclease I (Fermentas) and 1h incubation at 37°C and inactivation for 15 min at 80°C.

The template was cleaned-up with the Macherey Nagel NucleoSpin Extract II Kit (NTC buffer). The template concentration was determined by measurement of the absorbance at 260 nm with a Nanodrop spectrophotometer ND-1000 (Peqlab). Successful circularization was controlled by running the samples on a 15% PAA gel with 7M Urea, acrylamide/ bis-acrylamide (19:1) (Sigma-Aldrich). The gel was run in TBE-buffer (89 mM Tris, 89 mM Borate, 2 mM EDTA, pH 8.3; Merck) for 30 min at 200V before loading the samples in urea loading buffer (8M urea, 20 mM EDTA, 5 mM Tris-HCl, 0.5% (w/v) xylene cyanol, bromphenole blue, pH 7.5) and running for further 2h. SYBR Green II (Invitrogen) staining in TBE buffer was carried out for 20 min while shaking gently. The read out was carried out with the GeneDoc X gel documentation system (Biorad).

5.3.2.2 RCA reaction

Per 50 µL reaction volume: 2 nM of circularized template, 10 U ϕ29 DNA polymerase, 0.3 µM BSA, ϕ29 buffer (50 mM TrisHCl, 10 mM MgCl$_2$, 10 mM (NH$_4$)$_2$SO$_4$, 4 mM dithiothreitol; pH 7.5; New England Biolabs), 1 mM dATP, dGTP, dCTP each (Fermentas), and1 µM Cy3- (GE Healthcare) / DY-555-dUTP (Dyomics) for direct labeling or 1 mM dTTP for post-synthetic labeling via *Hyb-Cy3* labeling (Fermentas) and were incubated at 37°C. For each slide a negative control with the same solutions and handling steps but without the circular template was run.

SSB and mutant ϕ29 DNA polymerase

For the experiments with *Tht*SSB and/ or the mutant ϕ29 DNA polymerases the same reaction solution was used, except that the mutant ϕ29 DNA polymerases replaced the regular polymerase and *Tht*SSB added. ThtSSB was provided by the group of Tsutumo Mikawa (Japan)[30], while the mutant D12A/D66A ϕ29 DNA polymerase was provided by the group of Margarita Salas (Spain).[108] MagniPhi was purchased from X-Pol Biotech.

5.3.3.1 DNA Microarray

Epoxide coated glass slides (Corning) were spotted with sciFLEXARRAYER S11 (Scienion AG). Spots: DNA primers *cF5* (15 µM), *cRCA15* (15 µM), Cy3-labeled spotting-control primer *F-prim* (0.15, 1.5, and 15 µM), and PBS buffer (137 mM NaCl, 2.7 mM KCl, 10 mM Na$_2$HPO$_4$, 2 mM KH$_2$PO$_4$, pH-value 7.4; Carl Roth GmbH).

The slides were immobilized at room temperature in a humidity chamber with saturated NaCl solution in the dark for 48 h. The slides were washed 1x 5 min in 0.1% Triton X-100, 2x 2 min in 1 mM HCl, 1x 10 min in 100 mM KCl and 1x 2 min in ultrapure H$_2$O prior to blocking. The blocking was performed with 50 mM ethanolamine and 0.1 % SDS in 0.1 M Tris-HCl (pH 9.0) at 50°C for 15 min. The slides were rinsed for 2 min in ultrapure H$_2$O before being dried by centrifugation and vacuum shrink-wrapped with DryCaps.

The slides were shaken gently for 2 min at room temperature after adding the RCA reaction solution before incubation at 37°C. The wells were washed for 5 min. each with 120 µL PBST (PBS, 0.05% Tween 20; Serva), PBS, and 0.1x PBS consecutively. The unlabeled strands (dTTP) were incubated for 30 min with 50 µL hybridization solution (1 µM *Hyb-Cy3* in PBST) while shaking at room temperature. Washing steps were carried out for 5 min each with 120 µL PBST, PBS, 0.1x PBS consecutively.

The read out was performed with the Axon GenePix 4300A microarray-scanner and GenePix Programs. For each read out, the setting of the photomultiplier was adjusted in order to exploit the full dynamic range of the microarray scanner. The fluorescence signals given in Mean F532 – B532 were calculated by correcting the fluorescence signals of the individual spots (F532) for their local background (B532).

5.3.3.2 Antibody Microarray

The antibody arrays were spotted as the DNA microarrays. Spots: 0.01, 0.1 and 1 mg/ ml antiHCG-ß mAb (mouse), 1 mg/ ml antiHCG-ß pAb (goat) as specificity control and PBS buffer.

The immobilisation was performed overnight at 4°C in the dark. The slides were washed with PBS and ultrapure H_2O for 30 sec. The blocking was performed with 3% skim milk (Applichem) in PBS for 45-60 min. The slides were rinsed with PBS and ultrapure H_2O. The slides were dried with pressurized nitrogen, vacuum shrink-wrapped with DryCaps and stored at 4°C.

Incubation with Anti-mouse-IgG with *Antibody-primer* and Hybridization probe *AB-Cy3* (IBA GmbH). The preincubation of 30 µL Anti-mouse-IgG with DNA primer (2.5 ng/ µL) and 0.1 pmol circularized *RCA15* template in PBST was carried out by shaking gently for 1h at room temperature per 50 µL final reaction volume. The antibody template was applied to the microarray and 20 µL RCA reaction solution was added (for 50 µl final volume). The arrays were shaken gently for 2 min before being incubated for 3h at 37°C. Washing and hybridization see DNA microarrays.

The read out was performed with the Axon GenePix 4300A microarray-scanner and GenePix Programs. For each read out, the setting of the photomultiplier was adjusted in order to exploit the full dynamic range of the microarray scanner. The fluorescence signals given in Mean F532 – B532 were calculated by correcting the fluorescence signals of the individual spots (F532) for their local background (B532).

6 RESULTS AND DISCUSSION
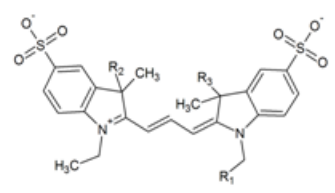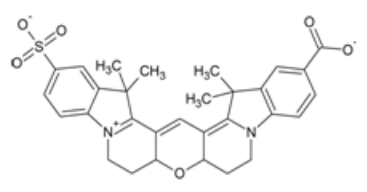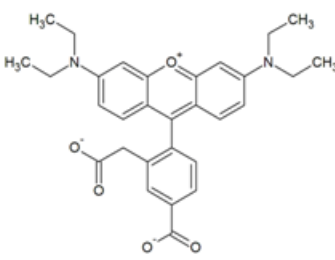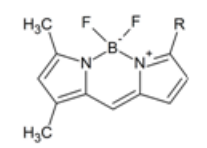
6.1 STEADY-STATE SPECTROSCOPY

6.1.1 Fluorophores

The spectroscopic properties and photochemical stability of seven fluorescent labels differing in dye class, charge and rigidity were studied (Table 1).

Next to the most common green excitation dye Cy3, six fluorophores were chosen to spectrally resemble it: DY-547, DY-548, DY-549 - cyanines with non-bridged double bonds that can undergo *cis-trans* isomerization and differ in the number of sulfonate groups attached to the dyes, Cy3B - a bridged, rigified cyanine and derivate of Cy3, DY-555 (rhodamine), and BODIPY FL (boron-dipyrromethene).

Table 1: Chemical structures and properties of the fluorescent labels investigated. The cyanines Cy3, DY-547, DY-548, and DY-549 share the same main chromophore, yet differ slightly in substitution pattern and in the number of sulfonate groups and thus, chromophore charge. The chemical structures of the DY-547/8/9 that closely resemble Cy3 with just very few photophysically not really important groups distinguishing the DY-54x series from Cy3, were provided to us by the manufacturer only confidentially. The molecular formulas of the carbocylic acids of these dyes are: DY-547 $C_{30}H_{35}N_2O_8S_2Na$, DY-548 $C_{31}H_{36}N_2O_{11}S_3Na_2$, DY-547 $C_{33}H_{39}N_2O_{14}S_4Na_3$. These dyes were chosen to systematically assess the influence of chromophore charge on the spectroscopic properties of such dye-DNA systems.

Cy3	charge -1, trimethine chain	cyanine $R_1, R_2, R_3 = CH_3$	
DY-547	charge -1	cyanine	
DY-548	charge -2	cyanine	
DY-549	charge -3	cyanine	
Cy3B	charge -1 (free dye), zwitterionic (dUTP), rigid	cyanine	
DY-555	charge -1 (free dye), zwitterionic (dUTP), rigid	rhodamine	
BODIPY FL	zwitterionic, rigid	boron-dipyrromethene dye $R = C_5H_9O_2$	

The cyanines Cy3 and the Dy-54x group are similar in structure, yet differ in the position of their linkers attached to the aromatic end group.

BODIPY FL, that absorbs and emits at shorter wavelength as Cy3, was chosen because of its rigidity and neutral charge and its promisingly high fluorescence quantum yield of nearly 1.0 for the free dye (Figure 19, Table 2).[109]
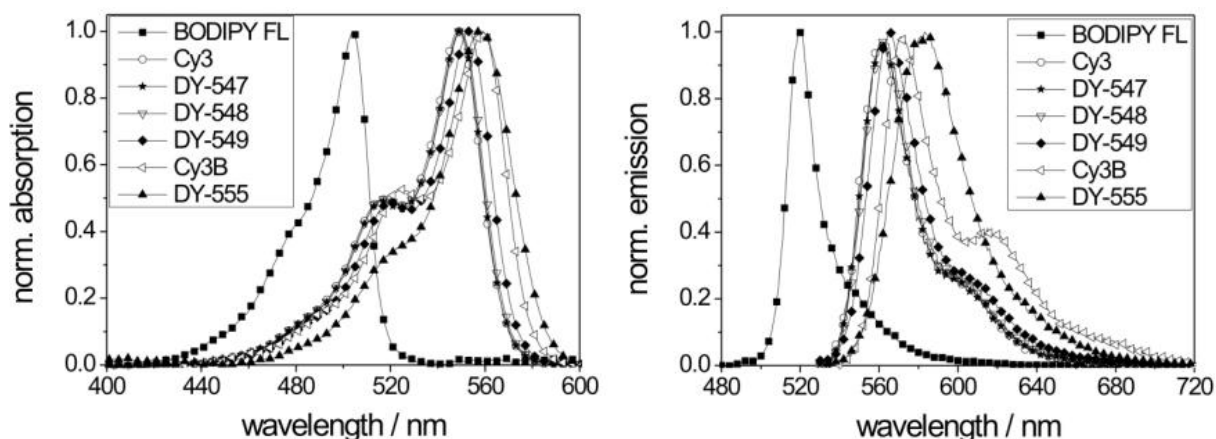
Figure 19: Normalized absorption spectra (left) and normalized corrected emission spectra (right) of Cy3, DY-547, DY-548, DY-549, Cy3B, and DY-555 (λ_{ex} = 525 nm) as well as BODIPY FL (λ_{ex} = 480 nm) in DNA buffer. The excitation wavelengths used are given in brackets.

6.1.2 Template design

The template design can be crucial for direct labeling approaches as a close spacing of the incorporated fluorophores may lead to dye-dye quenching, resulting in less signal at greater costs. But to obtain a high signal the overall output could be greater in templates offering more integration sites, justifying higher costs.

For the choice of the optimum label from the fluorophores shown in Table 1, two model sequences, a single (1A) and a triple (3A) labeled 91mer, were designed based on preliminary studies with Cy3. [9] The strands were labeled internally, the fluorophores having a minimum distance from the end of 35 and 25 bases for the single and triple labeled strand, respectively. The next guanosine that could engage in PET-induced fluorescence quenching, as reported e.g. for certain BODIPY and rhodamines dyes, is four bases from the labeling site in ssDNA and two bases in dsDNA.[110] The dyes in the triple-labeled samples were 10 bases, i.e., one helix turn, apart. The labeling sites were surrounded by mirrored base sequences to provide the same microenvironment for the fluorophore-labeled nucleotides.

Table 2: Absorption and emission spectra maximum and shoulder of Cy3, DY-547, DY-548, DY-549, Cy3B, and DY-555 (λ_{ex} = BODIPY FL (λ_{ex} = 480 nm) in DNA buffer.

Dye-microenvironment	Maximum λ_{abs} [nm]	Shoulder λ_{abs} [nm]	Maximum λ_{em} [nm]	Shoulder λ_{em} [nm]
Cy3				
free dye	549	517	561	606
dUTP	550	519	564	606
1A ssDNA	549	517	562	608
1A dsDNA	549	518	563	608
3A ssDNA	549	517	563	609
3A dsDNA	550	517	564	610
DY-547				
free dye	549	518	563	605
dUTP	551	518	564	604
1A ssDNA	551	518	565	603
1A dsDNA	551	517	564	605
3A ssDNA	551	519	565	608
3A dsDNA	551	520	566	608
DY-548				
free dye	549	518	562	608
dUTP	551	519	565	608
1A ssDNA	551	519	565	607
1A dsDNA	552	520	563	608
3A ssDNA	552	520	565	609
3A dsDNA	555	519	565	610
DY-549				
free dye	553	520	565	607
dUTP	555	522	568	607
1A ssDNA	554	522	567	607
1A dsDNA	554	521	566	608
3A ssDNA	555	521	570	609
3A dsDNA	559	522	570	609
Cy3B				
free dye	559	525	571	615
dUTP	561	525	573	617
1A ssDNA	562	528	575	618
1A dsDNA	562	528	574	618
3A ssDNA	563	529	575	622
3A dsDNA	562	528	576	622
DY-555				
free dye	558	520	583	638
dUTP	561	521	588	648
1A ssDNA	560	521	584	637
1A dsDNA	560	522	584	639
3A ssDNA	560	524	596	640
3A dsDNA	560	527	597	640
BODIPY FL				
free dye	505	478	509	546
dUTP	504	478	510	547
1A ssDNA	513	485	520	558
1A dsDNA	513	485	521	558
3A ssDNA	514	484	521	559
3A dsDNA	513	487	520	561

6.1.3 Internal Cy5 primer standard

A Cy5-labeled primer served as internal standard in early setups for DNA quantification as the signal of the absorption spectra could be normalized for the DNA concentration A_{260} but not for the fluorescence emission spectra.

To prevent FRET from the studied dyes to Cy5, Cy5 was spaced at minimum 40 base pairs (i.e. *ca.* 130 Å) apart from the first labeling site (see 3.3.8).

If the dye-dUTPs were incorporated successfully into the DNA strand by ϕ29 DNA polymerase, the signal ratio for the fluorophores should be 1:3 for the single (1A) and triple (3A) strand.

The Cy5 absorption/ emission peak at 650 nm/ 660 nm, respectively, can provide an internal standard for both measurements as it should be in 1:1 ratio to the total DNA. Normalizing the absorption peak of Cy5 should yield matching spectra for DNA at A_{260} as well (Figure 20).
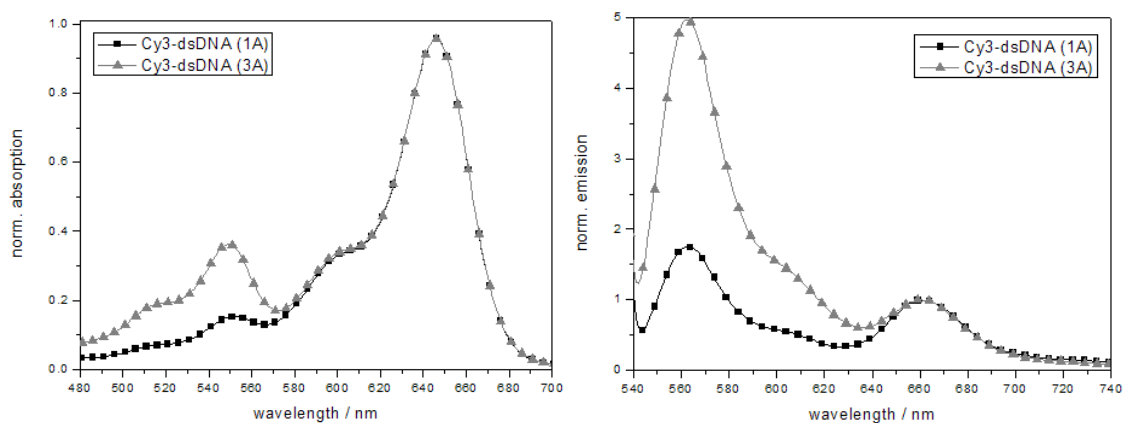
Figure 20: Normalized spectra of single (1A) and triple (3A) labeled Cy3-dsDNA (peak: 550 nm) with Cy5-primer (peak: 650 nm) as internal standard. Left: aborption spectra, right: emission spectra (λ_{ex} = 525 nm).

As Figure 20 and 21 show, the normalized absorption spectra at 260 nm (DNA absorption maximum) and at 650 nm (Cy5 absorption maximum) are matching (Figure 21). All other dyes employed yielded the same results. Therefore, the Cy5 primer was used to normalize the emission spectra as well to determine the signal ratio for the single (1A) and a triple (3A) strands.
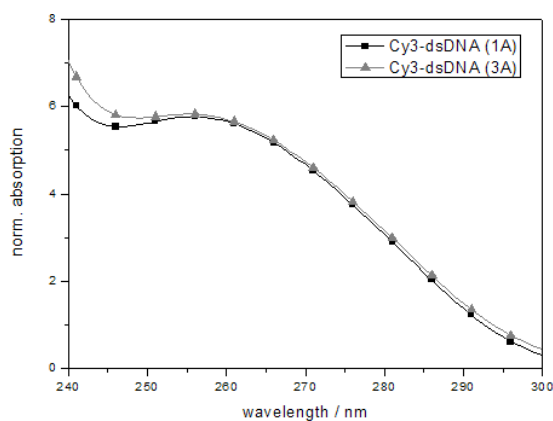
Figure 21: DNA absorption at 260 nm of the normalized absorption spectra of Figure 20.

35

The samples were excited at 525 nm which is the favorable wavelength for Cy3 but not Cy5. Cy5 is excited as well but to a lesser extent resulting in a reduced fluorescence. The normalized absorption and the emission spectra yielded the expected signal ration of 3:1 for 3A to 1A showing that the labeled dye-dUTPs were integrated successfully.,

Normalized Absorption	550 nm	2.8 +/- 0.2
Normalized Emission	560 nm	3.1 +/- 0.2

All following measurements were performed with samples lacking Cy5 at the 5' end of the primer to ensure that the observed effects were solely due to the fluorophores within the DNA strand and not due to dye-dye interactions with Cy5.

6.1.4 Microenvironment-induced spectral shifts

The shape, intensity and spectral position of the absorption and emission spectra provide information on the fluorophores microenvironment (see 3.3.2). Therefore, the spectra of the free dye, dye-labeled dUTP and single dye-labeled model sequences (dsDNA/ ssDNA) were investigated for microenvironment-induced spectral shifts.
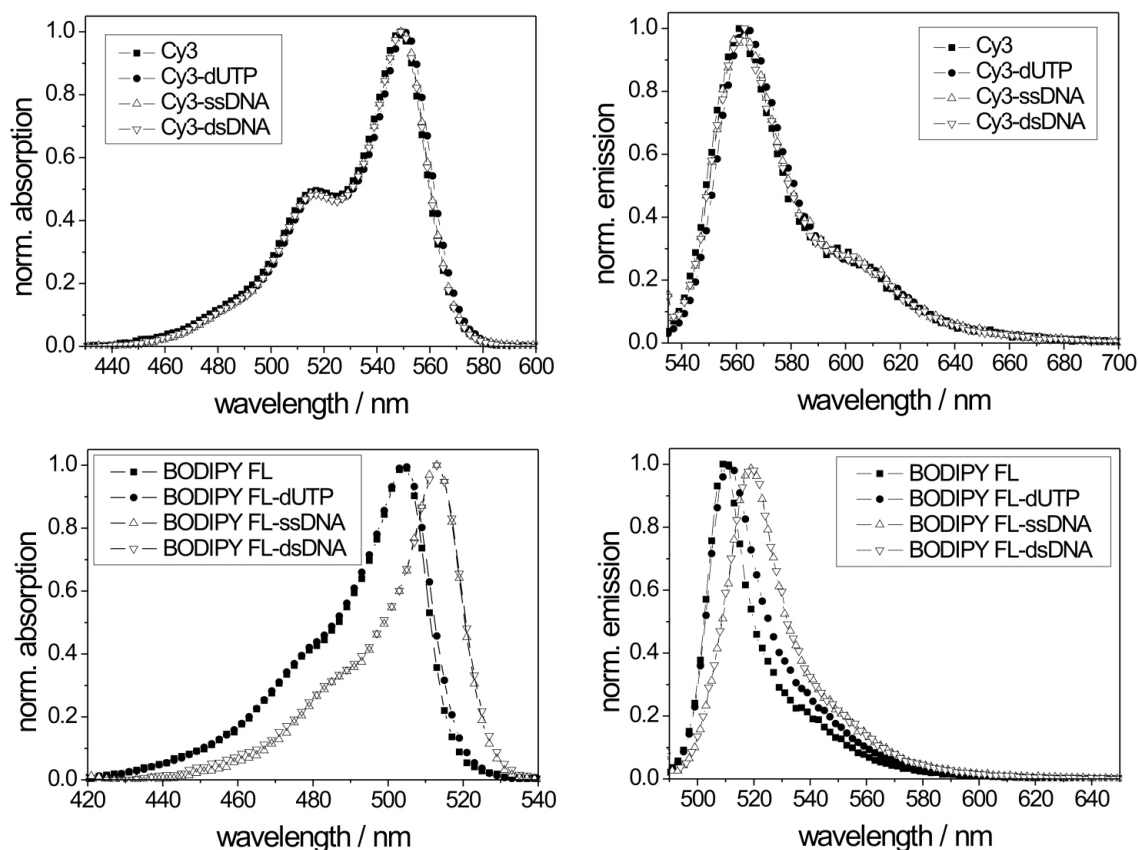
Figure 22: Normalized absorption spectra (left) and normalized corrected emission spectra (right) of Cy3 top and BODIPY FL (bottom) in dependence of dye microenvironment.

Attachment to dUTP and incorporation into the DNA strand barely affected the spectral features of the cyanine dyes and the rhodamine (Table 2) and is exemplary shown in Figure 22 for Cy3, (spectral shifts of 1-3 nm, Figure 22, top).

In contrast, in the case of BODIPY FL (Figure 22, bottom, right), attachment to dUTP resulted in a slight broadening of the emission band in comparison to the free fluorophore and pronounced red shifts of *ca*. 10 nm in absorption and emission for the DNA-bound fluorophore compared to the free and dUTP-linked dye.

BODIPY dyes with a core of lower symmetry as the fluorophore used here are known to display spectral changes especially in fluorescence in dependence of solvent polarity, with a red shift in emission typically indicating an increase in the polarity of the dye microenvironment.[111][112] This could suggest a close neighborhood of BODIPY FL to the negatively charged phosphate backbone of the DNA. As similar effects are observed for single and double stranded DNA, dye intercalation seems not to be likely.

6.1.5 Fluorescence quantum yield

As a high signal output is desired, a high fluorescence quantum yield Φ_f is favourable (see 3.3.5). At the same time the signal should be influenced as little as possible by the local microenvironment. Accordingly, the spectroscopic properties of the free dye and dye-dUTP were compared to the single labeled sequences.
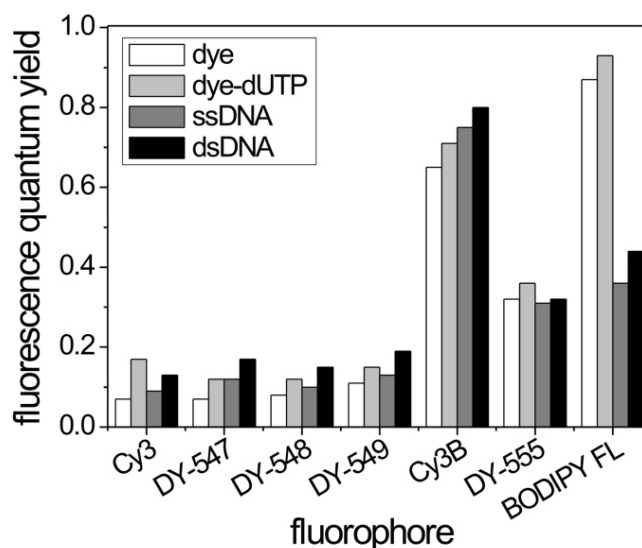
Figure 23: Fluorescence quantum yields of the seven fluorophores as a measure of their fluorescence efficiency in dependence of dye microenvironment.

All the dyes underwent a small increase in fluorescence upon attachment to dUTP (Figure 23) that was least pronounced for DY-555. Incorporation into the DNA strand resulted in no to little fluorescence enhancement for the non-bridged cyanines as well as for rigid Cy3B.

These effects render intercalation of these dyes into the grooves of the dsDNA or into the base stacks not very likely as this is expected to lead to a considerable increase of the fluorescence quantum yield, at least for the non-bridged cyanines. Similar effects resulted for the rhodamine DY-555.

For BODIPY FL, however, a strong reduction in Φ_f by *ca.* 50% occurred. Guanosine, the DNA base with the lowest oxidation potential, has been reported to quench the fluorescence of BODIPY FL via PET.[97] For the templates, the nearest guanosine in the single strand is four bases apart from the dye-labeled uracil and only two bases in the double strand. The diminution in fluorescence of BODIPY FL was thus attributed to PET involving the neighboring guanosine(s) within the strand.[113]

6.1.6 Influence of labeling density

An increase in the number of dye labels does not necessarily result in a linear increase in fluorescence signal as dye-dye interactions can result in undesired fluorescence quenching and thus in a reduced fluorescence quantum yield per label with increasing labeling density (see. 3.3.11.4). [70][114] This can hamper quantification from measurements of fluorescence intensity and results in unnecessary high costs. The occurrence and size of such effects, that should be thus minimized, are dye-specific and difficult to predict. Accordingly, the single and triple labeled strands were compared to determine if, and to what extent, the fluorescence is quenched by dye-dye interactions.
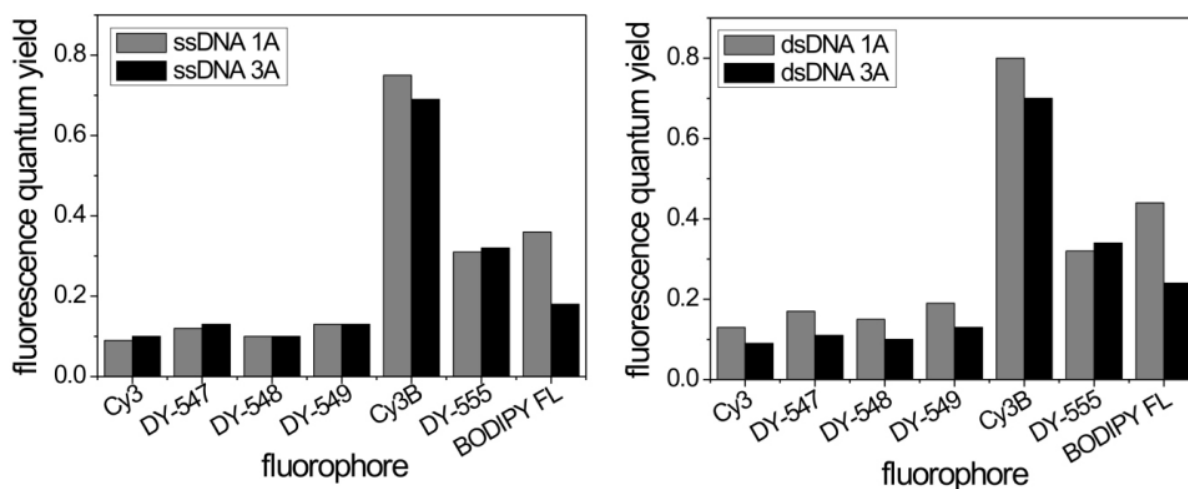
Figure 24: Fluorescence quantum yield of single labeled (1A) versus triple labeled (3A) DNA: ssDNA (left), dsDNA (right).

As shown in Figure 24 (left), for ssDNA, the fluorescence quantum yield of the triple labeled strand, where the dyes are spaced 10 nucleotides apart, was reduced for BODIPY FL by 50% compared to the (already quenched) single labeled strand and by 8% in the case of Cy3B.

All other dyes displayed similar Φ_f values for 3A and 1A ssDNA, meaning that the fluorescence efficiencies are independent of label density at this spacing. The fact, that BODIPY FL is especially prone to fluorescence quenching, is in accordance with other literature reports on self-quenching and dye-dye interactions of BODIPY dyes for distances ranging from 20 to 80 Å.[115]

The corresponding 3A dsDNA sequences (Figure 24, right), where the fluorophores are one helix turn apart, showed a decrease in fluorescence quantum yield for all dyes, except DY-555. Unlike the flexible ssDNA, the rigid helix forces the dyes on top of each other, thereby favoring dye-dye interactions. This can possibly account for the more pronounced fluorescence quenching in the dsDNA compared to the ssDNA strands.[114]

6.1.7 Photostability

A good photostability is a prerequisite for the suitability of fluorescent labels for fluorescence techniques using intense excitation light sources as it enables frequent remeasuring without signal loss and permits longer exposition times to collect more photons (see 3.3.9).
Thus, photostability studies were performed with the seven fluorophores, illuminating the dye-dUTPs in DNA buffer with a 150 W Xe-lamp.

Dye	Photobleaching [%]
Cy3	5
DY-547	2
DY-548	1
DY-549	0
Cy3B	20
DY-555	0
BODIPY FL	98
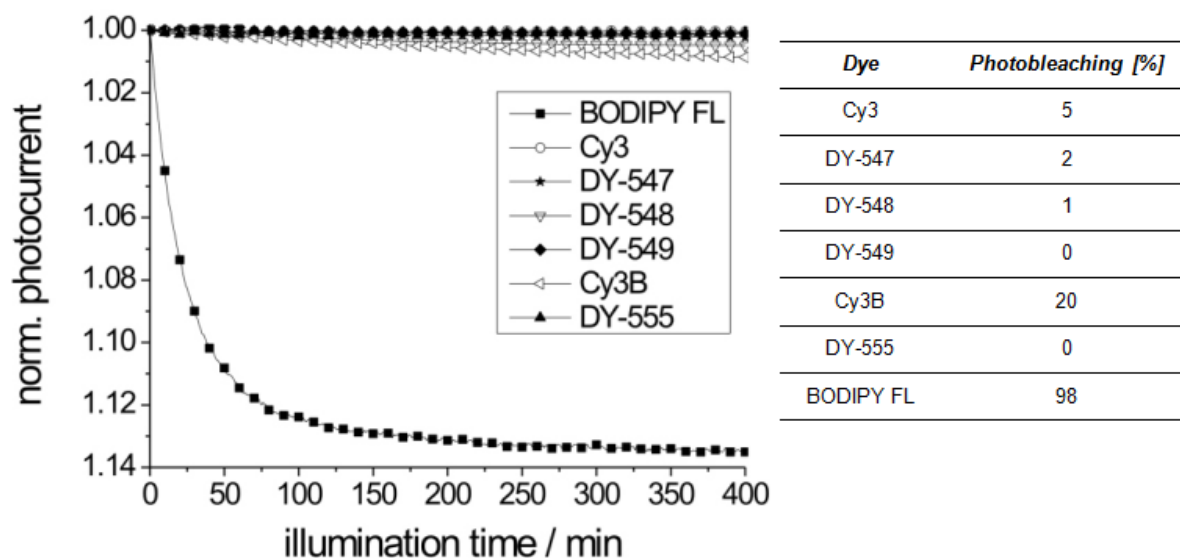
Figure 25: Left: Photocurrent as a function of illumination time measured within the over a period of 400 min of the illumination of the dye-labeled dUTPs in DNA buffer. The photocurrent correlates with dye absorbance and thus, dye concentration. The results obtained after 1000 min. of illumination are summarized on the right: The percentage of photobleaching was calculated from the light-induced decrease of the initial absorbance of the dye.

As summarized in Figure 25, the cyanines with non-bridged double bonds and the rhodamine DY-555 showed little to no photobleaching over an illumination period of 400 min and even after 1000 min. Astonishingly, the rigid cyanine Cy3B displayed a slow, but continuous loss in absorption and thus, in dye concentration as function of illumination time, eventually resulting in a 20% loss in signal. However, BODIPY FL lost 50% of its original absorption within the first 30 min. and was completely photobleached after *ca.* 4 h. Such a photoinstability has been reported for other BODIPY dyes as well.[17]

Interesting is here the decreased photostability of Cy3B compared to its analogue Cy3 with non-bridged double bonds as often, rigid chromophores are more photostable than unbridged ones,

especially for dyes, where photostability is linked to cis-trans isomerization. However, this finding is in agreement with the data provided by the manufacturer of the Cy dyes, GE Healthcare (former Amersham).[116]

6.2 TIME-RESOLVED SPECTROSCOPY

To understand the photophysical nature of the effects observed with steady-state spectroscopy and to determine their suitability for time-gated detection the dyes were further investigated with time-resolved fluorescence detection.

6.2.1 Emission Anisotropy and Average Fluorescence Lifetime

6.2.1.1 Emission Anisotropy

The emission anisotropy r is a measure for the polarization dependence of the emission of a fluorophore (see 3.3.7) Although principally, r can provide information on dye mobility and thus, interaction with biomolecules such as intercalation into dsDNA [101][117] care must be taken as r depends also strongly on fluorescence lifetime τ.
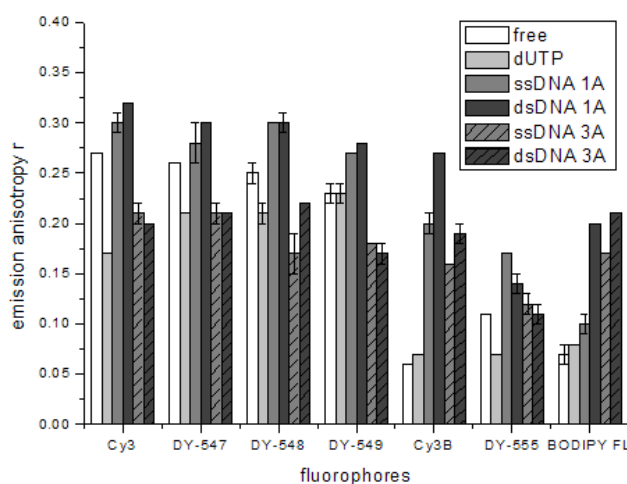
Figure 26: Emission anisotropy r of the seven fluorophores in different the different samples. The error bars given for the selected samples represent relative standard deviations derived from three independent measurements.

The emission anisotropy of the dye-dUTPs decreases compared to the free fluorophores for Cy3, DY-547, DY-548, and DY-555 whereas for DY-549, Cy3B and BODIPY FL, the r values are similar. In the case of the former four cyanines, this is attributed to the increased fluorescence lifetime upon attachment of the fluorophore to dUTP as detailed in the lifetime analysis for Cy3 and the DY-54x series in the following sections. All dyes undergo an increase in r when bound to the large DNA strand ssDNA/ dsDNA 1A. The triple labeled DNA strands, however, display reduced emission anisotropies compared to the single labeled strands for all fluorophores except for BODIPY FL (Figure 26).

This trend is more pronounced for the cyanine dyes with non-bridged double bonds compared to rigid Cy3B and rhodamine DY-555. The reduced emission anisotropy of the triple labeled samples could suggest energy transfer between the labels on the DNA strand. The Φ_f values indicate no quenching for the dyes in ssDNA/ dsDNA 3A compared to ssDNA/ dsDNA 1A, with the exception of BODIPY FL.

The rigid dyes, DY-555, Cy3B and BODIPY FL, on the other hand, display an increase in emission anisotropy from ssDNA to dsDNA for both 1A and 3A, with the enhancement being less pronounced for the latter system. This indicates a possible groove interaction for Cy3B.

An overall decrease in fluorescence lifetime seems to be a more plausible explanation for this observation as will be subsequently detailed.

Table 3: Fluorescence quantum yields, average fluorescence lifetimes, and steady-state emission anisotropy for the free dyes, dye-dUTP and ssDNA 1A systems.

sample	free dye			dUTP			ssDNA 1A		
	Φ_f	τ_{av}	r	Φ_f	τ_{av}	r	Φ_f	τ_{av}	r
Cy3	0.07	*0.18*	0.27	0.17	*0.71*	0.17	0.09	*1.03*	0.30
DY-547	0.07	*0.18*	0.26	0.12	*0.71*	0.21	0.12	*0.90*	0.28
DY-548	0.08	*0.21*	0.25	0.12	*0.6*	0.21	0.10	*0.58*	0.30
DY-549	0.11	*0.28*	0.23	0.15	*0.54*	0.23	0.13	*0.56*	0.27
Cy3B	0.65	*2.22*	0.06	0.71	*2.35*	0.07	0.75	*2.78*	0.20
DY-555	0.32	*1.68*	0.11	0.36	*2.17*	0.07	0.31	*2.12*	0.17
BODIPY FL	0.87	*5.63*	0.07	0.93	*6.34*	0.08	0.36	*6.80*	0.10

Table 4: Fluorescence quantum yields, average fluorescence lifetimes, and steady-state emission anisotropy of the dye dsDNA 1A, ssDNA 3A, and dsDNA 3A systems.

sample	dsDNA 1A			ssDNA 3A			dsDNA 3A		
	Φ_f	τ_{av}	r	Φ_f	τ_{av}	r	Φ_f	τ_{av}	r
Cy3	0.13	*0.66*	0.32	0.10	*0.37*	0.21	0.09	*0.29*	0.20
DY-547	0.17	*0.79*	0.30	0.13	*0.5*	0.21	0.11	*0.40*	0.21
DY-548	0.15	*0.63*	0.30	0.10	*0.38*	0.17	0.10	*0.36*	0.22
DY-549	0.19	*0.56*	0.28	0.13	*0.44*	0.18	0.13	*0.35*	0.17
Cy3B	0.80	*2.65*	0.27	0.69	*2.82*	0.16	0.70	*2.83*	0.19
DY-555	0.32	*2.05*	0.14	0.32	*1.79*	0.12	0.34	*1.75*	0.11
BODIPY FL	0.44	*6.79*	0.20	0.18	*5.01*	0.17	0.24	*4.82*	0.21

All fluorophores undergo an increase in r when bound to the large DNA strand ssDNA/ dsDNA 1A. The triple labeled DNA strands, however, display reduced emission anisotropies compared to the single labeled strands for all fluorophores except for BODIPY FL. This trend is more pronounced for the cyanine dyes with non-bridged double bonds compared to rigid Cy3B and rhodamine DY-555.

The reduced emission anisotropy of the triple labeled samples may be due to an energy transfer between the labels on the DNA strand. The Φ_f values indicate no quenching for the dyes in ssDNA/ dsDNA 3A compared to ssDNA/ dsDNA 1A, with the exception of BODIPY FL. Contrary to DY-555, Cy3B and BODIPY FL also display an increase in emission anisotropy from ssDNA to dsDNA for both 1A and 3A, with the enhancement being less pronounced for the latter system. This may indicate possible groove interaction for Cy3B. BODIPY FL, on the other hand, reveals a reduction in Φ_f for the DNA strands.

An overall decrease in fluorescence lifetime seems to be a more plausible explanation for this observation.

6.2.1.2 Average Fluorescence Lifetime

To determine whether the observed changes in emission anisotropy can be at least partly attributed to changes in fluorescence lifetime, the average fluorescence lifetimes τ_{av} of the fluorophores in the different samples were investigated (Figure 27, Table 3 and 4). τ_{av} was used as the fluorescence decay kinetics as all dyes typically decay tri-exponential within the DNA strand (see 5.2.5).
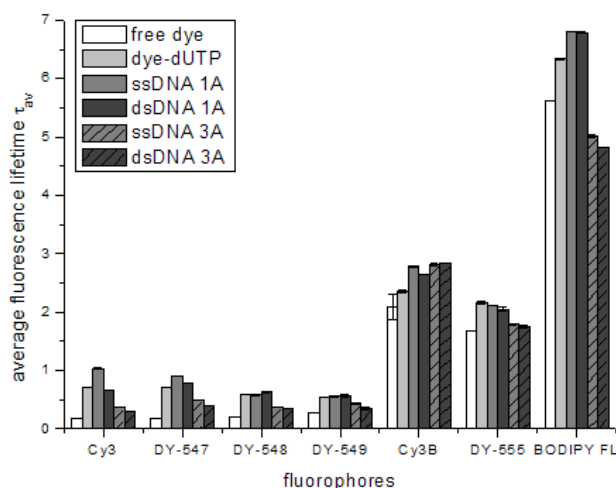
Figure 27: Average fluorescence lifetime τ_{av} of the seven fluorophores in the different samples. The error bars given for the selected samples represent relative standard deviations derived from three independent measurements.

τ_{av} significantly increases for the cyanines Cy3, DY-547, DY-548, and DY-549 upon binding to dUTP. This τ_{av} increase most likely accounts for the decrease in emission anisotropy observed for these systems. For the single negatively charged Cy3 and DY-547, τ_{av} further increases in ssDNA 1A. In ssDNA 3A and dsDNA 3A, the τ_{av} values are slightly reduced compared to the 1A DNA systems.

The average fluorescence lifetimes of the rigid chromophores Cy3B and DY-555 are less affected by binding to the DNA strand. Both dyes display only minor change in τ_{av} in all samples, especially compared to the dyes Cy3 and DY-547. The effects for DY-555 are less pronounced as for Cy3B, thereby paralleling the trends observed for the fluorescence quantum yields of these systems (Figure 23). Accordingly, the increase in emission anisotropy is mainly attributed to an increase in size.

This suggest that a blocking of the photoisomerization mechanisms of the non-bridged dyes that can undergo *cis-trans* isomerization is at least partially responsible for the increase in τ_{av} and Φ_f. Similar effects have been reported e.g. for Cy3 in various DNA systems and were ascribed to stacking interactions between the dye and the DNA bases. [70][118] In the case of BODIPY FL, τ_{av} and Φ_f reveal similar trends for ssDNA/dsDNA 1A and ssDNA/dsDNA 3A contrary to the effects observed for the emission anisotropies.

This suggests that an observed decline in *r* is mainly due a rise in fluorescence lifetime and vice versa. It also underlines the importance of considering fluorescence lifetimes when analyzing steady-state anisotropies.

6.2.2 Fluorescence Decay Behavior and Lifetime Analysis

The vast majority of fluorophores reveal bi-, tri- or multi-exponential decay kinetics due to a heterogeneous label environment or formation of different conformers that can provide distinctly different fluorescence quenching or enhancing efficiencies. Although a complex decay behavior of the labels bound to dUTP or within the DNA strands is to be expected the differences between these structurally closely related dyes are interesting.
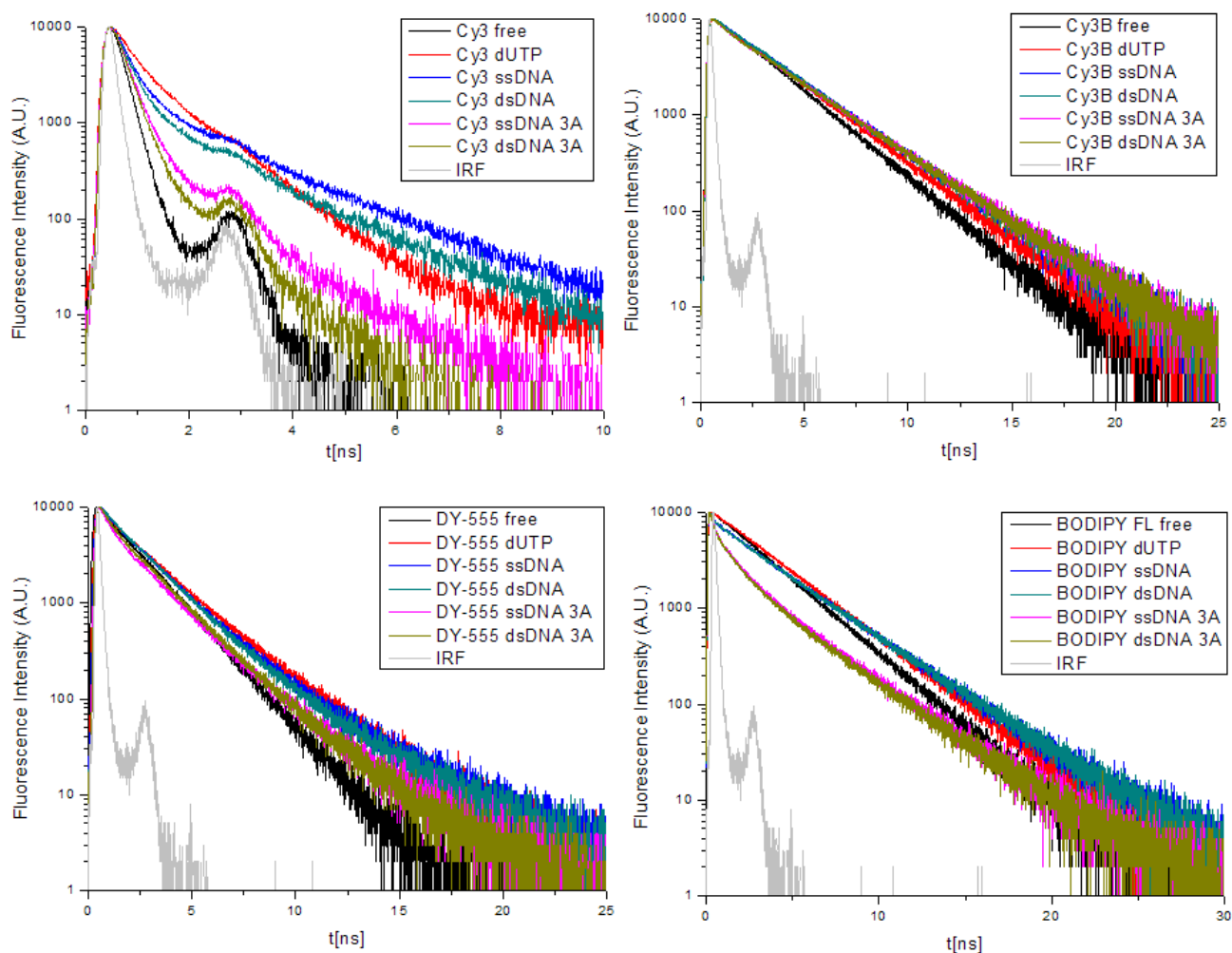
Figure 28: Fluorescence decays of Cy3, Cy3B, DY-555, and BODIPY FL obtained for the free dye, dye-dUTP, ss/dsDNA 1A and ss/dsDNA 3A.

6.2.2.1 Cy3 and DY-54x

The fluorescence decay kinetics of the cyanine dyes Cy3 and DY-54x are summarized in Table 5 and shown in Figure 28 for Cy3. These non-bridged cyanines are very similar in their chromophore structure but are attached in the positions to the linker. Also the the number of sulfonate groups differs: two for Cy3, Dy-547, three for DY-548 and four for DY-549 (Table 1).

Table 5: Fluorescence lifetimes of Cy3 and the DY-54x series and their relative amplitudes in % in the different samples.

sample	Φ_f	τ_1	A_1	τ_2	A_2	τ_3	A_3
Cy3	0.07					0.18	100
Cy3-dUTP	0.16			0.95	34.5	0.26	65.5
Cy3 ssDNA 1A	0.08	2.20	7.5	0.90	11.0	0.24	81.5
Cy3 dsDNA 1A	0.12	1.87	5.5	0.73	8.5	0.23	86.0
Cy3 ssDNA 3A	0.09	1.46	1.6	0.46	11.6	0.22	86.8
Cy3 dsDNA 3A	0.08			0.86	2.4	0.23	97.6
DY-547	0.07					0.18	100
DY-547-dUTP	0.11	1.39	5.7	0.48	30.5	0.20	63.8
DY-547 ssDNA 1A	0.11	1.90	5.7	0.61	28.8	0.23	65.5
DY-547 dsDNA 1A	0.16	2.01	4.8	0.65	26.5	0.24	68.7
DY-547 ssDNA 3A	0.12	1.26	4.0	0.47	38.1	0.22	57.9
DY-547 dsDNA 3A	0.10	1.14	2.7	0.38	53.6	0.18	43.7
DY-548	0.08					0.21	100
DY-548-dUTP	0.11	1.28	5.4	0.48	35.1	0.21	59.5
DY-548 ssDNA 1A	0.09	1.73	3.0	0.58	23.5	0.23	73.5
DY-548 dsDNA 1A	0.14	1.93	2.7	0.66	20.5	0.25	76.8
DY-548 ssDNA 3A	0.09			0.79	9.1	0.28	90.9
DY-548 dsDNA 3A	0.09			0.73	8.1	0.26	91.9
DY-549	0.10					0.29	100
DY-549-dUTP	0.14			0.92	18.4	0.35	81.6
DY-549 ssDNA 1A	0.12	1.34	3.2	0.60	28.9	0.32	67.9
DY-549 dsDNA 1A	0.18	1.28	5.0	0.48	57.0	0.24	38.1
DY-549 ssDNA 3A	0.12			0.70	12.6	0.36	87.4
DY-549 dsDNA 3A	0.12			0.51	27.6	0.28	72.4

All free dyes decay mono-exponentially (lifetime τ_3) as to be expected for a free fluorophore in a homogeneous environment. Interestingly, the fluorescence lifetime of the DY-54x series increases slightly from 0.18 ns to 0.29 ns with greater label charge. The fluorescence lifetime found for Cy3 equals the lifetime reported for this dye in 2007.[119] This trend in τ_3 parallels the increase in fluorescence quantum yield.

Attachment of these cyanine labels to dUTP results in biexponential decay kinetics for Cy3 and DY-549 and in triple-exponential decay kinetics for DY-547 and DY-548, with longer lived new decay components τ_2 (Cy3 and DY-549) and τ_1 and τ_2 (DY-547 and DY-548), respectively, appearing. Incorporation into ssDNA and dsDNA yields triple exponential decay kinetics for all fluorophores in the case of the 1A systems with τ_1 of *ca.* 1.3 to 2.0 ns, τ_2 of *ca.* 0.5 to 0.9 ns, and τ_3 of *ca.* 0.2 to 0.3 ns.

For the triple labeled DNA strands, three decay components can be observed for DY-547 (ssDNA/ dsDNA 3A) and Cy3 (ssDNA 3A only) and two lifetimes for DY-548 and DY-549. The decay component with the lifetime τ_3 closely resembling the lifetime of the free dye, is attributed to fluorophores that do not interact with the DNA.

Cyanines are known to interact with DNA through minor groove binding, intercalation or base stacking. [69][120] Minor grove binding cannot be the cause for the long lived decay component (τ_1) as this

decay component appears in both ssDNA and dsDNA. The fluorescence lifetimes τ_1 and τ_2 are ascribed to fluorophores interacting with DNA bases via π-stacking which results in a restricted dye motion and thus, a reduced rate of *cis-trans* photoisomerization. Another hint for this assumption seems to be the increased emission anisotropies of these systems. While the quantum yields point in this direction as well, they are below the 0.39 reported for ssDNA sequences.[97][101]

Both papers employ short 5' labeled sequences but other reports show that Φ_f increased only to 0.21 when labeling internally since no end-stacking can take place.[77] The values here are below those reported which is attributed to the far higher purine content of his sequences, as purines are resulting in a greater quantum yield for Cy3.

Comparing the three DY-54x dyes, τ_1 disappears consecutively from some species with the increase in chromophore charge. This suggests that the interaction of the DY-54x dyes with DNA is concomitantly hindered by their increasing charge. This influence of label charge and thus, electrostatic repulsion on the dye´s fluorescence decay behavior reflects and explains some of the trends observed for the emission anisotropies of the DY-54x fluorophores in the different microenvironments. The difference in *r* between the free dyes and the dye-dUTPs is disappearing from Cy3 to DY-549. A decrease in dye-DNA and dye-dye interaction with an increase in dye hydrophilicity / number of sulfonate groups attached to the fluorophores was also reported previously.[70]

6.2.2.2 Cy3B, DY-555, BODIPY FL

The fluorescence decay kinetics of the rigid dyes, i.e., the cyanine Cy3B, rhodamine DY-555, and BODIPY FL, are summarized in Table 6 and Figure 28.

Table 6. Fluorescence lifetimes of the rigid fluorophores and their relative amplitudes in % in the different samples.

sample	Φ_f	τ_1	A_1	τ_2	A_2	τ_3	A_3	τ_4	A_4
Cy3B	0.61			2.22	100				
Cy3B-dUTP	0.67			2.43	88.5	1.23	11.5		
Cy3B ssDNA 1A	0.70			2.99	70.9	1.85	29.1		
Cy3B dsDNA 1A	0.75	4.22	7.9	2.42	92.1				
Cy3B ssDNA 3A	0.65			3.10	61.5	1.88	20.3	0.39	18.2
Cy3B dsDNA 3A	0.66	5.24	2.3	2.82	78.7			0.52	19.0
DY-555	0.30			1.74	13.9	0.58	86.1		
DY-555-dUTP	0.34	2.78	34.7	1.48	49.9	0.25	15.4		
DY-555 ssDNA 1A	0.29	3.52	11.7	1.73	74.5	0.35	13.8		
DY-555 dsDNA 1A	0.30	3.67	7.8	1.76	79.6	0.38	12.6		
DY-555 ssDNA 3A	0.30	2.79	14.0	1.53	46.0	0.36	40.0		
DY-555 dsDNA 3A	0.32	3.24	5.4	1.69	59.4	0.40	35.2		
BODIPY FL	0.79	5.63	100						
BODIPY FL-dUTP	0.84	6.34	100						
BODIPY FL ssDNA 1A	0.33	7.34	54.9	3.66	14.0	0.29	31.1		
BODIPY FL dsDNA 1A	0.40	7.38	52.9	3.72	15.0	0.27	32.1		
BODIPY FL ssDNA 3A	0.16	6.84	24.2	2.21	33.8	0.39	42.0		
BODIPY FL dsDNA 3A	0.22	6.78	19.0	2.09	31.8	0.31	49.2		

Free Cy3B and BODIPY FL show monoexponential decay kinetics. The lifetime τ_3 of 2.2 ns found for Cy3B is slightly shorter than the value of 2.7 ns reported in Tris buffer. [77] This is in agreement with the tendency observed for the fluorescence quantum yield (Φ_f = 0.65 vs. Φ_f = 0.85 previously reported). DY-555 is the only dye which decays biexponentially with lifetimes τ_2 of 1.7 ns and τ_3 of 0.6 ns.

Attachment to dUTP leads to the appearance of an additional lifetime in the case of Cy3B and DY-555, whereas the decay kinetics of BODIPY FL remains mono-exponential. Contrary to the other cyanines, Cy3B shows a shorter lifetime τ_3 of 1.2 ns that is also present in the ssDNA systems.

Within the DNA strands, all rigid fluorophores reveal triple exponential decay kinetics. The only exception is Cy3B in ssDNA/ dsDNA 1A. Interestingly, Cy3B displays a new long lived decay component in both dsDNA systems, with lifetimes τ_1 of 4.2 ns and 5.2 ns resulting for the 1A and 3A system.

This suggests an interaction with the structure of the DNA double helix, most likely via minor groove binding, as reported for other cyanines. This is also supported by the increase in emission anisotropy that occurs exclusively for the dsDNA systems despite the increase in fluorescence quantum yield and lifetime. The short lived decay component with τ_4 of 0.4 to 0.5 ns, present only in the triple labeled strands, is attributed to fluorescence quenching dye-dye-interactions. In the case of DY-555, the three lifetimes τ_1, τ_2, and τ_3 are present in all DNA samples differing only slightly for the systems studied.

The main change is a decrease in the amplitude of the longest lived decay component τ_1 when comparing ssDNA and dsDNA. Although the fluorophore clearly senses a heterogeneous environment as reflected by the more complex decay kinetics compared to the free label or the dUTP system, this suggests only little interaction of the chromophore with the strand or other labels within the strand.

DY-555 is the only dye which decays biexponentially and one would expect a monoexponetial decay for a free dye. To rule out an error in interpretation or calculation of these lifetimes, a support plane analysis of the data was conducted. This analysis showed that these lifetimes are indeed distinct (Figure 29). According to the dye manufacturer, DY-555 can contain another isomer, yet only at a very low concentration, the presence of which can possibly result in a bi-exponential decay behavior.
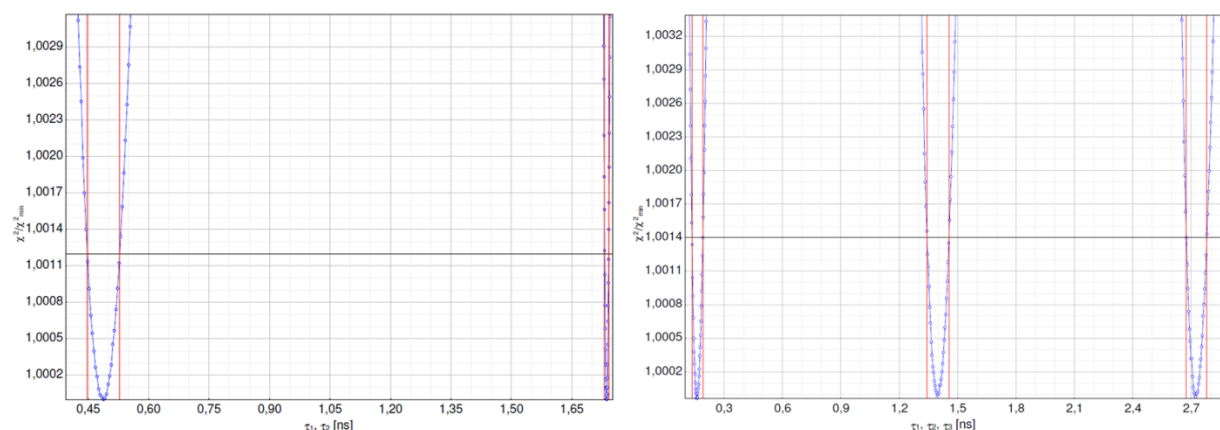

Figure 29: Support plane analysis of the fluorescence decays of DY-555 free (left) and DY-555-dUTP (right).

The fluorescence quantum yields, emission anisotropies, and fluorescence decays of DY-555 in the different environments studied do not provide an obvious hint for PET-induced quenching although such effects have been reported for other rhodamines like TAMRA.[69] DY-555 is structurally very similar to TAMRA, differing only in a second carboxyl group on the phenyl ring. This very is likely influencing the interaction with the dUTP and DNA as an increase in negative charge has already proven for the DY-54x series to hamper dye-DNA interactions. Dye-dye or guanosine induced quenching as reported for other rhodamines could not be observed. [97][121]

BODIPY FL displays two new shorter lifetimes τ_2 and τ_3 upon DNA integration whereas τ_1 increases from 5.6 ns found for the free label to *ca.* 7.3 ns in ssDNS/ dsDNA 1A and 6.8 ns in the triple labeled systems. The short lifetime τ_3 of *ca.* 0.3 ns that is present in all DNA systems, is ascribed to PET-induced fluorescence quenching due to the presence of neighboring guanosines in accordance with other reports on BODIPY FL. [97][122] This is also responsible for the decrease in fluorescence quantum yield.

When comparing the 1A to the 3A DNA systems, the following trends are obvious: The decay component τ_2 decreases from 3.7 ns in single labeled DNA to *ca.* 2.2 ns in the triple labeled systems. Simultaneously, the amplitude A_2 of the lifetime τ_2 increases by a factor of two which is paralled by a corresponding decrease in the amplitude A_3 of the longest lifetime τ_3. Moreover, the amplitude of the decay component with the lifetime τ_3 increases for the triple labeled system.

These changes in fluorescence lifetime of BODIPY FL seem to be responsible for the alterations in emission anisotropy and account for the reduction in fluorescence quantum yield shown in Figure 23. The observed fluorescence decay behavior suggests either the occurrence of additional fluorescence diminishing dye-dye interactions in the 3A systems, slightly different dye-guanosine distances and orientations in 3A DNA favoring PET-induced fluorescence quenching or a combination of both effects.

6.2.3 Dye-DNA interactions

Based on the results of the steady-state and time-resolved data, five states within the DNA strand for the fluorophore labels investigated are proposed that could account for the observed spectroscopic effects and changes in fluorescence decay behavior (Figure 30).

The fluorescence properties of Cy3 and the DY-54x series are ascribed to blocking of the *cis-trans* photoisomerization via nucleotide stacking and a general effect of the heterogeneous microenvironment of the DNA strand.

Among the rigid dyes studied, only DY-555 seems to be prone to such stacking interactions as suggested e.g. by its increased lifetime upon dUTP binding. The fluorescence behavior of BODIPY FL in the DNA strands is dominated by dGTP-induced quenching although a minor contribution from dye-dye interaction cannot be excluded.

Dye-dye interactions may also affect the emission of Cy3B in triple labeled DNA as suggested by the appearance of a new short lived decay component with a lifetime τ_4 of 0.4 ns or 0.5 ns exclusively in these systems although the absorption spectra of both BODIPY FL and Cy3B DNA systems do not display signs for dye aggregation. Cy3B seems to be the only dye that exhibits a double strand specific fluorescence lifetimes increase of τ_4 of 4.2 ns and 5.2 ns, suggesting an interaction with the dsDNA structure.
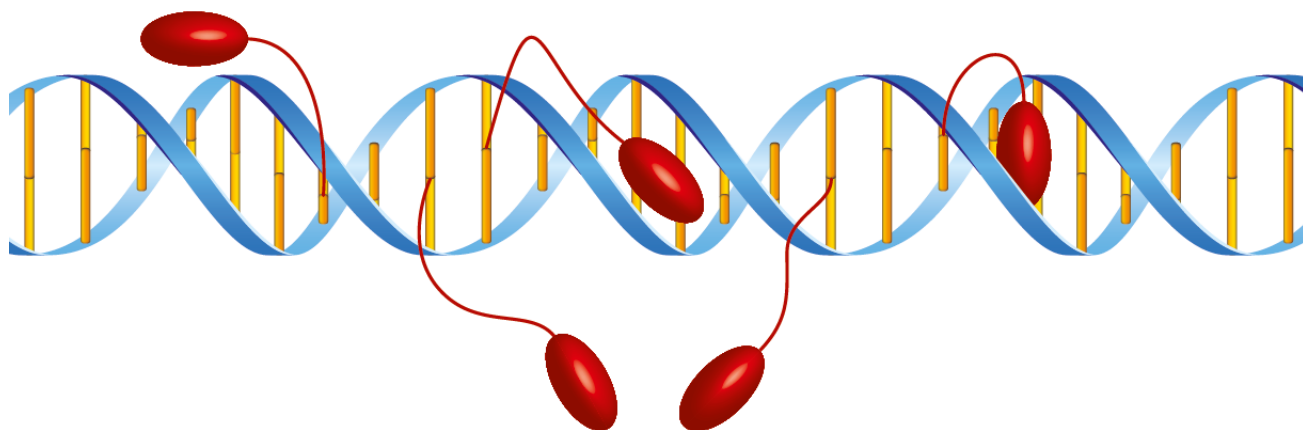
Figure 30: Dye-DNA interactions. From left to right: General interaction with the heterogeneous environment of the DNA strand (Cy3, DY-54x, BODIPY FL); dye-dye-quenching in multi-labeled strands (Cy3B, BODIPY FL); stabilization by minor groove binding (Cy3B); stabilization via nucleotide stacking (Cy3, DY-54x, DY-555) or dGTP-induced quenching (BODIPY FL).

In conclusion, Cy3B and DY-555 are both attractive candidates for application studies on microarrays but Cy3B's application is hampered by the fact that Cy3B-labeled dUTP is commercially unavailable requiring custom synthesis, resulting in a comparatively high price of the label.

All over DY-555 displayed the best spectroscopic properties, like stable signal output in the different microenvironment, no dye-dye or PET induced quenching and good fluorescence quantum yield, and was consequently in direct labeling RCA on microarrays.

6.3 RCA ON MICROARRAYS

After identifying DY-555 as the best candidate for RCA-based labeling assays, the fluorophore was used in designing an improved RCA protocol for direct enzymatic labeling with dye-dUTPs. It was compared to the currently most common microarray label Cy3 and therefore, most test were run with both dyes in parallel.

To increase the signal yield in RCA-based formats, either the runtime can be extended or the amount of circular template added can be increased. For practicable diagnostics, an assay runtime of several hours is rarely desirable. The increase of circular template has no counter-indication but the high costs of its preparation. For simple signal amplification proximity-ligation of the template is not needed. This combination is only crucial for formats that need to ensure the specificity of the signal, e.g. single nucleotide polymorphism (SNP) detection (see 3.2.4.1).[123][124]

To obtain an increase in signal yield with the same assay runtime and constant template concentration, the influence of the label, template design, temperature and composition of the reaction solution as well as the labeling strategy to obtain an increase in signal yield were systematically assessed and optimized.

6.3.2 Reaction solution and template design

6.3.2.1 Reaction solution

Studies of the influence of template design and composition of the RCA reaction solution were carried out on DNA microarrays. The reaction solution was optimized for template *RCA15*, which spaces the dye-dUTPs 13 or 14 bases apart to avoid dye self-quenching, based on the spectroscopic studies. For direct labeling during synthesis, usually templates with randomly spaced integration sites are employed and a solution of modified and unmodified dNTP is used, e.g., for PCR labeling protocols.[125] Despite ϕ29 DNA polymerase's high fidelity and exonucleic activity[22][23] it has integrated all dyes into the short single and triple labeled oligonucleotides for the spectroscopic studies in solution. But now the RCA is run on a microarray slide that provides an altered surrounding and a far larger reaction product. Therefore, several reaction solutions were tested to obtain a high signal at low cost, providing dye-dUTP/ dTTP ratios or solely dye-dUTP in various concentrations (Figure 31).

	A	B	C	D	E	F	G
dA/G/CTP [mM]	1	1	1	2	1	1	1
dTTP [µM]	-	-	2	-	10	-	20
dye-dUTP [µM]	2	1	1	1	1	0.1	1
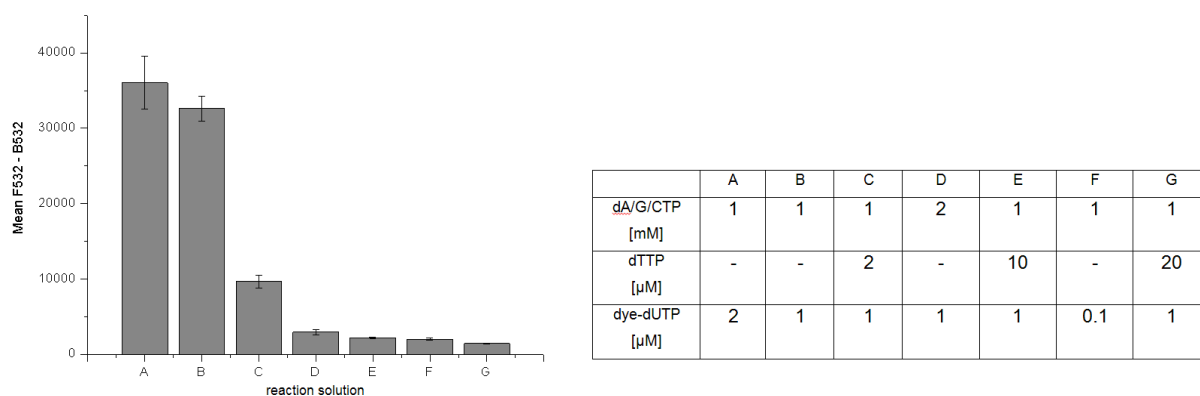
Figure 31: Rolling circle amplification reaction solutions. Left: Cy3 signal yield. Right: Reaction solution composition.

The results for Cy3-dUTP are presented in Figure 33 but DY-555-dUTP displayed the same order of signals and signal sizes. While reaction solution A and B are equally good, solution A is twice as expensive. Therefore, reaction solution B was used for the experiments presented.

6.3.2.2 Template design

For the direct labeling template *RCA15*, a 88 mer, the five integration sites were spaced 14 or 15 bases apart, a little further as for the linear triple labeled sequence 3A, to omit dye-dye quenching. The design was compared to a template that was successfully used for labeling with fluorescent hybridization probes in the past, *F1F9F10F5*, a 74 mer with 29 randomly distributed labeling sites.[107][126]

The immobilized primer *cF5* acted as specificity control for template *RCA15* and *cRCA15* for *F1F9F10F5* (Figure 32). Each slide had Cy3-labeled primers spotted in three concentrations that would allow a comparison between different slides. Compared to the widely spaced *RCA15*, the signal yield of *F1F9F10F5* was diminished by a factor of more than ten. This diminution may not be solely due to intramolecular dye-dye quenching.

Figure 32: Comparison of Cy3-dUTP and DY-555-dUTP signal yield for the templates *RCA15* and *F1F9F10F5*.

In addition, as template *F1F9F10F5* contains more integration sites, a diffusion-limitation of the enzymatic reaction may occur due to the low concentration of fluores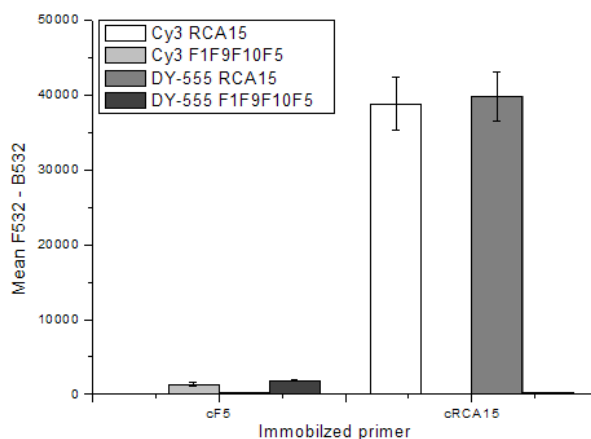cent dUTPs in the reaction solution. This probably slows down the reaction, diminishing the product yield compared to *RCA15* and therefore, could account for some signal reduction.

A depletion of dye-dUTP is unlikely as the experiments were usually run for 30 – 60 min and a linear signal rise could be observed for 4 h (Figure 33).
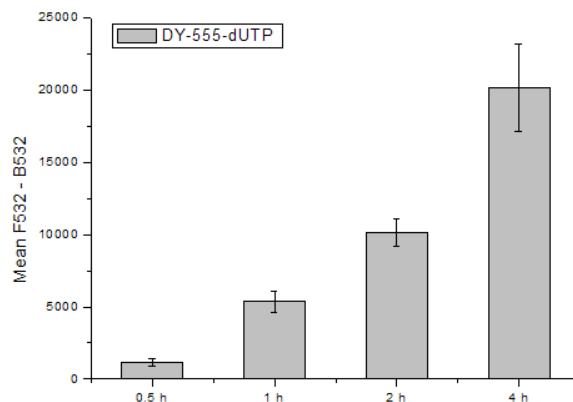
Figure 33: Comparison of RCA runtime with DY-555-dUTP.

This demonstrates the importance of optimizing the employed template for signal amplification with direct incorporation of fluorescent dNTPs.

6.3.3 Fluorescent labels

Fluorescent dNTPs are an important cost factor in DNA labeling assays. Cy3, the most commonly used label, is a comparatively expensive dye for microarray experiments using the green detection channel. Based on the spectroscopic investigations of the previous sections 6.1 and 6.2, DY-555-dUTP was chosen and studied along with Cy3-dUTP and a Cy3 hybridization probe (*Hyb-Cy3*) on DNA- and antibody microarrays.

While both fluorophores display similar signal yields for the systems examined (Figure 32), Cy3-dUTP is six times as expensive as DY-555-dUTP. For the reaction solution B, direct labeling with DY-555-dUTP lead to the same cost as *Hyb-Cy3*-labeling of the RCA product.

6.3.4 Control of ligation products

The template can be circularized by enzymatic ligation, and cleaned up in larger amounts before the RCA reaction, saving time and simplifying handling. Also, the success of the ligation can be controlled beforehand ensuring a consistent quality of the circular template, and thus the comparability of results.

While the ligation was successful in most instances, Figure 34 shows that it cannot be guaranteed even if two samples were ligated in parallel reactions on the same day. RCA15 I failed to yield a circularized template while RCA15 II was successfully ligated.
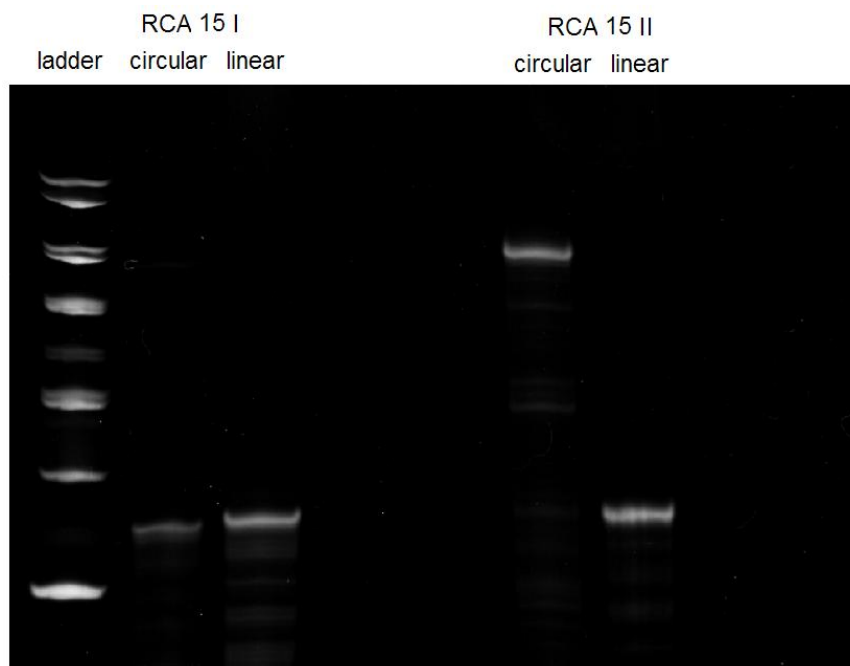
Figure 34: 15% PAA gel with 7M Urea of circularized and linear templates for two RCA15 samples (I and II).

6.3.5 Template concentration

The plain statement "the more, the better" is true for the concentration of the circular template (Figure 35). Yet, after the expense of the labeled nucleotides this is probably the second most costly aspect of the RCA reaction due to the ligation enzymes. For high throughput or parallel screening as little as possible will be applied.
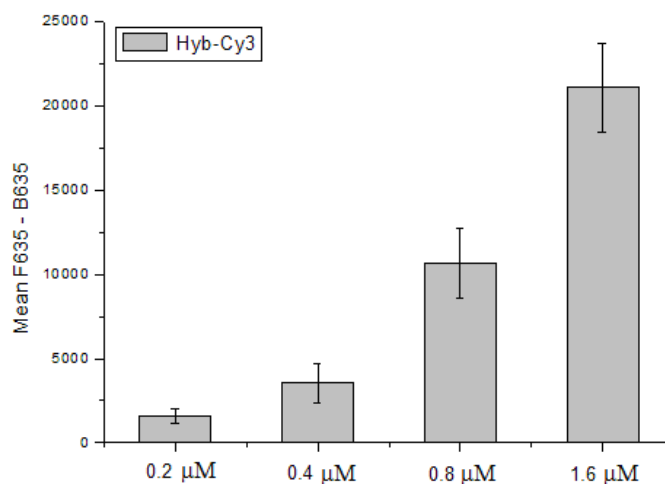
Figure 35: Signal yield for 0.2, 0.4, 0.8 and 1.6 µM template concentration. Hyb-Cy3 with 2h runtime.

6.3.6 Reaction temperature

One advantage of RCA is its isothermal nature that allows the reaction to be run at room temperature – a feature desirable for the use of simple read-out devices. In the literature, different temperatures are employed, ranging from 25 – 37°C.[48][50] Choosing the right temperature is a further, very simple, tool to increase the signal yield.
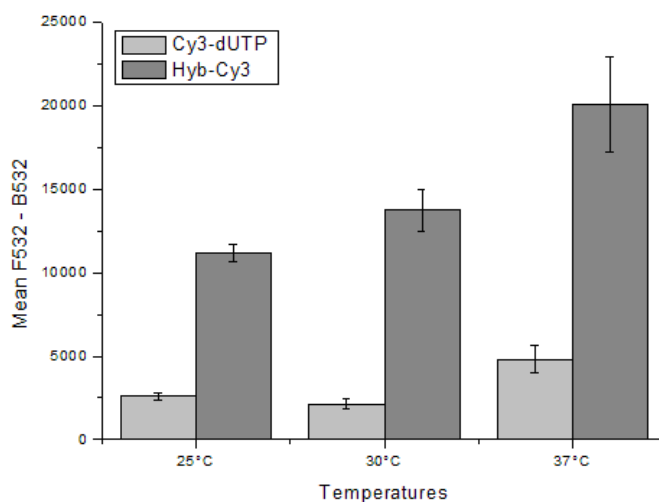
Figure 36: Signal yield for direct labeling with Cy3-dUTP and Hyb-Cy3 for incubation at 25, 30 and 37C for 1h runtime.

Incubating ϕ29 DNA polymerase for one hour at 37°C raised the signal by a factor of 2 compared to reaction at 25°C (Figure 36) and should be used whenever possible, as done in these studies.

6.3.7 Assay runtime and labeling strategies

As unmodified dNTPs are probably integrated more readily into the nascent strand, post-synthetic labeling via hybridization with *Hyb-Cy3* yields higher signals than direct labeling with dye-dUTPs - given that the same time for the RCA reaction is employed.

However, the overall assay runtime can be reduced while increasing the RCA reaction time. By separating polymerization and labeling in post-synthetic labeling via hybridization, two handling steps (*washing/ hybridization*) are added and the overall assay runtime is increased. The time saved by reducing the handling steps with the direct labeling protocol was thus added to the reaction time of the direct labeling RCA. This resulted in an overall higher signal output (Figure 37).
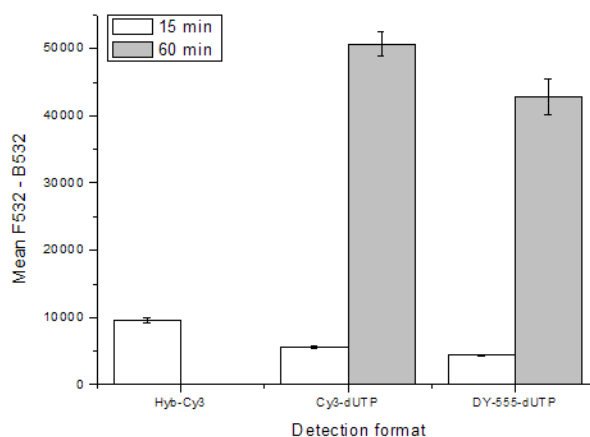
Figure 37: Signal yields of *Hyb-Cy3*, Cy3-dUTP and DY-555-dUTP for the same runtime (15 min.) compared to the signal increase for Cy3-dUTP and DY-555-dUTP when the handling time saved is added to the overall runtime (60 min.).

The assay runtime was further reduced by adding the template and the reaction solution simultaneously to the microarray. Hence, compared to typically employed protocol steps for post-synthetic labeling: *template hybridization* (30 min), *washing* (3x5min), *RCA*, *washing* (3x5min), *fluorescent-probe hybridization* (30 min), *washing* (3x5min), the experimental procedure was reduced to: *RCA*, *washing* (3x5min) - saving in this case 90 min and four handling steps. Although the dye-dUTP signals were well visible after 15 min it is better to reinvest at least part of the savings in RCA reaction time.

A positive side effect of omitting template *hybridization/ washing* was that the overall signal increased significantly (Figure 38).

Apparently, most of the hybridized template is usually washed away. Stringent washing before the RCA reaction is unnecessary in this case and has even proven to be counterproductive for the signal yield. It should be employed only when the specificity of the sequence must be guaranteed. As the primers are bound to the surface, there is no risk of a reaction in solution. For the post-reaction washing, the direct labeling allows more stringent washing as possible with hybridization probes, since the labeled strand is now covalently bound to the primer.
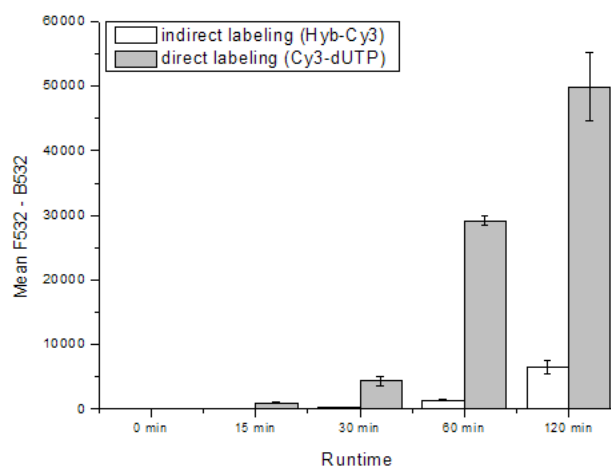
Figure 38: Comparison of the signal yields of the direct and indirect labeling protocol for the RCA reaction on microarray. The indirect labeling included washing and hybridization steps (*Hyb-Cy3*) while for the direct labeling, the template was added with the reaction solution (Cy3-dUTP).

55

6.3.8 SSB and mutant φ29 DNA polymerase

As single strand binding (SSB) proteins have been reported to enhance the efficiency of the RCA and thus enable a greater signal yield they were given to the reaction solution (see 3.2.3) .[30][31] Also a mutant φ29 DNA polymerase produced and investigated by the group of M.Salas was added.[108] The mutant, D12A/ D66A, was reported to have a reduced fidelity but increased DNA yield. This could integrate labeled dUTPs better and faster as the wild type.

Therefore, both SSB and D12A/D66A were tested on DNA microarrays hoping to further increase the signal yield (Figure 39).
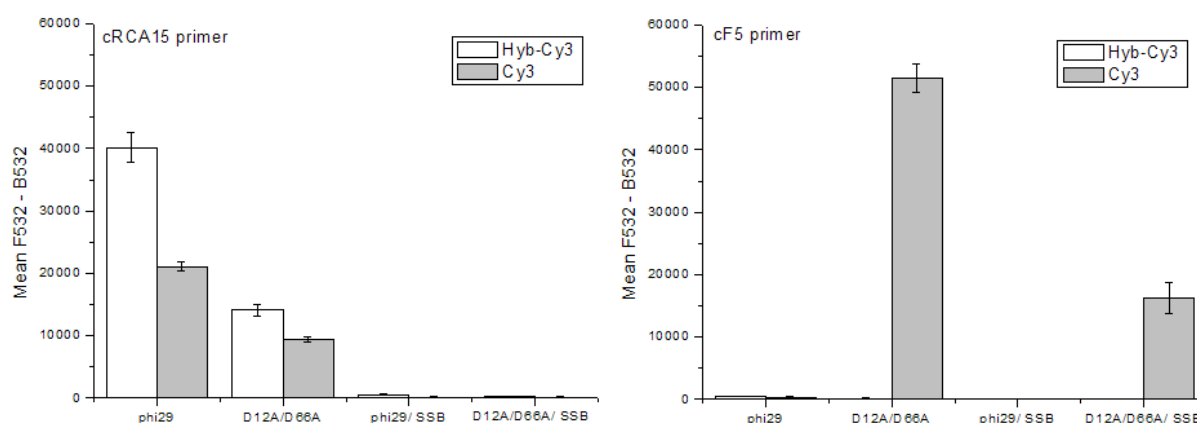
Figure 39: Comparison of signal intensities for wild type (phi29) and mutant (D12A/D66A) φ29 DNA polymerases with and without single strand binding protein (SSB) for the cRCA15 (left) and cF5 primer (right) incubated with template *RCA_15*.

Figure 40: Exemplary DNA microarray image, Spotting layout (left) and microarray scanner images (right) of the DNA microarray. Negative control: circular template omitted. *RCA_15*: circular template added.

As only template *RCA_15* was added the scanner image should look like the one shown in Figure 40 but this was true only for the regular reaction solution without SSB or D12A/D66A.

The addition of the SSB to the reaction had a negative effect on the signal yield as it seems to hinder the reaction substantially. The experiments reporting a good yield were performed in solution and were said to eliminate unwanted side products.[30] For the reaction on microarrays the SSB may block spotted primers and by this hinder the hybridization.

The mutant polymerase D12A/D66A did not yield a greater signal as hoped but rather only 40-50% of that achieved by the wild type. As this trend can be observed for Cy3-dUTP and *Hyb-Cy3* the direct labeling cannot be the cause but the overall performance of D12A/D66A is less than that of the wild type for the set up here.

Entirely unexpected was the effect on the cF5 primer spots. Though no template *F1F9F10F5* was added these spots yield a 5x greater signal for direct labeling with Cy3-dUTP than the *cRCA_15* primers that were provided with the template *RCA_15*. Even for the reactions containing SSB a clear signal can be seen, indicating that the loss of signal in the *cRCA_15* spots maybe do to hindering the template hybridization. The experiment with D12A/D66A was repeated with a reaction solution containing no template at all - yielding the same results as shown in Figure 39.

Hairpin formation could be the source of this template free replication, although it should have been observed for wild type φ29 DNA polymerase as well. The primers are not prone to hairpin formation offering only 2 base overlaps and both having the same number of possible hairpin hybridization sites (Table 7).

Table 7: Possible Hairpin formations (orange/ bold), cF5 primer and cRCA15 primer, calculated with OligoCalc.

Possible Hairpin formations

cF5 primer	cRCA15 primer
5' CTTA**TC**GCTTTATGACCG**GA**CC 3'	5' TCAA**GC**CAGACGAACTCAA**GC**C 3'
5' CTTAT**CG**CTTTATGAC**CG**GACC 3'	5' TCA**AG**CCAGACGAA**CT**CAAGCC 3'
5' CTTA**TC**GCTTTAT**GA**CCGGACC 3'	5' TCAAGCC**AG**ACGAA**CT**CAAGCC 3'
5' CTT**AT**CGCTTT**AT**GACCGGACC 3'	5' **TC**AAGCCAGAC**GA**ACTCAAGCC 3'
5' CT**TA**TCGCTT**TA**TGACCGGACC 3'	5' **TC**AAGCCA**GA**CGAACTCAAGCC 3'

The group of M. Salas that created and investigated D12A/D66A could not explain this phenomenon as well. They suggested that the wild type might digest the unprotected primers by its exonuclease activity which is greatly reduced for D12A/D66A. But since the reaction solution without any template yielded the same specific amplification for *cF5* this can be ruled out.

They did not know the cause of this effect but recommended trying another, commercially available mutant, N62D mutant, which is sold as MagniPhi. It has a higher strand displacement activity and only 10% of the exonuclease activity of the wild type.

MagniPhi did provide a higher yield for the direct labeling RCA than the wild type. But it demonstrated the same amplification of naked primers as D12A/D66A (Figure 41).
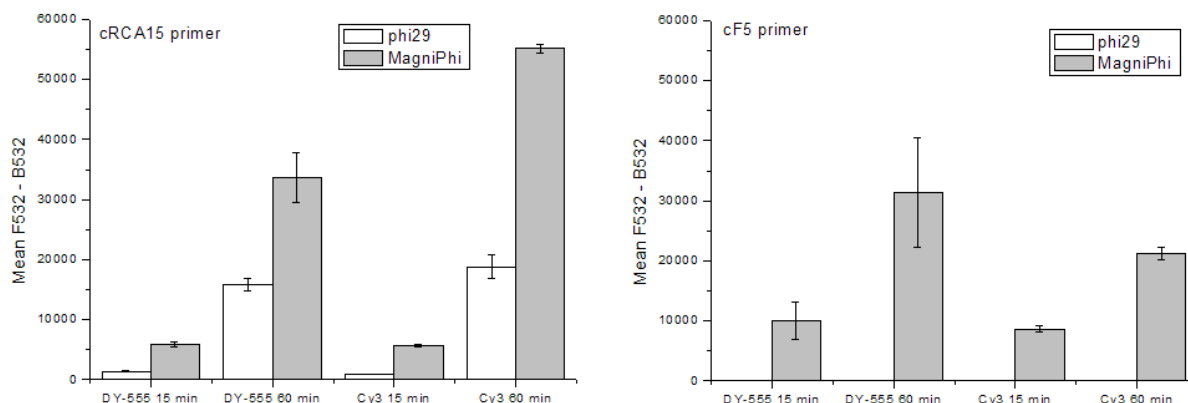
Figure 41: Comparison of signal intensities for wild type (phi29) and MagniPhi φ29 DNA polymerases for the cRCA15 (left) and cF5 primer (right) incubated with template *RCA_15*.

This makes the polymerase mutants tested unsuitable for this run of experiments as they effectively removed all specificity with the false positives yielding a far greater signal than the actual RCA reaction.

In an experimental set up that offers only one primer to be labeled, with or without RCA, MagniPhi maybe recommendable but the specificity has to be ensured at another level of the detection.

6.3.9 Antibody microarrays

To further demonstrate the versatility of the protocol, it was tested on an antibody microarray.

The microarray was spotted with antiHCG-ß mAb (mouse) in three concentrations to determine if the detection limits improved with direct labeling RCA. AntiHCG-ß pAb (goat) was spotted as a specificity control for the anti-mouse-IgG covalently modified with DNA primers. The RCA product signal of Cy3-, DY-555-dUTP, and *Hyb-Cy3* was compared to that of the unamplified primer with *AB-Cy3*. The 1 and 0.1 mg/ mL spots of antiHCG-ß mAb (mouse) could be clearly detected with all labels (Figure 42).
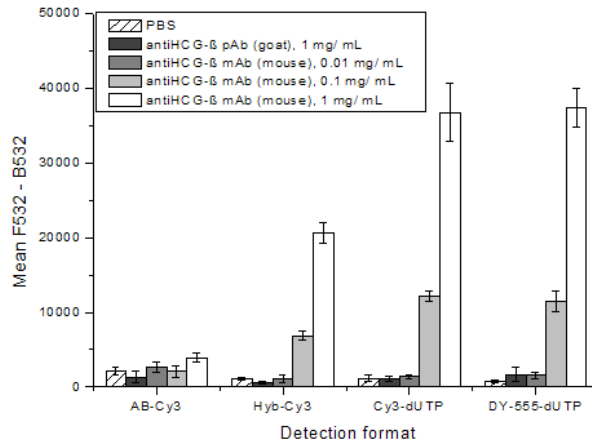
Figure 42: Detection of antiHCG-ß mAb (mouse; 0.01, 0.1 and 1 mg/ ml), antiHCG-ß pAb, (goat; 1 mg/ mL) as specificity control and PBS buffer for *AB-Cy3*, *Hyb-Cy3*, Cy3- and DY-555-dUTP.

For the unamplified primer, the 1 and 0.1 mg/ mL spots are in effect indistinguishable from the background and the specificity control. Therefore, with this approach, at least two orders of magnitude above the unamplified primer with *AB-Cy3* could be detected.

7 CONCLUSION

The straightforward enzymatic incorporation of dye-labeled dNTPs into the designed template sequences for RCA-based signal amplification with direct fluorophore labeling was successfully demonstrated.

Six fluorophores spectrally closely resembling Cy3 were tested as potential Cy3 alternatives and, with together with Cy3, investigated with steady-state and time-resolved spectroscopy. For the envisaged RCA-based detection they should provide a high and constant signal output in a DNA template with defined integration site spacing for the dye-dUTPs. Several dyes did provide this and had the same signal output as Cy3 at lesser cost (DY-547/8/9) or even a greater signal at lesser cost (DY-555). While BODIPY FL promised the highest signal based on the data of the free and dUTP-bound dye, its fluorescence drastically declined when it upon integration into the DNA strand and even further when multiple labels were present within the strand. This environmental sensitivity renders BODIPY FL unsuitable for RCA applications but it can be valuable in other experiments aimed at monitoring environmental changes by the fluctuations of its spectroscopic properties. For this, the nature of these changes must be known. The spectroscopic characterizations of the seven fluorophores can be, for example, used as a roadmap toward DNA probe design and label screening.

The time-resolved measurements of the dyes in the different microenvironments provided further information on the nature of the dye-oligonucleotide dynamics within the DNA compared to the free and dUTP-bound dye. For the cyanines with non-bridged double bonds (Cy3/ DY-547/8/9) the DNA strand allows for stacking interactions that hinder the *cis-trans* isomerization and thereby yields a greater signal than the free dye does. Their fluorescence lifetimes are less than a tenth of the rigid dyes (Cy3B/ DY-555/ BODIPY FL) and thus they are not well suited for time-gated detection. Cy3B and DY-555 are both apt as fluorophores for multiplexed time-resolved detection formats and the direct labeling RCA for signal amplification. But as Cy3B-dUTP is not commercially available DY-555 was subsequently the best candidate and used in further studies.

On the DNA microarrays different parameters of the signal amplification assay were investigated and the protocol improved for direct enzymatic labeling RCA. For example, the composition of the labeled and unlabeled dNTPs was varied, mutant ϕ29 DNA polymerases were tried, and a reduction of handling steps was achieved. The resulting improved signal amplification protocol for biological assays using direct enzymatic labeling RCA was simplified down to two steps: reaction and washing. It reduced the assay runtime and while increasing the signal yield and was successfully applied to antibody microarrays as well.

Conclusion

The mutant ϕ29 DNA polymerases were unsuited for the assay on DNA microarrays due to their unspecific amplification of the single stranded DNA primers. Yet, they may be valuable for detection platforms that ensure the specificity of the signal at a stage prior to the amplification reaction. For these they will provide an overall greater signal output as there is always an excess of primers and both naked and template binding primers will be labeled.

The direct labeling strategy developed here can be applied to many other assay formats using DNA primers to improve their detection limits. This straightforward detection protocol is attractive for many detection formats but especially for point-of-care diagnostic kits that need to be cost-efficient, fast, and easy to handle for untrained personnel.

That is why the RCA-based approaches have attracted attention of diagnostics-oriented biotech companies and research centers. Important future applications of RCA-based signal amplification include monitoring biomarkers to tell how effective a cancer treatment is or identifying STDs to prevent their spread. The aspect of multiplexing can play an important in identifying pathogens in minutes or hours to treat patience with bloodstream infections quickly with the right antibiotics to prevent septic shock.

References

8 REFERENCES

[1]   D. Howe and S. Yon, "The future of biocuration," *Nature*, vol. 455, no. 9, pp. 47-50, 2008.

[2]   M. M. Hann and T. I. Oprea, "Pursuing the leadlikeness concept in pharmaceutical research.," *Curr. Opin. Biotechnol*, vol. 8, no. 3, pp. 255-263, Jun. 2004.

[3]   S. Min, J. H. Choi, S. Y. Lee, and N. C. Yoo, "Applications of DNA Microarray in Disease Diagnostics," *J Microbiol Biotechnol*, vol. 19, no. 2008, pp. 635-646, 2009.

[4]   F. F. Bier, E. Reiß, E. Ehrentreich-Förster, J. Henkel, and R. Strehlow, "DNA Microarrays," in *Advances in Biochemical Engineering/Biotechnology*, no. 2007, Heidelberg: Springer, 2008, pp. 433-453.

[5]   U. Maskos and E. M. Southern, "Oligonucleotide hybridisations on glass supports: a novel linker for oligonucleotide synthesis and hybridisation properties of oligonucleotides synthesised in situ," *Nucleic Acids Res*, vol. 20, no. 7, pp. 1679-1684, 1992.

[6]   M. W. Shafer, L. Mangold, A. W. Partin, and B. B. Haab, "Antibody Array Profiling Reveals SerumTSP-1as a Marker to Distinguish Benign From Malignant Prostatic Disease," *Prostate*, vol. 67, pp. 255-267, 2007.

[7]   B. Schweitzer et al., "Multiplexed protein profiling on microarrays by rolling-circle amplification," *Nature Biotech*, vol. 20, no. 4, pp. 359-365, 2002.

[8]   L. Yang, S. Guo, Y. Li, S. Zhou, and S. Tao, "Protein microarrays for systems biology," *Acta Biochimet Biophys Hungarica*, vol. 43, no. 3, pp. 161 - 171, 2011.

[9]   S. H. Mayer-Enthart E., Sialelli J., Rurack K., Resch-Genger U., Koester D., "Toward Improved Biochips Based on Rolling Circle Amplification — Influences of the Microenvironment on the Fluorescence Properties of Labeled DNA Oligonucleotides," *Ann N.Y. Acad Sci*, vol. 292, pp. 287-292, 2008.

[10]   Anon, "Microarray steps." [Online]. Available: http://en.wikipedia.org/wiki/DNA_microarray.

[11]   V. Gubala, L. F. Harris, A. J. Ricco, M. X. Tan, and D. E. Williams, "Point of Care Diagnostics: Status and Future," *Anal Chem*, pp. 487-515, 2012.

[12]   M. R. Melo, S. Clark, and D. Barrio, "Miniaturization and globalization of clinical laboratory activities.," *Clin Chem Lab Med*, vol. 49, no. 4, pp. 581-586, Apr. 2011.

[13]   D. Andresen, M. von Nickisch-Rosenegk, and F. F. Bier, "Helicase dependent OnChip-amplification and its use in multiplex pathogen detection.," *Clin Chim Acta*, vol. 403, no. 1-2, pp. 244-248, May 2009.

[14]   B. Schweitzer and S. Kingsmore, "Combining nucleic acid amplification and detection," *Curr. Opin. Biotechnol*, vol. 12, pp. 21-27, 2001.

[15]   R. P. Novick, "Contrasting lifestyles of rolling-circle phages and plasmids.," *Trends Biochem Sci*, vol. 23, no. 11, pp. 434-438, Nov. 1998.

[16]   T. Brown, "Genome Replication," in *Genomes*, xford: Wiley-Liss., 2002, p. Chapter 13.

[17]   P. M. Lizardi, X. Huang, Z. Zhu, P. Bray-ward, D. C. Thomas, and D. C. Ward, "Mutation detection and single-molecule counting using isothermal rolling-circle amplification," *Nat Genet*, vol. 19, pp. 225-232, 1998.

References

[18] V. V. Demidov, *Rolling-circle amplification (RCA)*. New York: Dekker, M, 2005, pp. 1175-1179.

[19] L. Linck, E. Reiß, F. F. Bier, and U. Resch-Genger, "Direct labeling rolling circle amplification (RCA) as straightforward signal amplification for biodetection formats.," *Anal Meth*, vol. accepted, 2012.

[20] D. C. Thomas, G. A. Nardone, and S. K. Randall, "Amplification of Padlock Probes for DNA Diagnostics by Cascade Rolling Circle Amplification or the Polymerase Chain Reaction," *Arch Pathol Lab Med*, vol. 12, no. 123, pp. 1170-1176, 1999.

[21] O. a Alsmadi et al., "High accuracy genotyping directly from genomic DNA using a rolling circle amplification based assay.," *BMC Genomics*, vol. 4, no. 1, p. 21, May 2003.

[22] C. Garmendia, A. Bernad, J. a Esteban, L. Blanco, and M. Salas, "The bacteriophage phi 29 DNA polymerase, a proofreading enzyme.," *J Biol Chem*, vol. 267, no. 4, pp. 2594-2599, Feb. 1992.

[23] S. Kamtekar et al., "Insights into Strand Displacement and Processivity from the Crystal Structure of the Protein-Primed DNA Polymerase of Bacteriophage φ29," *Mol Cell*, vol. 16, pp. 609-618, 2004.

[24] J. G. Paez et al., "Genome coverage and sequence fidelity of f29 polymerase-based multiple strand displacement whole genome amplification," *Genome*, vol. 32, no. 9, pp. 1-11, 2004.

[25] V. Gadkar and M. C. Rillig, "Suitability of genomic DNA synthesized by strand displacement amplification (SDA) for AFLP analysis: genotyping single spores of arbuscular mycorrhizal (AM) fungi.," *J Microbiol Meth*, vol. 63, no. 2, pp. 157-164, Nov. 2005.

[26] S. Panelli, G. Damiani, L. Espen, G. Micheli, and V. Sgaramella, "Towards the analysis of the genomes of single cells: further characterisation of the multiple displacement amplification.," *Gene*, vol. 372, pp. 1-7, May 2006.

[27] F. B. Dean et al., "Comprehensive human genome amplification using multiple displacement amplification.," *P Natl Acad Sci USA*, vol. 99, no. 8, pp. 5261-5266, Apr. 2002.

[28] C. a Hutchison, H. O. Smith, C. Pfannkoch, and J. C. Venter, "Cell-free cloning using phi29 DNA polymerase.," *Proc Natl Acad Sci USA*, vol. 102, no. 48, pp. 17332-17336, Nov. 2005.

[29] V. V. Demidov and H. Thorne, "Rolling-circle amplification in DNA diagnostics: the power of simplicity," *Expert Rev . Mol. Diagn.*, vol. 2, no. 6, pp. 89-95, 2002.

[30] J. Inoue, Y. Shigemori, and T. Mikawa, "Improvements of rolling circle amplification (RCA) efficiency and accuracy using Thermus thermophilus SSB mutant protein," *Nucleic Acids Res*, no. June, 2008.

[31] T. Mikawa, J. Inoue, and Y. Shigemori, "Single-stranded DNA binding protein facilitates specific enrichment of circular DNA molecules using rolling circle amplification," *Anal Biochem*, vol. 391, no. 2, pp. 81-84, 2009.

[32] A. Fire and S. Q. Xu, "Rolling replication of short DNA circles," *Proc. Natl. Acad. Sci*, vol. 92, pp. 4641-4645, 1995.

[33] W. Zhao, M. M. Ali, M. A. Brook, and Y. Li, "Minireviews Rolling Circle Amplification: Applications in Nanotechnology and Biodetection with Functional Nucleic Acids," *Angew. Chem.*, pp. 6330-6337, 2008.

References

[34]   B. Schweitzer et al., "Immunoassays with rolling circle DNA amplification: A versatile platform for ultrasensitive antigen detection," *Proc Natl Acad Sci USA*, vol. 97, no. 4, pp. 10113-10119, 2000.

[35]   H. Zhou et al., "Two-color, rolling-circle amplification on antibody microarrays for sensitive, multiplexed serum-protein measurements.," *Genome Biol*, vol. 5, no. 4, p. R28.1-R28.12, Jan. 2004.

[36]   E. J. Cho, L. Yang, M. Levy, and A. D. Ellington, "Using a Deoxyribozyme Ligase and Rolling Circle Amplification To Detect a Non-nucleic Acid Analyte , ATP," *J Am Chem Soc*, vol. 127, no. 7, pp. 2021-2023, 2005.

[37]   M. Strömberg, J. Göransson, K. Gunnarsson, M. Nilsson, P. Svedlindh, and M. Strømme, "Sensitive Molecular Diagnostics Using Volume-Amplified Magnetic Nanobeads 2008," *Nano Lett*, vol. 8, no. 3, pp. 816-821, 2008.

[38]   M. Nilsson, "Lock and roll: single-molecule genotyping in situ using padlock probes and rolling-circle amplifcation," *Histochem Cell Biol*, vol. 126, pp. 159-164, 2006.

[39]   C. Ma, W. Wang, Q. Yang, C. Shi, and L. Cao, "Cocaine detection via rolling circle amplification of short DNA strand separated by magnetic beads.," *Biosens Bioelectron*, vol. 26, no. 7, pp. 3309-3312, Mar. 2011.

[40]   Y. P. Bao et al., "Detection of protein analytes via nanoparticle-based bio bar code technology.," *Anal Chem*, vol. 78, no. 6, pp. 2055-2059, Mar. 2006.

[41]   N. Li, J. Li, and W. Zhong, "CE combined with rolling circle amplification for sensitive DNA detection.," *Electrophoresis*, vol. 29, no. 2, pp. 424-432, Jan. 2008.

[42]   L. J. Ou, S. J. Liu, X. Chu, G. L. Shen, and R. Q. Yu, "Amplification Immunoassay as a Versatile Platform for Ultrasensitive Detection of Protein," *Anal Chem*, vol. 81, no. 23, pp. 9664-9673, 2009.

[43]   C. Larsson, J. Koch, A. Nygren, G. Janssen, A. K. Raap, and U. Landegren, "In situ genotyping individual DNA molecules by target-primed rolling-circle amplification of padlock probes," *Nature Methods*, vol. 1, no. 3, pp. 1-6, 2004.

[44]   M. Stougaard, S. Juul, F. F. Andersen, and B. R. Knudsen, "Strategies for highly sensitive biomarker detection by Rolling Circle Amplification of signals from nucleic acid composed sensors.," *Integr Biol*, vol. 3, no. 10, pp. 982-92, Oct. 2011.

[45]   J. Banér, M. Nilsson, M. Mendel-Hartvig, and U. Landegren, "Signal amplification of padlock probes by rolling circle replication.," *Nucleic Acids Res*, vol. 26, no. 22, pp. 5073-5078, Nov. 1998.

[46]   F. A. Faruqi et al., "High-throughput genotyping of single nucleotide polymorphisms with rolling circle amplification," *BMC Genomics*, 2001.

[47]   C. R. Sabanayagam, C. Berkey, U. Lavi, C. R. Cantor, and C. L. Smith, "Molecular DNA switches and DNA chips," in *Micro- and Nanofabricated Structures and Devices for Biomedical and Environmental Applications II*, vol. 3606, M. Ferrari, Ed. Bellingham, WA: Proceedings of the Society for Optical Engineering, 1999, pp. 90-98.

[48]   W. Van Dessel, F. Vandenbussche, M. Staes, N. Goris, and K. De Clercq, "Assessment of the diagnostic potential of immuno-RCA in 96-well ELISA plates for foot-and-mouth disease virus.," *J Virol Methods*, vol. 147, no. 1, pp. 151-156, Jan. 2008.

References

[49]   W. Shao et al., "Optimization of Rolling-Circle Amplified Protein Microarrays for Multiplexed Protein Profiling.," *J Biomed Biotech*, vol. 2003, no. 5, pp. 299-307, Jan. 2003.

[50]   Y. Gusev et al., "Rolling circle amplification: a new approach to increase sensitivity for immunohistochemistry and flow cytometry.," *Am J Pathol*, vol. 159, no. 1, pp. 63-69, Jul. 2001.

[51]   Olink, "Duolink system." [Online]. Available: http://www.olink.com/products-services/duolink.

[52]   L. Zhou, L. J. Ou, X. Chu, G. L. Shen, and R. Q. Yu, "Aptamer-Based Rolling Circle Amplification: A Platform for Electrochemical Detection of Protein," *Anal Chem*, vol. 79, no. 19, pp. 7492-7500, 2007.

[53]   J. Lee, K. Icoz, A. Roberts, A. D. Ellington, and C. A. Savran, "Diffractometric Detection of Proteins Using Microbead-Based Rolling Circle Amplification," *Anal Chem*, vol. 5699, no. 1, pp. 197-202, 2010.

[54]   D. a Di Giusto, W. a Wlassoff, J. J. Gooding, B. a Messerle, and G. C. King, "Proximity extension of circular DNA aptamers with real-time protein detection.," *Nucleic Acids Res*, vol. 33, no. 6, p. e64, Jan. 2005.

[55]   L. Yang, C. W. Fung, E. J. Cho, and A. D. Ellington, "Real-Time Rolling Circle Amplification for Protein Detection Real-Time Rolling Circle Amplification for Protein Detection," *Anal Chem*, vol. 79, no. 9, pp. 3320-3329, 2007.

[56]   E. Reiß, R. Hölzel, and F. F. Bier, "Preparations of DNA Nanostructures with Repetitive Binding Motifs by Rolling Circle Amplification," in *DNA Nanotech*, vol. 749, no. 3, G. Zuccheri and B. Samorì, Eds. Totowa, NJ: Humana Press, 2011, pp. 151-168.

[57]   S. Beyer, P. Nickels, and F. C. Simmel, "Periodic DNA nanotemplates synthesized by rolling circle amplification.," *Nano letters*, vol. 5, no. 4, pp. 719-22, Apr. 2005.

[58]   Y. Xiao, V. Pavlov, T. Niazov, A. Dishon, M. Kotler, and I. Willner, "Catalytic beacons for the detection of DNA and telomerase activity.," *JACS*, vol. 126, no. 24, pp. 7430-7431, Jun. 2004.

[59]   H. Y. Hsu and Y. Y. Huang, "Short communication RCA combined nanoparticle-based optical detection technique for protein microarray: a novel approach," *Biosens Bioelectron*, vol. 20, pp. 123-126, 2004.

[60]   L. Linck and U. Resch-Genger, "Identification of efficient fluorophores for the direct labeling of DNA via rolling circle amplification (RCA) polymerase φ29.," *Eur J Med Chem*, vol. 45, no. 12, pp. 5561-5566, Sep. 2010.

[61]   G. Nallur et al., "Signal amplification by rolling circle amplification on DNA microarrays," *Nucleic Acids Res*, vol. 29, no. 23, p. e118, 2001.

[62]   K. Kolmakov et al., "Red-Emitting Rhodamine Dyes for Fluorescence Microscopy and Nanoscopy," *Chem Eur J*, vol. 16, pp. 158-166, 2010.

[63]   A. Berr and I. Schubert, "Direct labelling of BAC-DNA by rolling-circle amplification," *Plant J*, vol. 29, no. 45, pp. 857-862, 2006.

[64]   J. R. Lakowicz, *Principles of Fluorescence Spectroscopy*, 3rd ed. New York: Springer, 2006.

[65]   A. Rolinski and O. J. W. G. Visser, "Basic Photophysics," 2010. [Online]. Available: http://www.photobiology.info/Visser-Rolinski.html.

[66]   W. Schmidt, *Optische Spektroskopie*, 2nd ed. Weinheim: Wiley-VCH, 2000.

References

[67] S. Das et al., "Molecular Fluorescence, Phosphorescence, and Chemiluminescence Spectrometry," *Anal Chem*, vol. 84, pp. 597-625, 2012.

[68] U. Resch-Genger, M. Grabolle, S. Cavaliere-Jaricot, R. Nitschke, and T. Nann, "Quantum dots versus organic dyes as fluorescent labels," *Nature Meth*, vol. 5, no. 9, pp. 763-775, 2008.

[69] J. R. Unruh, G. Gokulrangan, G. H. Lushington, C. K. Johnson, and G. S. Wilson, "Orientational dynamics and dye-DNA interactions in a dye-labeled DNA aptamer.," *Biophys J*, vol. 88, no. 5, pp. 3455-3465, May 2005.

[70] J. B. Randolph and A. S. Waggoner, "Stability , specificity and fluorescence brightness of multiply-labeled fluorescent DNA probes," *Nucleic Acids Res*, vol. 25, no. 14, pp. 2923-2929, 1997.

[71] G. Giraud et al., "Solution state hybridization detection using time-resolved fluorescence anisotropy of quantum dot-DNA bioconjugates," *Chem Phys Lett*, vol. 484, no. 4-6, pp. 309-314, 2010.

[72] "Stokes shift." [Online]. Available: http://en.wikipedia.org/wiki/File:Stokes_shift.png.

[73] "Beer Lambert Law." [Online]. Available: http://en.wikipedia.org/wiki/Beer–Lambert_law.

[74] S. E. Braslavsky, "Subcomitte on Photochemistry Glossary of Terms used in Photochemistry 3 rd EDITION Glossary of terms used in photochemistry , 3 rd edition (IUPAC Recommendations 2006)," *Pure and Applied Chemistry*, vol. 79, no. 3, pp. 293-465, 2007.

[75] B. J. Mccranor and R. B. Thompson, "Long Wavelength Fluorescence Lifetime Standards for Front-Face Fluorometry," *Biochemistry*, vol. 20, no. 2, pp. 435-440, 2011.

[76] W. Lei, A. Duerkop, Z. Lin, M. Wu, and O. S. Wolfbeis, "Detection of Hydrogen Peroxide in River Water via a Microplate Luminescence Assay with Time-Resolved ('Gated') Detection," *Microchim Acta*, vol. 143, no. 4, pp. 269-274, Dec. 2003.

[77] M. E. Sanborn, B. K. Connolly, K. Gurunathan, and M. Levitus, "Fluorescence Properties and Photophysics of the Sulfoindocyanine Cy3 Linked Covalently to DNA," *J Phys Chem B*, pp. 11064-11074, 2007.

[78] S. Wang, C. Zhang, S. K. Nordeen, and D. J. Shapiro, "In vitro fluorescence anisotropy analysis of the interaction of full-length SRC1a with estrogen receptors alpha and beta supports an active displacement model for coregulator utilization.," *J Biol Chem*, vol. 282, no. 5, pp. 2765-2775, Feb. 2007.

[79] B. A. Armitage, "Cyanine dye-Nucleic acid interaction," in *Top Heterocycl Chem*, Heidelberg: Springer, 2008, pp. 11-29.

[80] D. M. Jameson and J. A. Ross, "Fluorescence polarization/anisotropy in diagnostics and imaging.," *Chem Rev*, vol. 110, no. 5, pp. 2685-2708, May 2010.

[81] B. Instruments, "An Introduction to Fluorescence Resonance Energy Transfer (FRET) Technology and its Application in Bioscience," 2006.

[82] K. E. Sapsford, L. Berti, and I. L. Medintz, "Materials for Fluorescence Resonance Energy Transfer Analysis: Beyond Traditional Donor – Acceptor Combinations," *Angew Chem*, no. 45, pp. 4562 - 4588, 2006.

[83] J. Croney, "Fluorescence spectroscopy in biochemistry: teaching basic principles with visual demonstrations," *Biochem Mol Biol Edu*, vol. 29, no. 2, pp. 60-65, Mar. 2001.

References

[84]   F. P. Zamborini, L. Bao, and R. Dasari, "Nanoparticles in Measurement Science," *Anal Chem*, vol. 541-576, 84AD.

[85]   G.-il Kim, K.-woo Kim, M.-kyu Oh, and Y.-mo Sung, "The detection of platelet derived growth factor using decoupling of quencher- oligonucleotide from aptamer / quantum dot bioconjugates," *Nanotech*, vol. 20, 2009.

[86]   A. Miyawaki, "Proteins on the move: insights gained from fluorescent protein technologies," *Nature Rev Mol Cell Biol*, vol. 12, no. 10, pp. 656-668, Sep. 2011.

[87]   E. a Jares-Erijman and T. M. Jovin, "FRET imaging.," *Nature Biotech*, vol. 21, no. 11, pp. 1387-1395, Nov. 2003.

[88]   M. Schäferling and S. Nagl, "Optical technologies for the read out and quality control of DNA and protein microarrays.," *Anal Bioanal Chem*, vol. 385, no. 3, pp. 500-517, Jun. 2006.

[89]   L. E. Morrison, "Basic Principles of Fluorescence and Energy Transfer Applied to Real-Time PCR," *Mol Biotech*, vol. 44, no. 2, pp. 168-176, 2010.

[90]   Applied Gene, "TaqMan probe and Molecular beacon." [Online]. Available: Http://www.appliedgene.com/realTimePCR_2.html.

[91]   H. S. Rye et al., "Stable fluorescent complexes of double-stranded DNA with bis-intercalating asymmetric cyanine dyes: properties and applications," *Nucleic Acids Res*, vol. 20, no. 11, pp. 2803-2812, 1992.

[92]   Invitrogen, "Molecular Probes," in *Molecular Probes - The Handbook*, 11th ed., .

[93]   K. Licha and U. Resch-Genger, "Probes for optical imaging: new developments," *Drug Discovery Today: Technologies*, 2011.

[94]   M. Grabolle, R. Brehm, J. Pauli, F. M. Dees, and I. Hilger, "Determination of the Labeling Density of Fluorophore−Biomolecule Conjugates with Absorption Spectroscopy," *Bioconjugate Chem*, vol. 23, pp. 287-292, 2012.

[95]   K. Natte, T. Behnke, G. Orts-gil, C. Wu, and U. Resch-genger, "Synthesis and characterisation of highly fluorescent core – shell nanoparticles based on Alexa dyes," *J Nanopart Res*, 2012.

[96]   "Amino linker modified nucleotides." [Online]. Available: http://www.biomers.net/de/index/Technische_Informationen/Modifikationen/Linker_Spacer_Haptene.html.

[97]   M. Torimura et al., "Fluorescence-quenching phenomenon by photoinduced electron transfer between a fluorescent dye and a nucleotide base.," *Analytical Scienc*, vol. 17, no. 1, pp. 155-160, Jan. 2001.

[98]   C. Agbavwe and M. M. Somoza, "Sequence-dependent fluorescence of cyanine dyes on microarrays.," *PloS one*, vol. 6, no. 7, p. e22177, Jan. 2011.

[99]   G. Vamosi, C. Gohike, and R. M. Clegg, "Fluorescence Characteristics of 5-Carboxytetramethylrhodamine Linked Covalently to the 5' End of Oligonucleotides: Multiple Conformers of Single-Stranded and Double-Stranded Dye-DNA Complexes," *Biophysic J*, vol. 71, no. August, pp. 972-994, 1996.

[100]   Z. Zhu and A. S. Waggoner, "Molecular mechanism controlling the incorporation of fluorescent nucleotides into DNA by PCR," *Cytometry*, vol. 28, pp. 206-211, 1997.

References

[101] B. J. Harvey, C. Perez, and M. Levitus, "DNA sequence-dependent enhancement of Cy3 fluorescence.," *Photochem Photobiol*, vol. 8, no. 8, pp. 1105-1110, Aug. 2009.

[102] H. Yu, J. Chao, D. Patek, R. Mujumdar, S. Mujumdar, and A. S. Waggoner, "Cyanine dye dUTP analogs for enzymatic labeling of DNA probes," *Nucleic Acids Res*, vol. 22, pp. 3226-3232, 1994.

[103] R. F. Delgadillo and L. J. Parkhurst, "Spectroscopic properties of fluorescein and rhodamine dyes attached to DNA.," *Photochem Photobiol*, vol. 86, no. 2, pp. 261-272, 2010.

[104] U. Resch-Genger et al., "Traceability in Fluorometry: Part II . Spectral Fluorescence Standards," *J. Fluoresc.*, vol. 15, no. 3, pp. 315-336, 2005.

[105] R. P. Haugland, "Fluorescein Substitutes for Microscopy and Imaging.," in *Optical Microscope for Biolology*, 1st ed., J. K. Herman, B., Ed. Wilmington: Wiley-Liss Inc., 1990, pp. 143-157.

[106] C. Würth, M. Grabolle, J. Pauli, M. Spieles, and U. Resch-Genger, "Comparison of Methods and Achievable Uncertainties for the Relative and Absolute Measurement of Photoluminescence Quantum Yields.," *Anal Chem*, vol. 83, no. 9, pp. 3431-3439, May 2011.

[107] E. Reiß, R. Hölzel, and F. F. Bier, "Synthesis and stretching of rolling circle amplification products in a flow-through system.," *Small*, vol. 5, no. 20, pp. 2316-2322, Oct. 2009.

[108] A. Bernad, L. Blanco, J. Y. Lkaro, G. Martin, and M. Salas, "A Conserved 3 + S Exonuclease Active Site in Prokaryotic and Eukaryotic DNA Polymerases," *Cell*, vol. 59, pp. 219-226, 1988.

[109] R. P. Haugland, *Optical Microscopy for Biology - Fluorescein Substitutes for Microscopy and Imaging*, 1st ed. Wilmington: , 1990, pp. 143-157.

[110] L. Wang, A. K. Gaigalas, J. Blasic, and M. J. Holden, "Spectroscopic characterization of fluorescein- and tetramethylrhodamine-labeled oligonucleotides and their complexes with a DNA template," *Spectrochim Acta*, vol. 60, pp. 2741-2750, 2004.

[111] D. Marushchak, S. Kalinin, and I. Mikhalyov, "Pyrromethene dyes (BODIPY) can form ground state homo and hetero dimers: Photophysics and spectral properties," *Spectrochim Acta*, vol. 65, pp. 113-122, 2006.

[112] R. Hu et al., "Twisted Intramolecular Charge Transfer and Aggregation-Induced Emission of BODIPY Derivatives," *J Phys Chem C*, vol. 113, pp. 15845-15853, 2009.

[113] T.-C. Chang, C.-T. Kuo, C.-C. Chiang, J.-Y. Cheng, C.-S. Yan, and K. Peck, "Investigation of guanine-rich DNA telomeric structure by a covalently linked BODIPY dye," *PCCP*, vol. 1, no. 16, pp. 3783-3787, 1999.

[114] T. L. Netzel, K. Nafisi, M. Zhao, J. R. Lenhard, and I. Johnson, "Base-Content Dependence of Emission Enhancements, Quantum Yields, and Lifetimes for Cyanine Dyes Bound to Double-Strand DNA: Photophysical Properties of Monomeric and Bichromophoric DNA Stains," *Pharmacia*, pp. 17936-17947, 1995.

[115] I. Mikhalyov, N. Gretskaya, F. Bergstro, B. Chemistry, U. E-mail, and A. Article, "Electronic ground and excited state properties of dipyrrometheneboron difluoride (BODIPY): Dimers with application to biosciences.," *PCCP*, vol. 4, pp. 5663-5670, 2002.

[116] A. Biosciences, "Properties of CyDye fluors," in *Fluorescence screening reagents guide*, 1st ed., Uppsala: Amersham, 2003, pp. 1-3.

[117] B. J. Harvey and M. Levitus, "Nucleobase-specific enhancement of Cy3 fluorescence.," *J. Fluoresc.*, vol. 19, no. 3, pp. 443-448, May 2009.

References

[118] A. C. Fogarty, A. C. Jones, and P. J. Camp, "Extraction of lifetime distributions from fluorescence decays with application to DNA-base analogues.," *PCCP*, vol. 13, no. 9, pp. 3819-3830, Mar. 2011.

[119] A. Tomlinson, B. Frezza, M. Kofke, M. Wang, B. Armitage, and D. Yaron, "A structural model for cyanine dyes templated into the minor groove of DNA," *Chem Phys*, vol. 325, no. 1, pp. 36-47, Jun. 2006.

[120] T. Heinlein, J.-P. Knemeyer, O. Piestert, and M. Sauer, "Photoinduced Electron Transfer between Fluorescent Dyes and Guanosine Residues in," *J Phys Chem B*, pp. 7957-7964, 2003.

[121] C. A. M. Seidel, A. Schulz, and M. H. M. Sauer, "Nucleobase-Specific Quenching of Fluorescent Dyes. 1. Nucleobase One-Electron Redox Potentials and Their Correlation with Static and Dynamic Quenching Efficiencies," *J Phys Chem A*, pp. 5541-5553, 1996.

[122] D. P. Mcewen, K. R. Gee, H. C. Kang, and R. R. Neubig, "Fluorescent BODIPY-GTP Analogs: Real-Time Measurement of Nucleotide Binding to G Proteins 1," *Anal Biochem*, vol. 117, pp. 109 -117, 2001.

[123] X. Qi, S. Bakht, K. M. Devos, M. D. Gale, and A. Osbourn, "L-RCA (ligation-rolling circle amplification): a general method for genotyping of single nucleotide polymorphisms (SNPs)," *Nucleic Acids Res*, vol. 29, no. 22, pp. 1-7, 2001.

[124] J. Jarvius et al., "Digital quantification using amplified single-molecule detection," *Nat. Methods*, vol. 3, pp. 725-727, 2006.

[125] Z. Zhu, J. Chao, H. Yu, and A. S. Waggoner, "Directly labeled DNA probes using fluorescent nucleotides with different length linkers," *Nucleic Acids Res*, vol. 22, no. 16, pp. 3418-3422, 1994.

[126] U. Feldkamp, R. Wacker, H. Schroeder, W. Banzhaf, and C. M. Niemeyer, "Microarray-based in vitro evaluation of DNA oligomer libraries designed in silico.," *Chemphyschem*, vol. 5, no. 3, pp. 367-372, Mar. 2004.

9 APPENDIX

9.1 MATERIALS

9.1.1 Chemicals

BODIPY-FL, -dUTPs	Invitrogen
Cy3, -dUTPs	GE Healthcare
Cy3B-NHS	GE Healthcare
DNA	Integrated DNA Technology/ Biomers
dNTPs	Fermentas
DY-dyes, -dUTPs	Dyomics
Ethanol	Merck
Ethanolamine	Carl Roth GmbH
HCl	Carl Roth GmbH
KCl	Carl Roth GmbH
Loading dye	Fermentas
NucleoSpin Extract II	Macherey-Nagel
NaCl	Carl Roth GmbH
NaPi	Carl Roth GmbH
PAA acrylamide/ bis-acrylamide (19:1)	Sigma-Aldrich
PBS buffer	Carl Roth GmbH
SDS	Carl Roth GmbH
Skim milk	Applichem
TBE-buffer	Merck
TEMED	Carl Roth GmbH
Tris-HCl	Carl Roth GmbH
Triton X-100	Carl Roth GmbH
Tween 20	Serva

9.1.2 Enzymes

BSA	New England Biolabs
CircLigase II	Epicentre
CircLigase II buffer	Epicentre
Exonuclease I	Fermentas

9.1.2 Enzymes (cont.)

ϕ29 DNA polymerase	New England Biolabs
ϕ29 DNA polymerase buffer	New England Biolabs
λ-exonuclease	Fermentas

9.1.3 Instruments and Consumption Materials

1 cm-quartz microcuvettes	Hellma
15 mL falcon tubes	Orange Scientific
50 mL falcon tubes	Orange Scientific
Autoklav	SHP Steriltechnik AG
Accuracy scales	Satorius
CARY 5000 spectrometer	Varian Inc.
Epoxide glass slides	Corning
FluoTime200 time-resolved spectrometer	Picoquant
Freezer –20ºC	Liebherr
Freezer 4ºC	Liebherr
GeneDoc X	Biorad
GenePix 4300A microarray-scanner	Axon
Gloves	NeoLab
Incubation chamber	Heraeus
Mini-PROTEAN Tetra Electrophoresis System	Biorad
Nanodrop spectrophotometer ND-1000	Peqlab
Reaction Tubes, 1.5 ml	Eppendorf
Parafilm	Pechiney
Pipettes	Eppendorf
Pipette Tips	Eppendorf
Purest Water Installation (Milli–Q)	Millipore
Scales	Kern EW
sciFLEXARRAYER S11	Scienion AG
Shaker Rotamax 120	Heidolph
Spectronics Instruments 8100	Spectronics Instruments
SYBR Green II	Invitrogen
Tissues	Kimwipes
Table–top Centrifuge	Eppendorf
Thermomixer	Eppendorf
Vortex	Labdancer IKA

9.1.4 Buffers

DNA buffer, pH 7.2

10 mM NaPi

250 mM NaCl

CircLigase II buffer, pH 7.5

0.033 M tris-acetate

0.066 M potassium acetate

0.5 mM DTT

ϕ29 DNA polymerase reaction buffer, pH 7.5

50 mM Tris-HCl

10 mM $MgCl_2$

10 mM $(NH_4)_2SO_4$

4 mM dithiothreitol

Loading Buffer for Agarose Gel (6x)

0.03% Bromphenolblue

0.03% Xylencyanol

60% Glycerol

10 mM Tris-HCl (pH 7.5)

60 mM EDTA (pH 8.0)

Phosphate–Buffered Saline, pH 7.4

137 mM NaCl

2.7 mM KCl

10 mM Na_2HPO_4

2 mM KH_2PO_4

Phosphate–Buffered Saline with Tween, pH 7.4

Phosphate–Buffered Saline

0.05% Tween 20

TBE-buffer, pH 8.3

89 mM Tris

89 mM Borate

2 mM EDTA

9.1.4 Buffers (cont.)

Urea loading buffer, pH 7.5

8M urea

20 mM EDTA

5 mM Tris-HCl

0.5% (w/v) xylene cyanol, bromphenole blue

9.1.4 Buffers (cont.)

Appendix

9.2 ABBREVIATIONS

A	Adenosine
Å	Angstrom
A_{260}	Absorption at 260 nm
A_{280}	Absorption at 280 nm
AB	Antibody
°C	Celsius
C	Cytosine
dATP	Deoxyadenosine triphosphate
dCTP	Deoxycytidine triphosphate
dGTP	Deoxyguanosine triphosphate
dNTP	Deoxynucleoside triphosphate
dTTP	Deoxythymine triphosphate
dUTP	Deoxyuridine triphosphate
DNA	Deoxyribonucleic acid
ds double–stranded	ds double–stranded
ε	Molar absorption coefficient
EDTA	Ethylenediaminetetraacetic acid
ELISA	Enzyme-linked immunosorbent assay
FLIM	Fluorescence-lifetime imaging microscopy
FRET	Foerster resonance energy transfer
ϕ_f	Fluorescence quantum yield
G	Guanosine
GFP	Green fluorescent protein
h	Hour(s)
kb	Kilobase
λ_{ex}	Excitation wavelength
λ_{ill}	Illumination light wavelength
l	Liter
MDA	Multiple displacement amplification
min	Minute(s)
mol	Mole(s)
mM	Millimolar
mM	Micromolar
mRNA	Messenger ribonucleic acid
nM	Nanomolar
nmol	Nanomol
nt	Nucleotide(s)

9.2 ABBREVIATIONS (cont.)

PAA	Polyacrylamid
PCR	Polymerase chain reaction
PET	Photoinduced electron transfer
PMT	Photomultiplier tube
POC	Point-of-care
r	Emission anisotropy
RCA	Rolling circle amplification
RCP	Rolling circle product
RCR	Rolling circle replication
RD	Reference detector
RT	Reverse transcription
OD	Optical density
PBS	Phosphate–Buffered Saline
PBST	Phosphate–Buffered Saline with Tween 20
QD	Quantum dot
s	second(s)
SSB	Single strand protein
T	Thymine
TBE	Tris-borate with EDTA
TOTO-1	1-1'-[1,3-propanediylbis[(dimethyliminio)-3,1-propanediyl]]bis[4-[(3-methyl-2(3H)-benzothiazolylidene)methyl]]-tetraiodide
U	Unit(s)
UV	Ultraviolet
V	Volt(s)
VFP	Verde fluorescence protein
w/v	weight per volume

Appendix

9.3 FORMULAS

Beer Lambert Law

$$\log \frac{I}{I_0} = \varepsilon \times c \times d$$

I	light before sample
I_0	light after passing through the sample
ε	molar absorption coefficient
c	concentration
d	Pathway through sample

Radiative lifetime τ_0

$$\tau_0 = \frac{\Phi_f}{\tau}$$

τ_0	radiative lifetime
Φ_f	fluorescence quantum yield
τ	fluorescence lifeitme

Rate constant k

$$k = k_F + k_N$$

k	rate constant
k_F	radiative rate constant
k_N	non-radiative rate constant

Appendix

9.3 FORMULAS (cont.)

Fluorescence quantum yield Φ_f

$$\Phi_{f,x} = \Phi_{f,st} \times \frac{F_x}{F_{st}} \times \frac{f_{st}(\lambda_{ex})}{f_x(\lambda_{ex})} \times \frac{n_x^2}{n_{st}^2}$$

Φ_f	fluorescence quantum yield
$f(\lambda_{ex})$	absorption factor
λ_{ex}	excitation wavelength
F	fluorescence
x	sample
st	standard
n	refractive index of the solvent

Emission anisotropy r

$$r = \frac{F_{0°/0°} - F_{0°/90°}}{F_{0°/0°} + 2F_{0°/90°}}$$

r	emission anisotropy
0°/ 90°	emission polarizer setting
F	fluorescence

Relative amplitudes A_i

$$A_i = a_i / \Sigma a_i \times 100\%$$

A_i	relative amplitudes
a_i	single amplitudes
Σa_i	sum of amplitudes

9.3 FORMULAS (cont.)

Average fluorescence lifetime τ_{av}

$$\tau_{av} = \frac{\sum_i a_i \times \tau^2_i}{\sum_i a_i \times \tau_i}$$

τ_{av}	average fluorescence lifetime
τ_i	single lifetimes
a_i	single amplitudes
τ_{int}	intensity-weighted average fluorescence lifetimes

9.4 PUBLICA

Poster	*Direct Enzymatic Incorporation of Fluorophores on DNA-Microarrays via Rolling Circle Amplification (RCA).* Linck L, Mayer-Enthart E, Sialelli J, Rurack K, Köster D, Seitz H, Resch-Genger U, Panne U. Dechema Tagung Functional Genomics 06.03.2008
Poster	*Fluorescence Signal Amplification on DNA Microarrays via Rolling Circle Amplification (RCA).* Linck L, Mayer-Enthart E, Sialelli J, Rurack K, Köster D, Seitz H, Resch-Genger U, Panne U. ANAKON 2009 06.03.2008
Talk	*Optimized Fluorescence Detection for RCA-Assays on Microarrays* Linck L, Resch-Genger U Fraunhofer Institut 25.08.2010
Article	*Identification of efficient fluorophores for the direct labeling of DNA via rolling circle amplification (RCA) polymerase φ29.* Linck L, Resch-Genger U 2010. European Journal of Medical Chemistry, 45(12): 5561-6
Poster	*Optimization of fluorescence signals on rolling amplification-enhanced microarrays* Linck L, Resch-Genger U, Reiß E, Bier F, Sobek J Dechema Tagung Functional Genomics 03.02.2011
Proceedings	*Funktionelle Chromophor-Systeme, innovative Validierungskonzepte und rückführbare Standards für die fluoreszenzbasierte multiparametrische Bioanalytik* Resch-Genger U, Behnke T, Brehm R, Grabolle M, Hennig A, Hoffmann A, Hoffmann K, Linck L, Lochmann C, Pauli J, Spieles M, Würth C Senftenberger Innovationsforum Multiparameteranalytik 2011

9.4 PUBLICA (cont.)

Article   *Spectroscopic and Photophysical Properties of dUTP and internally DNA*
                 bound Fluorophores for Optimized Signal Detection in Biological Formats
                 Linck L, Kapusta P, Resch-Genger U
                 Photochemistry Photobiology, accepted 2012

Article   *Direct labeling rolling circle amplification (RCA) as straightforward signal*
                 amplification for biodetection formats.
                 Linck L, Reiß E, Bier F, Resch-Genger U
                 Analytical Methods, accepted 2012

9.5 CURRICULUM VITAE